CHARACTERISTICS OF OCEAN GRAVITY WAVES OFF THE CAPE SOUTH WEST COAST

by

F. A. Shillington

Submitted in partial fulfilment of the
requirements for the degree of Master of Science
in the Department of Oceanography in the
University of Cape Town
1974

Supervisors: Dr. T. F. W. Harris
Dr. T. R. Hennessy

Frontispiece. Sea tower at Melkbosstrand.

TABLE OF CONTENTS

LIST OF ILLUSTRATIONS

Figure 5.10 Extreme spectra compared with Pierson and Moskowitz (1964) fully developed spectra.

ABSTRACT

Ocean gravity waves have been recorded near Melkbosstrand with a Wemelsfelder float type wave recorder on a sea tower situated in water 13m deep and one Kilometre offshore. The half hour records, taken twice daily between July 1972 - June 1973, have been analysed in a format uniform with that of Draper (1966). Measurements have been made from the wave records to check the value of the statistical ratios of Longuet-Higgins (1952) and Draper (1963). Ratios of maximum wave height to root mean square amplitude are lower than the theoretical values and reasons for this are discussed in the light of the records being taken in shallow water. Ratios of maximum wave height to the average upper one tenth wave height and average upper one third wave height agree closely with the theoretical values.

Spectral analysis using the methods of Blackman and Tukey (1958), with 36 degrees of freedom and 100 lags have been applied to half hour records digitized once per second. Frequency, time diagrams contoured at equal energy values have been constructed for the period May and part of June 1973 on the basis of twice daily spectral measurements at 5 mHz intervals. The wave events, which include generation of swell from near South Georgia, (54^{o}S, 37^{o}W), have been compared with the South African Weather Bureau synoptic charts in order to identify generation centres. Repeated energy values near the 50 mHz band seem to be generated by winds of a lower velocity than required by Moskowitz (1964). Predominant siting of fetches at distances of the order of 1000 nautical miles accounts for the bulk of wave generation between latitudes 40^{o} - 50^{o}S. One storm appears to have originated near the Drake passage, but no events have been detected with waves passing through the passage.

Analysis of wave spectra from several storms generating maximum wave heights over 5 metres, show that fully developed seas are seldom, if ever, present in Cape waters.

CHAPTER 1

INTRODUCTION AND PURPOSE OF RESEARCH

Two main themes underly the research work on ocean gravity waves reported in this thesis.

a) Various wave statistics used in the routine analysis of analogue wave recordings have been investigated. The theoretical background to these statistics is by Longuet-Higgins (1952), and although his ratios have been found to apply under Northern Hemisphere wave conditions, it was felt that the long fetches, predominant swell characteristics, and possibly uncomplicated meteorological conditions pertaining to the Southern Hemisphere's ocean-weather system would provide a useful data set for comparison. Also, coastal engineers have an intrinsic need for the numerical values associated with the theoretically derived ratios.

b) The second purpose of the research was to study the synoptic meteorological conditions associated with wave generation into Cape waters. For this study, sections of the almost continuous one year's time series of wave heights, taken twice daily, were spectrally analysed. Energy, frequency, time diagrams provided the best method of summarising the available data. Synoptic weather charts from the South African Weather Bureau were then used to identify the origin of storm centres responsible for generating high waves at the Cape. A close understanding of the frequency spread of the wave energy arriving at the recording station, together with a knowledge of the predominant spectral shapes, is needed for the introduction of a wave forecasting scheme.

The data used in this thesis became available as a result of the oceanographic investigations by the Electricity Supply Commission into the feasibility of a sea water cooled Nuclear Power Station at Duynefontein, about 30 Km north of Cape Town. The engineering design of the sea water structures needed for the power station requires a basic knowledge of the ocean wave regime, amongst other factors. This information about waves in South African

waters was severely lacking, since most available wave recordings have until recently, been made on an intermittant basis during research cruises.

A wave data collection program was initiated by ESCOM in 1969. The Marine Effluent Research Unit in the Oceanography Department at the University of Cape Town was commissioned to carry out monthly cruises in Table Bay. Waves were recorded in various depths of water near Melkbosstrand with the NIO shipborne wave recorder on board the U. C. T. research vessel "Thomas B. Davie". Analysis of this data by van Ieperen (1970) revealed that conditions were generally suitable for the computation of one dimensional spectra from half hour records. The spectra were often rather sharply peaked indicating swell conditions, and situations were occasionally non stationary in a statistical sense during the recording interval.

An extension to the data collection program was made in 1971, when a Sea Tower was erected in 13 m deep water one Kilometre offshore, near Melkbosstrand. Instrumentation on this tower was to record automatically two half hour periods of wave heights per day, and monitor continuously other parameters such as sea temperature, and wind and current data.

The placement of the tower in shallow water provides an ideal platform from the engineering point of view. However, from the wave analysts viewpoint, the shallow water provides complications. Fortunately, the bottom topography near the tower is gently sloping at a uniform gradient of 1 : 150 (van Ieperen 1970) and this regular nature together with the rather predominantly sandy bottom structure minimises refraction effects.

Apart from equipment failure on some occasions, it has been possible to form a continuous time series of wave heights from the twice daily analogue records. Half hour records, telemetred ashore every two hours, provide digital records which can be spectrally analysed. However, telemetering problems sometimes rendered these records useless, although the closely spaced time grid was particularly useful for wave growth studies.

The entire time series of wave heights have, because of their invaluable nature, been tabulated in toto. The two hourly spectrally analysed records have been used in a preliminary study of the wave regime at the Cape by Harris, Marshall and Shillington (1972).

CHAPTER 2

2.1 Previous work on waves in South African Waters

Initial wave recordings in South African waters were made in 1960 aboard U.C.T.'s research vessel "John D. Gilchrist" with an echo sounder. In 1961, the division of Sea Fisheries research vessel "Africana II" was equipped with an NIO shipborne wave recorder. Wave records were made from the Africana II while on research cruises between Saldanha Bay and Cape Agulhas. These records were analysed by M. Darbyshire (1962) and wave hindcast studies made according to the scheme proposed by J. Darbyshire (1963) for North Atlantic conditions. On some occasions correlation was good, but M. Darbyshire comments on the paucity of both wave records and weather information over the South Atlantic.

M. Darbyshire and J. Darbyshire (1964) present the results of wave recordings taken on board the Africana II whilst she was on cruises in the area 31^{o}-38^{o}S and 15^{o}-22^{o}E. The wave records were of 15 minutes duration, taken at four hourly intervals while on the cruises. Some records were taken while the ship was steaming, but 318 records were available which were made while the ship was stopped. These are all records of opportunity taken while the ship was on deep sea cruises.

Darbyshire and Pritchard (1966) describe wave statistics in South African waters during the period 1962 - 1965. These records were taken aboard the Africana II while on cruises in the South Atlantic ocean, and the distribution of maximum wave heights versus zero crossing periods were plotted for different areas. Most frequent conditions were ones of maximum wave heights of 10 ft. and zero crossing periods of 10 seconds.

An Ocean Wave Research project was initiated in 1967 on a national scale in South Africa by the South African National Committee for Oceanographic Research (SANCOR). The work is being carried out by the Hydraulics Research Unit of the CSIR's National Mechanical Engineering Research Institute.

The main objectives of the Ocean Wave Research project are to record and analyse wave conditions along the 4000 Km of South African coastline. Zwamborn, van Schaik and Harper (1970) give details of the various instruments used in the program, as well as the situations of personnel doing visual observations. The results of the project are contained in Ocean Wave Research Reports 1 and 2 (1968, 1969).

The University of Cape Town's research vessel "Thomas B. Davie" was commissioned in 1966 and in 1968 it was equipped with an NIO shipborne wave recorder. Wave records taken while on cruises are to be added to the Ocean Wave Research project data bank. During the period 1968 - 1970, wave records were made on a monthly basis in Table Bay. These records, which were of twenty minutes duration, were made in water depths varying from 12 - 140 m. The analogue trace records were hand digitized at 2 second intervals in the Oceanography Department at the University of Cape Town. Van Ieperen (1970) used the records to test the assumptions of normality and stationarity so that the records could be spectrally analysed. The stationarity of three records was tested, and one record was found to be non stationary. Van Ieperen found that the total variances of the spectra decreased systematically in shoaling water. No frequency selective attenuation was found. He also determined a bottom friction factor which was higher than that of other workers. Van Ieperen (1973), used records taken aboard the T. B. Davie off Melkbosstrand to investigate the effect of shoaling water and bottom friction on the spectra. He suggests that a linear friction law may be more suitable than the quadratic law for this area.

In 1969, a program of monthly cruises was started to collect oceanographic data for ESCOM. Waves were measured from the T. B. Davie with an NIO wave recorder and analysed by Van Ieperen (see Interim Reports 1 and 2, 1969, 1971) in the Oceanography Department, UCT.

After the erection of a sea tower off Melkbosstrand in 1971, a program to record a continuous time series of wave heights with a Wemelsfelder float type recorder was started on behalf of ESCOM. Waves are recorded twice

daily as a half hour analogue trace on the tower and telemetered to a shore station every two hours in digital form. Harris, Marshall and Shillington (1972), have studied spectra from the telemetered records for July 1972 to gain a preliminary understanding of the wave regime at the Cape. A particularly interesting case of low frequency, (50 mHz), monochromatic waves has been examined by Harris, Marshall and Shillington (1973).

2.2 Meteorological conditions affecting waves in South African waters

a) General Introduction

To understand the origin and generation of wind waves and ocean swell recorded near Cape Town, it is essential to understand the meteorological conditions prevailing over the South Atlantic ocean between South America and South Africa, (see figure 2.1). Wind velocities, orientation of wind fields, fetch sizes, positions of cyclones and fronts, and typical cyclone tracks are some of the details that must be known for wave analysis and forecasting. The Southern Atlantic ocean suffers from a paucity of data of this nature, primarily due to the lack of shipping in the area.

b) Jet Stream

A fast moving upper current of air, called the jet stream, occurs at the meridional and vertical circulation boundary of the westerlies and Polar winds. The path of the jet stream and the upper westerlies meanders about the mid latitude around Antarctica. This meandering causes a series of wave like displacements of the polar front which are linked with cyclogenesis, and frontal waves observed at sea level. The migrating cyclones and anticyclones then furnish the heat exchange between high and low latitudes.

One of the earlier attempts at understanding the problems of the polar front, cyclogenesis and general meteorology of the Southern Hemisphere was made during the IGY of 1957. Meteorological data was collected extensively by many scientific research ships and was analysed chiefly by J. J. Taljaard of the South African Weather Bureau (SAWB) and H. van Loon, later attached to the National Centre for Atmospheric Research at Boulder, Colorado.

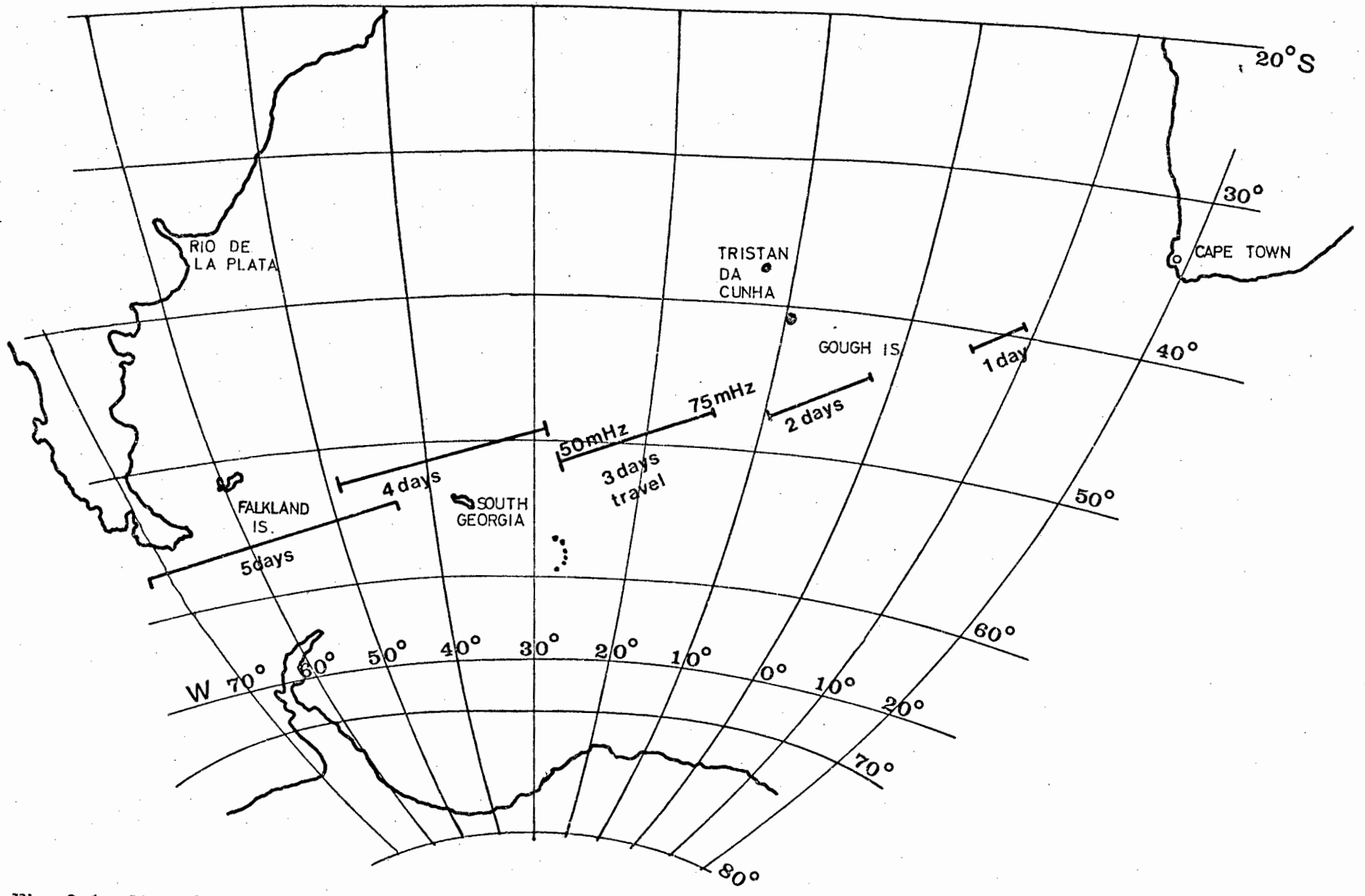

Fig. 2.1. Map of South Atlantic region. Travel times of 50 - 75 mHz swell indicated.

c) Fronts

There appears to be a close connection between the frequency spectrum of ocean waves recorded at the Cape and the velocity and nature of the frontal systems generating these waves. This is pursued later. For this reason, a synopsis of fronts, and features of cyclones and cyclogenesis is made below.

A clear exposition of fronts and frontal analysis was given by Taljaard, Schmitt, and van Loon (1961) in which they formulate the ideal front as follows:

"A front is a narrow sloping layer, with a vertical extent of at least 3 Km, across which the temperature changes in the horizontal direction by an average of at least 3^{o}C in subtropical regions (25^{o}S - 40^{o}S) and 4^{o} - 5^{o}C in middle latitude and polar regions".

Such cold fronts are the usual forerunners of occluded low pressure systems passing near the Cape.

(d) Cyclones and Cyclogenesis

Taljaard and van Loon (1962, 1963) analysed the 1957 IGY data for winter and spring, and summer of 1957 respectively. Taljaard (1967) summarises the development, distribution and movement of cyclones in the Southern Hemisphere. The results presented below are taken from Taljaard and van Loon (1962, 1963).

Cyclogenesis, that is the first appearance of a closed isobar, occurred frequently between 35^{o} - 55^{o}S off the east coast of South America in winter, (see figure 2.2). A notable exception was the area around La Plata (23^{o} - 35^{o}S). Cyclogenesis occurred infrequently south of 55^{o}S at this longitude. In summer, a high frequency band for cyclogenesis existed between 40^{o}S off South America to 50^{o}S in the Indian Ocean. The northern boundary for cyclogenesis in winter was 35^{o} - 40^{o}S and lay in a WNW to ESE

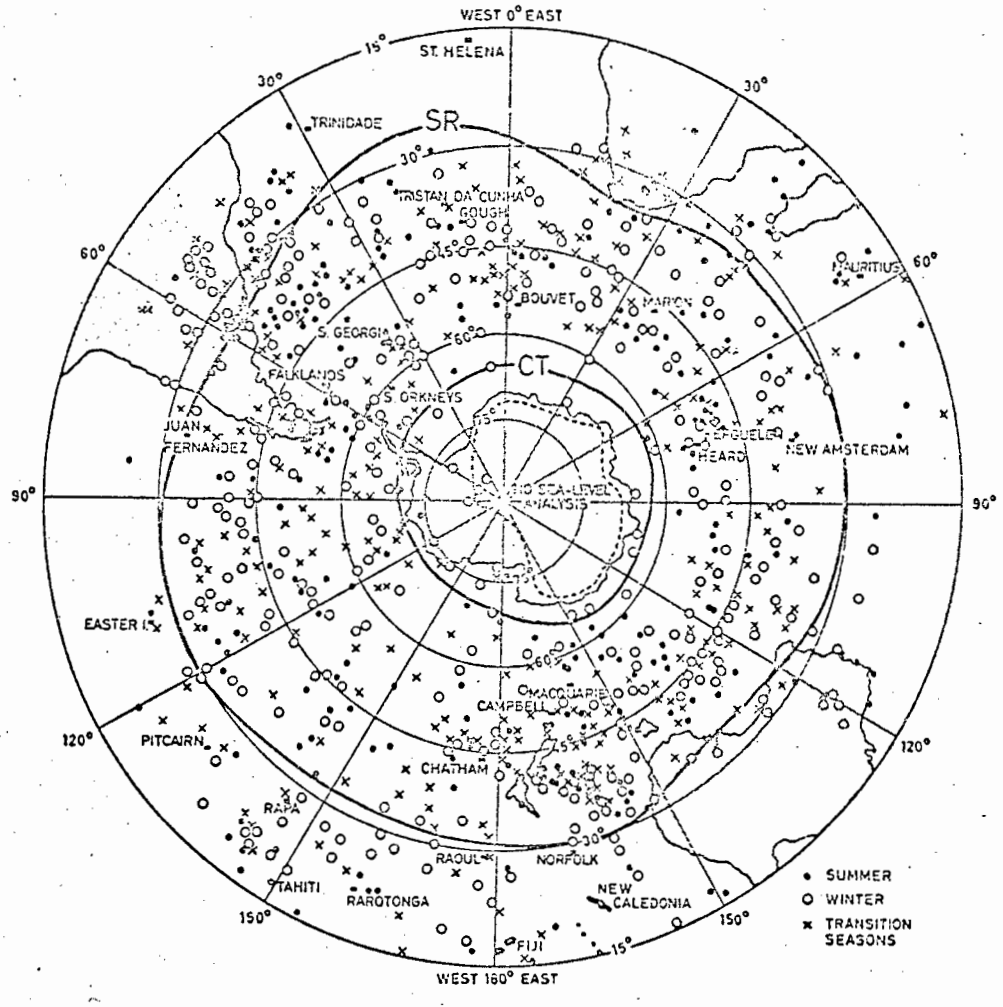

Fig. 2.2. Distribution of cyclogeneses (individual cases) during the IGY (compiled from data in Taljaard, 1967). SR is subtropical ridge and CT circumpolar trough.

orientation from (22°S, 55°W) to (40°S, 20°E) near Cape Town. A minimum area for cyclogenesis occurred between the Falkland Islands and Gough Island in winter. A frequent belt of cyclones extended from Paraguay to Tristan da Cunha as substantiated by shipping, but disappeared in spring.

In winter, the tracks of cyclones were ESE ward from Central - South America (at 23° - 35°S) past Gough Island (40°S, 10°W) and Marion Island (47°S, 38°E) off South Africa, (see figure 2.3). In October 1957, tracks of cyclones passing through the Drake passage continued almost due eastward until east of the Greenwich meridian where they turned southward until they disappeared in the "graveyard" off the Antarctica coast, south of South Africa.

In summer, a notable area devoid of cyclone tracks was the 20° of longitude south of South Africa, (see figure 2.4). This indicates the general southward migration of the cyclone belt in summer. The most predominant east and northward components of the cyclone tracks were found over the mid S.W. Atlantic ocean. The distribution of cyclone centres had a meridional maximum at 55°S but also increased steadily from 35° - 55°S.

Taljaard (1967) reaffirms most of the above results and indicates that cyclogenesis was most frequent at latitude 45°S in all seasons, and more frequent between 25° - 40°S in winter than in summer.

The SAWB now receives meteorological data regularly from the following stations in the Atlantic ocean:

a) Tristan da Cunha island (37°S, 12°W);
b) Gough Island (40°S, 10°W);
c) F. H. Hughes weathership stationed at 40°S, 10°E;
d) Marion Island (47°S, 38°E)

A history of the weathership is given below.

In 1969, the SAWB chartered a whaler from the Union Whaling Company to act as a weathership at 40°S, 10°E. This ship was later replaced by the F. H. Hughes. Under normal conditions, the weathership would be on or

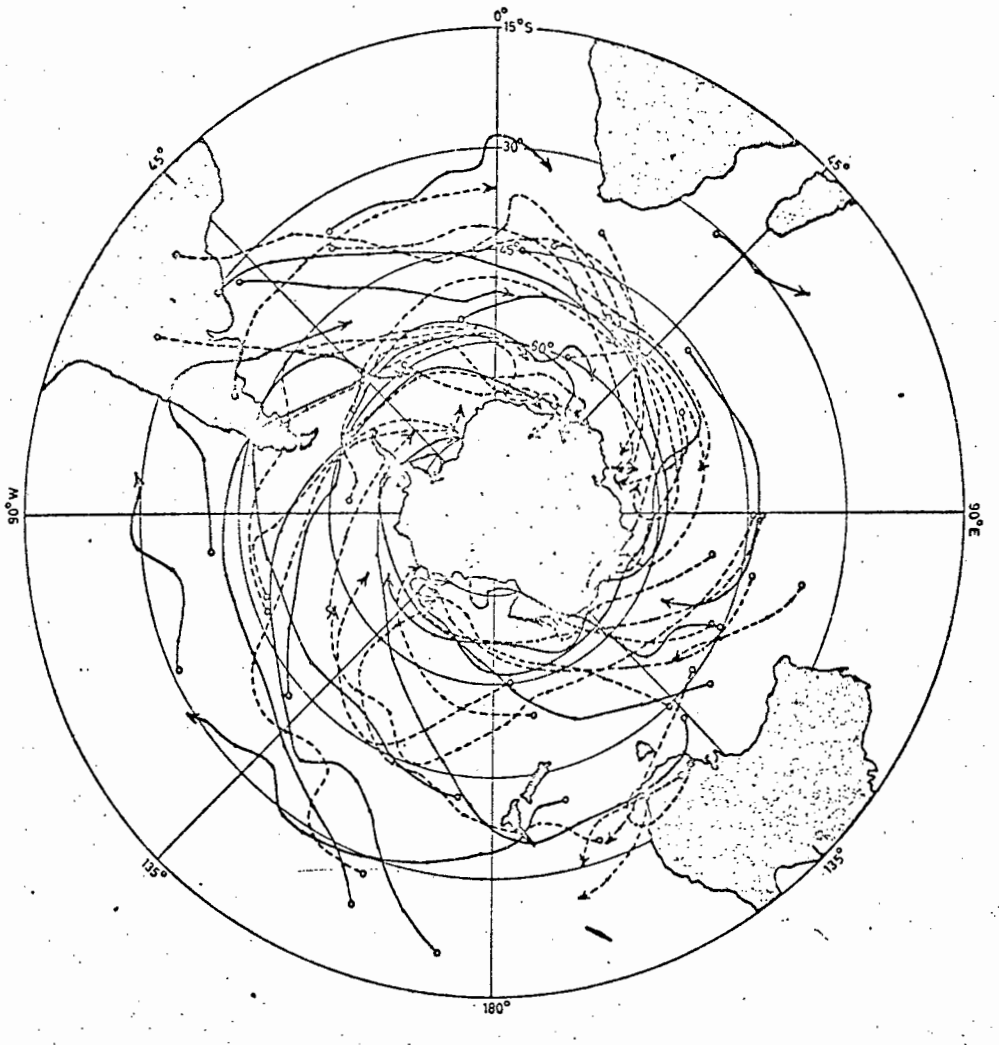

Fig. 2.3. Cyclone tracks for July 1957. (From Taljaard and van Loon, 1962.)

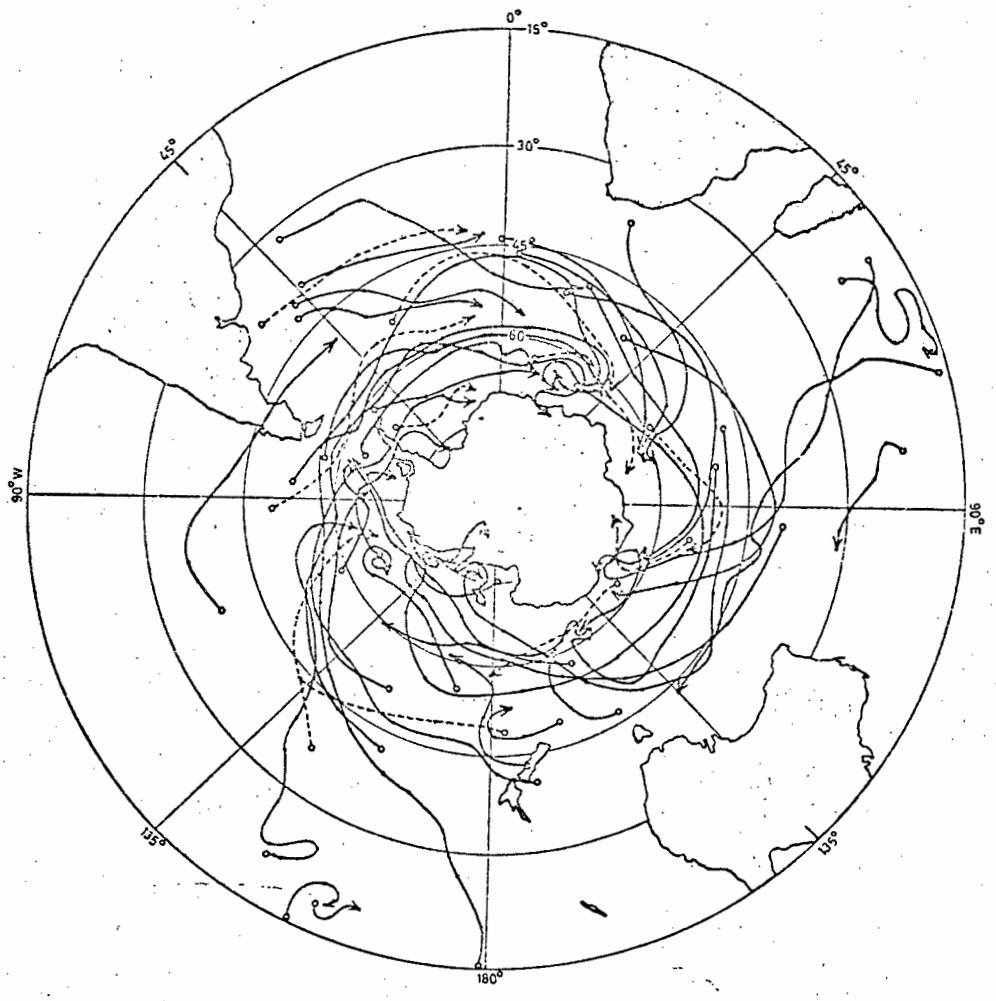

Fig. 2.4. Cyclone tracks for January 1958. (From Taljaard and van Loon, 1963.)

near its station point for three weeks of every month. Five days are spent in Cape Town taking on fuel and supplies. Sea surface temperature recordings are made while steaming to the site and these have been analysed to interpret the southern convergence. In 1970, an NIO shipborne wave recorder was installed on the F.H. Hughes, and regular six hourly wave recordings are now made.

The recent advances in satellite technology have had a profound effect on the quality of data now available to meteorologists in the Southern Hemisphere. Satellite photographs of the South West Atlantic ocean are used on a regular basis by the SAWB for preparation of synoptic weather maps. Consequently the positions of warm and cold polar fronts can now be more positively identified from satellite information.

Whereas Taljaard and van Loon only had use of data from Gough Island, Tristan da Cunha Island, and expedition ships, Neal (1972) used data collected at these island stations as well as data from the weathership, and wide spread satellite coverage. Extensive data collection for meteorological use in the Southern Hemisphere has been made by the Global Atmospheric Research Program (GARP). Twice daily mean sea level analyses have been made from the GARP basic data set for November 1969 and June 1970 by Phillpot, Price, Neal and Lajoie (1971).

Neal (1972) has calculated frequency distributions for cyclone and anticyclone centres for these two months. For November 1969, Neal found that the dominant feature of cyclone centre distribution was a high frequency belt extending around the Hemisphere between 55^{o}S and Antarctica, (see figure 2.5). In the mid latitudes, a high frequency finger stretched out from Brazil into a high frequency belt in the South Atlantic ocean between 45^{o} - 55^{o}S. In lower latitudes, persistent heat generated "lows" were evident off the SW coast of South Africa.

Neal used the same definition of cyclogenesis as Taljaard and found that in both months of observation, as in Taljaard (1967) that cyclogenesis occurred

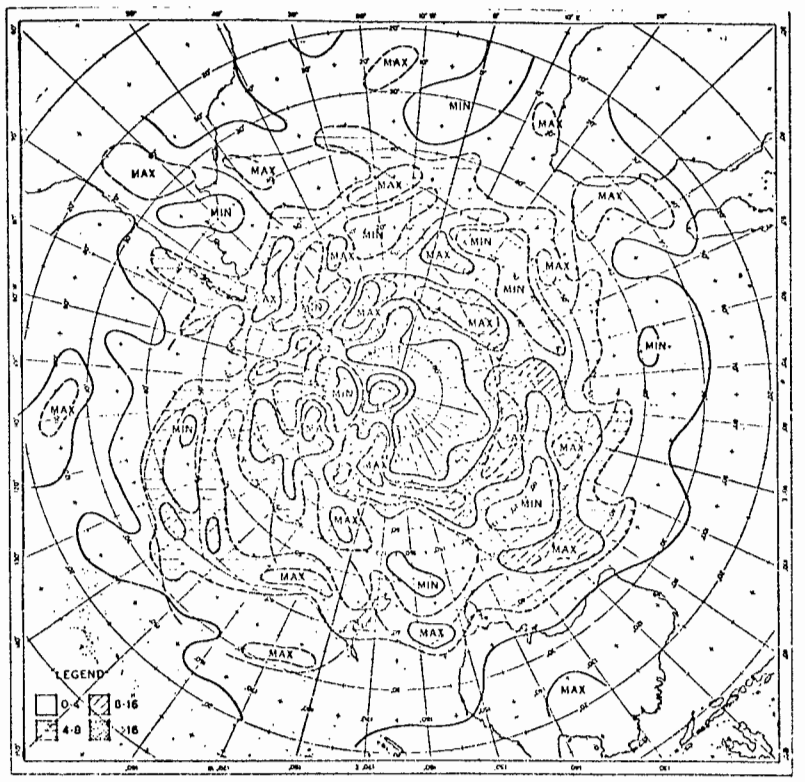

Fig. 2.5.

The normalised frequency distribution of cyclone centres in November 1969. Solid lines indicate major high frequency axes and dashed lines indicate minor high frequency axes.

The normalised frequency distribution of cyclone centres in June 1970. Solid lines are major high frequency axes. Dashed lines are minor high frequency axes.

(After Neal, 1972)

most frequently in mid latitudes between 35^{o} - 55^{o}S. Neal also reported several instances of cyclogenesis in subtropical latitudes (20 - 30^{o}S) in the South West Atlantic ocean west of 15^{o}W longitude.

According to Neal (1972), cyclone tracks can vary considerably in length, the largest measured being 7000 Km, and the lifetime of individual systems varied from twelve hours to ten days. It is of interest that from Neal's diagrams of cyclone tracks for November 1969, (see figure 2.6), that one cyclone lasting eight days followed a great circle path towards Cape Town passing through 50^{o}S. It ceased to exist before reaching 40^{o}S, 20^{o}E. This could, as will be later discussed, provide an ideal generator of ocean swell towards Cape Town.

The cyclone tracks for June 1970, showed that the majority of cyclone centres moved ESE past South Africa between latitudes 40 - 50^{o}S. Again one instance of a cyclone approaching Cape Town on a great circle path was noted.

Although the general circulation pattern of cyclone tracks of Neal (1972) and Taljaard (1967) are consistent, it must be remembered that different tracks can be followed by cyclones under different circumstances. Obviously many more similar studies must be made to consolidate the work of Neal and Taljaard.

Van Loon (1967) finds that the average velocities of the low pressure systems between latitudes 30^{o} - 40^{o}S, is 20,5 and 22,5 knots for summer and winter respectively. Further south, between latitudes 40^{o} - 50^{o}S, the velocities are higher - (28 to 29,5 knots). The importance attached to the speed of the "low" generating waves towards Cape Town will be further pursued.

Vowinckel (1954) found the frequency of frontal passages at Marion Island to be about two in five days. This is made up of the passage of three cold fronts in ten days, and one warm clear front in seven days.

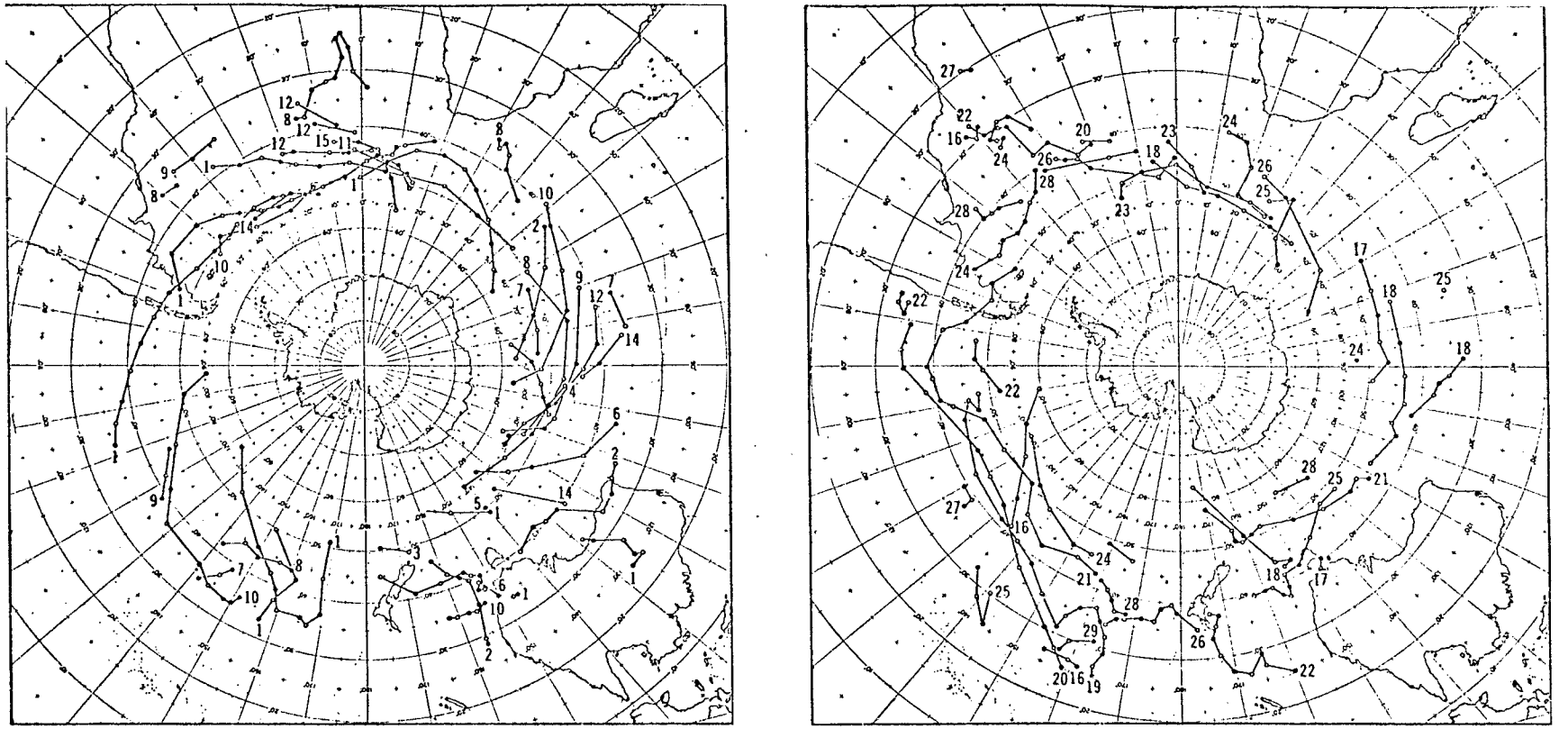

(A) 1-15 November

(B) 16-30 November

Fig. 2.6. Cyclone tracks from (20°S - 55°S) during November 1969 (After Neal 1972)

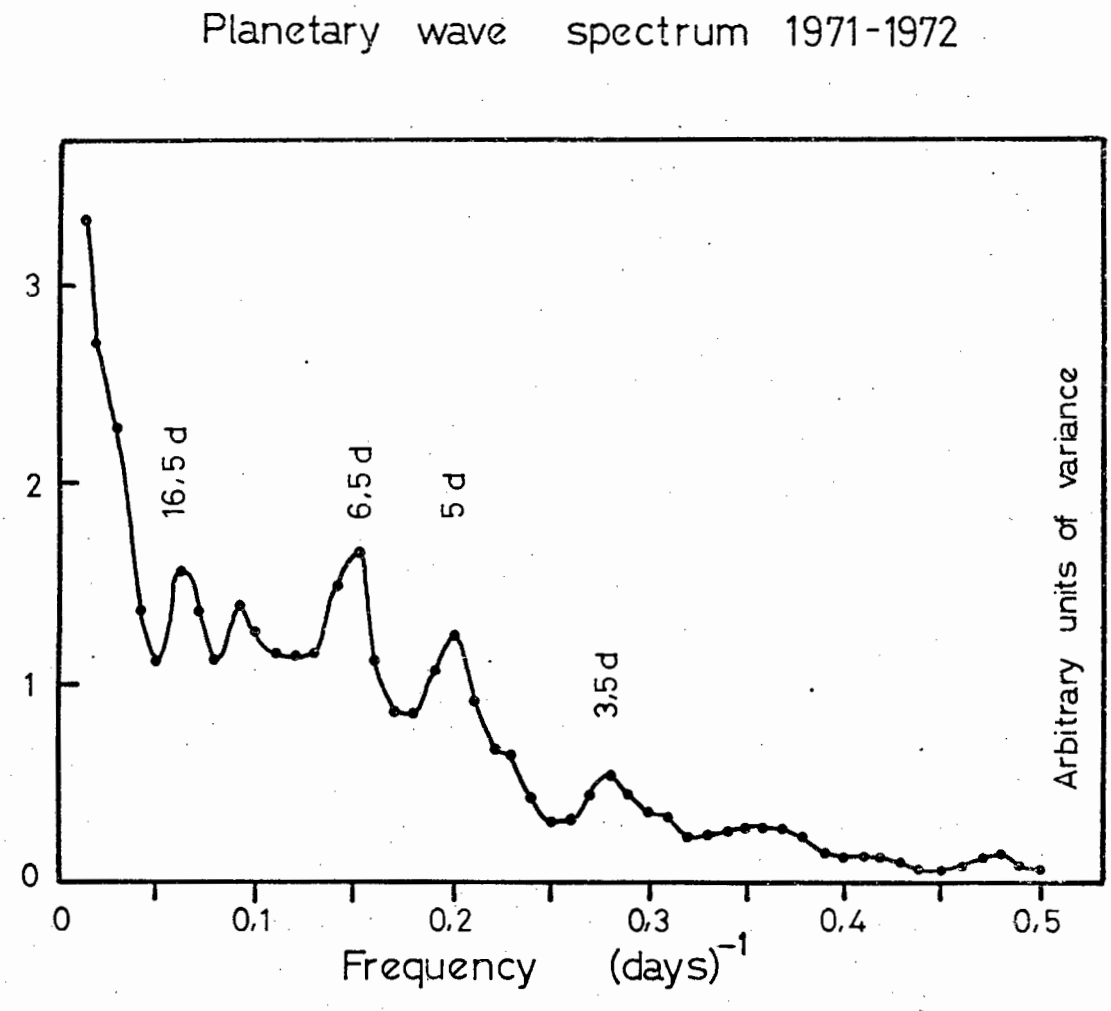

Fig. 2.7. Spectral distribution of frequencies of 1010 mb isobar excursion for 1971 and 1972 at longitude 10°E.

From spectral analysis of the excursion of the 1010 mb isobar along meridian 10°E, it has been found from research at the Insitute of Oceanography, U.C.T. (unpublished) that the frequency spectrum of the passage of "lows" past the Cape has peaks at periods of five, seven and seventeen days (see figure 2.7).

Taljaard (1972) classifies the frontal systems that affect the Cape as follows:

(a) the system that crosses the 20°E meridian between latitudes 30° - 40°S and subsequently moves SE on the poleward side of the semi-permanent Indian Ocean anticyclone.

(b) The systems which travel from La Plata across the South Atlantic ocean to the south of South Africa.

e) Geostrophic wind fields:

Van Loon (1972) gives figures for the zonal average geostrophic surface winds (see figure 2.8). The peak in the zonally averaged westerlies stays just south of latitude 50°S where the velocity is 14 m/s. At Cape latitudes (35°S) the average velocities are lower, about 5 m/s.

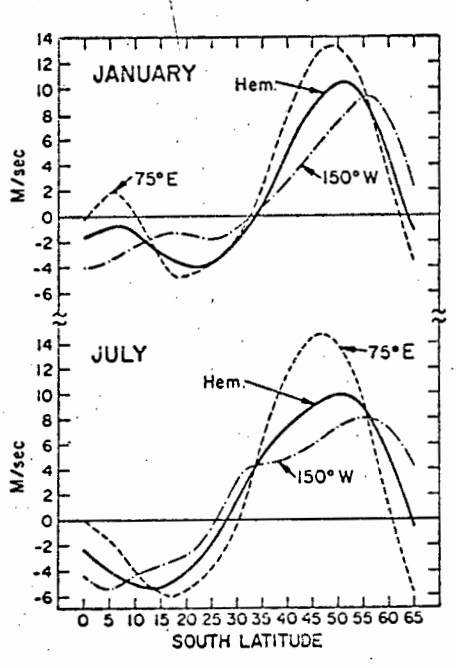

Fig. 2.8. Meridional profiles of the zonally averaged zonal geostrophic wind (m sec^{-1}) at sea level and profiles along 75°E and 150°W. North of 30°S the profiles are based on ships' winds. (After van Loon, 1972).

Harris, Marshall and Shillington (1972) explained the generation of waves at the Cape from fetches drawn in on SAWB synoptic charts at $\pm 30^{o}$ directions towards Cape Town. There appeared to be three major isobar patterns explaining the generation.

(a) long straight isobars stretching from N.W. to east across the South Atlantic ocean and ending on the South West Cape coast.

(b) the quickly moving and changing fetches associated with cyclones passing to the south of Cape Town.

(c) the short NW fetches associated with the heat generated coastal "lows" which travel down the South West African coast.

(b) has generated the largest waves measured to date, while (c) does not appear to be a significant cause of high waves at the Cape. Local South East winds do not have an appreciably large fetch associated with them, and are not a significant generator of any waves other than high frequency wind waves. However, for areas further north of Cape Town the above statement may not apply (for example near Lüderitz on the South West African coast).

The meandering nature of the surface pressure distribution, caused by the presence of cyclones on the polar front, results in a continual change of direction of the surface geostrophic winds. The general westerly orientation of the wind field is quickly changed from a short North Westerly direction to a long South Westerly direction.

This rapidly varying fetch orientation is the most likely cause of the very sharply pulsed nature of the wave energy arriving at the Cape. Non stationarity in wave energy is reflected also in the periodic variations measured by the meridional excursion of a specified isobar.

2.3 Classical wave analysis

Properties of surface waves generated by periodic impulses have been studied both empirically and analytically for a long time. A number of

simplifying assumptions can be made, depending on the nature of the fluid. Classical wave analysis, due mainly to Airy (see Lamb, 1932), has developed a number of relatively uncomplicated formulae.

Applications of the classical hydrodynamical equations were first made to ocean waves by investigators such as Cornish (1934). He attempted to verify that the velocity of surface waves obeyed the classical phase velocity equation. Cornish also made numerous investigations from ocean liners in order to deduce relationships between wind and wave velocity.

Some of the more useful classical hydrodynamical equations together with their underlying assumptions are presented below. Lamb (1932) gives a rigorous and elegant mathematical treatment of the problem, while Sverdrup, Johnson and Fleming (1942) or Kinsman (1965) give a more physically orientated version.

Airy theory

The waves are of very small amplitude, and infinitely long crested. The fluid is irrotational and the solution is of the first order. A disturbance of the form

$$\eta(x,t) = a \cos (kx - \sigma t) \qquad \ldots\ldots\ldots\ldots \quad (2.1)$$

a = amplitude, $k = \frac{2\pi}{L}$ - wave number, L - wavelength, $\sigma = \frac{2\pi}{T}$ - angular frequency, T - period

is propagated with phase velocity given by

$$c^2 = \frac{g}{k} \tanh (kd) \qquad \ldots\ldots\ldots\ldots \quad (2.2)$$

d - depth, g - acceleration due to gravity, c - phase velocity.

The dispersion relation is

$$\sigma^2 = gk \tanh (kd). \qquad \ldots\ldots\ldots\ldots \quad (2.3)$$

For practical purposes, (2.3) is replaced by the asymtotic form

$$\sigma^2 = gk, \qquad \ldots\ldots\ldots\ldots \quad (2.4)$$

when $d >> \frac{L}{4}$, (Cartwright, 1962). If the depth is small compared with the wavelength, $d \leq \frac{L}{200}$ then the wave train is non dispersive i.e.

$$c = \frac{\sigma}{k} = \sqrt{gd}. \qquad \ldots\ldots\ldots\ldots \quad (2.5)$$

The practical depth limit of shallow waves is $\frac{L}{20}$, which is used by most oceanographers (Kinsman, 1965).

A physical explanation, in terms of the orbital motion of the water particles, of the effect of shoaling water on the Airy wave was given by H. Jeffreys (Appendix to Cornish, 1934).

Sverdrup, Johnson and Fleming (1942) use classical formulae to describe ocean waves. Emphasising the restrictive assumptions, they apply the relations between wave lengths, periods and wave heights to the more conspicuous waves. Sverdrup and Munk (1947) devised the first wave forecasting system in terms of average wave heights, and periods. This work was motivated by the attempt to transport men safely through the surf zone in the second world war.

Group Velocity

An important implication of wave theory due to Cauchy and Poisson, is that waves of a certain period arrive at a specified location in space as if they had travelled from the disturbance centre with a velocity equal to that of the group velocity appropriate to that period.

The group velocity is given by

$$Cg = \frac{d\sigma}{dk}. \qquad \ldots\ldots\ldots\ldots \quad (2.6)$$

Because $\sigma = kc$ and $c = \left[\frac{g}{k} \tanh (kd)\right]^{\frac{1}{2}}$

$$Cg = \tfrac{1}{2}c \left[1 + \frac{2kd}{\sinh (2kd)}\right] \qquad \ldots\ldots\ldots\ldots \quad (2.7)$$

In deep water, $Cg = \frac{1}{2}c$ and in shallow water $Cg = c$.

An attempt to check that surface ocean gravity waves travel at their group velocity (depending in turn upon their period) was made by Barber and Ursell (1948). Their results agreed to within 5% of the value given by the hydrodynamical equations. Barber and Ursell (1948) successfully linked up generation centres on meteorological maps with storm fetches which were at distances calculated according to group velocities of waves.

The manner in which they did this was to construct a wave propagation diagram. The ordinate represents time and the abscissa gives the distance of the storm fetch from the measuring station. Waves of period T_1 are designated by (o,t_1) and waves of period T_2 by (o,t_2). The previous histories are designated by lines drawn with a slope equal to the appropriate group velocity of the period considered. An improved method of plotting this data is discussed later.

Coriolis deflection

When identifying storm fetches at great distances, it is important to know whether the waves are deflected by the Coriolis force. According to Sverdrup et al (1942) if the period of oscillation of the wave is short compared with the period of the earth's rotation, Coriolis forces can be neglected. This result is obtained by comparing wave particle accelerations with Coriolis force induced accelerations.

The Coriolis force is proportional to

$$(2\,\omega\,\sin\,\phi).\nu$$

where ω is the angular rotation of the earth,

ϕ is the angle of latitude,

ν is the horizontal velocity of the particle.

The horizontal acceleration of the wave particles is proportional to $\frac{2\pi}{T}\cdot\nu$ where T is the wave period. The ratio of the Coriolis force and wave acceleration is proportional to

$$(\frac{T}{2\pi})\ 2\,\omega\sin\,\phi. \qquad \ldots\ldots\ldots\ldots \quad (2.8)$$

If T_e is the period of rotation of the earth the ratio is

$$\frac{T}{Te} \cdot 2 \sin \phi = \frac{T}{12} \cdot \sin \phi, \quad (T_e = 24 \text{ hours.})$$

The Coriolis force is only important if T becomes of the order of one half pendulum day ($\frac{12}{\sin \phi}$ hrs).

Munk, Miller, Snodgrass and Barber (1963) found that wave sources were located as much as 0,1 radian to the left of generating areas as inferred from synoptic weather maps. This implied that possibly the Coriolis forces had deflected the wave propagation paths away from great circle paths. Backus (1962) showed that although the sense of the misalignment was correct, the discrepancy was too large by two orders of magnitude, to have been introduced by the earth's rotation.

In Figure 2.9 straight lines to Cape Town indicate possible great circle approaches of waves in high latitudes. Distances are marked in terrestrial degrees of latitude (1^o = 60 n.m. = 111 Km).

2.4 Spectral wave analysis

Theoretical approach

According to Kinsman (1965), wave analysis branched in a new direction, which was initiated by W.J. Pierson in 1952. Rice (1944, 1945) had developed statistical concepts for the analysis of noise problems in communications engineering and in 1949, J.W. Tukey applied these concepts to various practical problems.

Pierson's new approach to the wave problem assumed that the sea surface is composed of random fluctuations similar to the noise problem in electronics. The classical wave by wave treatment was to give way to finding statistics that would fully represent time series of sea surface observations.

A random process is one which is governed or described by probability laws. The exact representation of the process is non-deterministic. Most random

Fig. 2.9. Great circle paths to Cape Town as straight lines, with distances marked in terrestrial degrees (1^{o} = 60 n.m. = 111 km).

systems can be divided into three classes before an appropriate method of analysis can be applied.

a) Non-stationary, in which case one has to examine more than one ensemble of records to discover the laws of the process.

b) Stationary, which is time independent by definition, and one ensemble record will contain all the information.

c) Stationary and ergodic in which the ensemble averages may be replaced by time averages.

Most geophysical processes are assumed to be stationary and ergodic over the period of measurement.

So, the new approach to waves was to consider them as part of a random moving surface defined by a stationary Gaussian process (Cartwright, 1962).

To describe this Gaussian nature, Pierson (1955) introduces the concept of a stochastic type of integral

$$I = \int_0^1 f(\sigma) \sqrt{d\sigma} \qquad \ldots\ldots\ldots\ldots \quad (2.9)$$

where $\sigma = \frac{2\pi}{T}$ - angular frequency.

This integral is not to be used in the normal Riemannian sense, but as the integral of a probability governed function. Kinsman (1965) and Pierson (1955) describe the properties peculiar to this type of integral.

Pierson (1955) represents the waves arriving at a fixed point in space by a stochastic integral which in effect characterises the waves as having random amplitudes. The height of the sea surface $\eta(t)$ is given by

$$\eta(t) = \int_0^\infty \cos(\sigma t + \varepsilon(\sigma)) \sqrt{[A(\sigma)]^2 \, d\sigma} \qquad \ldots\ldots\ldots \quad (2.10)$$

$\varepsilon(\sigma)$ - random phase over σ - axis, $[A(\sigma)]^2$ - energy spectrum. The manner in which (2.10) is evaluated is determined by the partial summation

$$\eta(t) = \begin{cases} \text{Limit} \\ \sigma_{2r} \to \infty \\ \sigma_{2i+2} - \sigma_{2i} \to 0 \end{cases} \sum_{i=0}^{r} \cos\left[\sigma_{2i+1} t + \varepsilon(\sigma_{2i+1})\right] \sqrt{\left[A(\sigma_{2i+1})\right]^2 (\sigma_{2i+2} - \sigma_{2i})} \quad \ldots\ldots\ldots\ldots \quad (2.11)$$

where an ordered set of frequencies is chosen according to $\sigma_o < \sigma_1 < \sigma_2 \ldots\ldots < \sigma_{2r+2}$. If we suppose we have the value of $[A(\sigma)]^2$ in a deterministic sense, then we can plot its value at the frequencies σ_{2i+1}, with odd indices and multiply it by the difference $(\sigma_{2i+2} - \sigma_{2i})$. The square root of this quantity then gives in effect the amplitude of the sinusoid with frequency σ_{2i+1} whose phase is selected at random according to the probability of $\varepsilon(\sigma)$ given by

$$P(\alpha < \varepsilon(\sigma) < \alpha + d\alpha) = \frac{d\alpha}{2\pi}, \text{ for } o < \alpha < \alpha + d\alpha < 2\pi \quad \ldots\ldots\ldots\ldots \quad (2.12)$$

If the integral in (2.10) from zero to infinity is bounded, then equations (2.10) and (2.11) represent a stationary Gaussian process in one dimension.

The frequency spectrum $[A(\sigma)]^2$ is a non-negative function of frequency defined over zero to infinity so that the integral of this quantity represents the energy of the wave system, (to within a defineable constant).

$$\int_o^\infty [A(\sigma)]^2 \, d\sigma = E \quad \ldots\ldots\ldots\ldots \quad (2.13)$$

The spectral function $[A(\sigma)]^2 \, d\sigma$ represents the potential energy in the band $d\sigma$.

Longuet-Higgins (1957) proposed another linear model of the stationary Gaussian process which is realised by the sea surface. The displacement of the surface with time is composed of an infinite number of sinusoidal wave components with random phases and amplitudes,

$$\eta(x,t) = \sum_{n=1}^{\infty} a_n \cos(k_n x - \sigma_n t + \varepsilon_n) \quad \ldots\ldots\ldots\ldots \quad (2.14)$$

k_n - wave number, ε_n - random phase

The wave number k_n is densely distributed over $o < k_n < \infty$ and ε_n is randomly chosen from $(0, 2\pi)$. The energy in a particular frequency band is related to the amplitudes of the sinusoids by

$$E(\sigma)\, d\sigma = \sum_{\sigma}^{\sigma+d\sigma} \tfrac{1}{2} a_n^2 \qquad \ldots\ldots\ldots\ldots \quad (2.15)$$

From (2.13) and (2.15) we have that the Pierson amplitudes $[A(\sigma)]^2$ are equivalent to $2E(\sigma)$ in the Longuet-Higgins model.

From the discussion of the stochastic representation of the sea surface, it is clear that a thorough understanding of the nature of the waves implies a knowledge of the energy spectrum $[A(\sigma)]^2$. Neumann filled this gap with visual observations of waves from the M.S. Heidelberg. An outline of Neumann's procedure is given below according to Kinsman (1965).

$\tilde{T}$ denotes the deep water wave periods. Using a Fourier type description, if a period $\tilde{T}_1$ is observed, it must have been generated by in phase Fourier components $(\tilde{T}_1 - \frac{\Delta T}{2}, \tilde{T}_1 + \frac{\Delta T}{2})$ where the value of ΔT may not be a constant. The height of the wave H* will provide a measure of the energy associated with it.

Neumann then plotted values of $\log_e (\frac{H^*}{\tilde{T}^2})$ vs $(\frac{\tilde{T}}{U})^2$ where U is the wind speed for which the waves were considered to be fully developed. The marked result was that the graph had a distinct upper bound on $\log_e (\frac{H^*}{\tilde{T}^2})$ for each $(\frac{\tilde{T}}{U})^2$. See figure (2.10). This bound was given by

$$H^* = K_1 . \tilde{T}^2 . \exp\left[- (\frac{gT}{2\pi U})^2 \right]. \qquad \ldots\ldots\ldots\ldots \quad (2.16)$$

By formally squaring (2.16), we obtain the proportion of energy $(H^*)^2$ in a band ΔT. As ΔT is reduced, the number of components entering $(H^*)^2$ is reduced which implies that the constant K_1^2 tends to zero i.e.

$$K_1^2 = K_2 . dT \qquad \ldots\ldots\ldots\ldots \quad (2.17)$$

Thus

$$(H^*)^2 = K_2 . dT . T^4 . \exp\left[-2 (\frac{gT}{2\pi U})^2 \right] \ldots\ldots\ldots\ldots \quad (2.18)$$

where $\tilde{T}$ has become T since we now have a true spectral period. We can

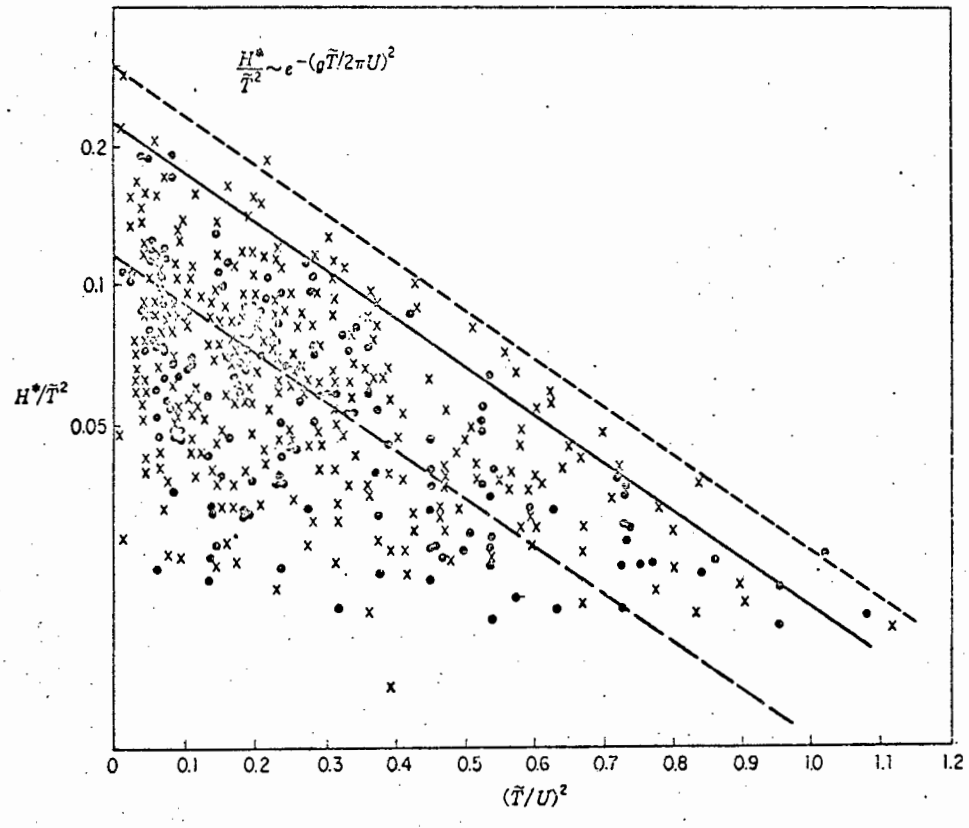

Fig. 2.10. Data supporting the Neumann spectrum as an upper bound. (From Pierson (1955)).

transform (2.18) into the frequency domain as follows:

$$\sigma = \frac{2\pi}{T}, \quad dT = -2\pi\sigma^{2}\, d\sigma, \quad C = -4(2\pi)^{4} K_{2}$$

$$\text{so} \qquad (H^{*})^{2} = [A(\sigma)]^{2}\, d\sigma = C.\frac{\pi}{2}.\ \sigma^{-6}.\ \exp\left(\frac{-2g^{2}}{\sigma^{2}U^{2}}\right) d\sigma \qquad \ldots (2.19)$$

An interesting feature of (2.19) is the sixth power dependence of the energy on the inverse of frequency. This implies that the constant is dimensional. Also, by integrating (2.19) from $o \longrightarrow \infty$, we see that the energy is proportional to U^{5} or wave height is proportional to $U^{5/2}$.

$$E = \int_{o}^{\infty} [A(\sigma)]^{2}\, d\sigma$$

$$= \int_{o}^{\infty} C.\ \frac{\pi}{2}.\ \sigma^{-6}.\ \exp\left[\frac{-2g^{2}}{\sigma^{2}U^{2}}\right] d\sigma$$

$$= 3.C.\ \left(\frac{\pi}{2}\right)^{3/2}.\ \left(\frac{U}{2g}\right)^{5} \qquad \ldots\ldots\ldots\ldots \quad (2.20)$$

Research workers have subsequently investigated the dependence of wave height on wind velocity and Darbyshire (1955) has evidence to support a U^{2} dependence of wind velocity with significant wave height. A different dependence of wind velocity on wave height implies a different spectral form.

Many workers have tried to evaluate the exact spectral form for waves. Darbyshire (1952, 1955, 1956a) has proposed an empirical wave spectrum to fit wave data collected in the North Atlantic ocean. A critical comparison of the different spectral shapes, including the form proposed by Roll and Fischer (1956), with the Neumann spectrum, as well as with the observations of the experiment SWOP, is given by Neumann and Pierson (1957). However as shown by Walden (1963) at the Easton conference on wave spectra, the problem has not been completely solved.

Phillips (1958) has argued that on dimensional grounds a fifth power dependence of energy on inverse wave frequency is more likely. His spectrum in the equilibrium range has the following shape:

$$\Phi(\sigma) \sim \alpha g^2 \sigma^{-5}, \quad \sigma_s < \sigma < \sigma_\gamma \qquad \ldots\ldots\ldots\ldots \quad (2.21)$$

The lower limit σ_s of the equilibrium range varies with fetch and wind duration while σ_γ, the upper limit is defined by the frequency at which the surface tension affects the motion.

A dimensionally consistent similarity spectrum which depends only on g, U, the wind fetch F_x, and its duration T can be specified by

$$\Phi(\sigma, t, x^1) = \alpha g^2 \sigma^{-5} f\left(\frac{\sigma_o}{\sigma}, \frac{U}{\sigma_o F_x}, \frac{1}{T\sigma_o}\right) \ldots\ldots \quad (2.22)$$

where σ_o is the frequency of a wave that moves at the wind velocity U ($\sigma_o = \frac{g}{U}$). For a large enough fetch and duration (F_x, $T \longrightarrow \infty$) (2.22) reduces to the fully developed state given by

$$\Phi(\sigma) = \alpha g^2 \sigma^{-5} f\left(\frac{\sigma_o}{\sigma}\right) \qquad \ldots\ldots\ldots\ldots \quad (2.23)$$

Pierson and Moskowitz (1964) investigating waves produced by various wind strengths propose a function for f of the form

$$f\left(\frac{\sigma_o}{\sigma}\right) = \exp\left[-A\left\{\frac{\sigma_o}{\sigma}\right\}^n\right] \qquad \ldots\ldots\ldots\ldots \quad (2.24)$$

where A = 0,74, $\sigma_o = \frac{g}{U}$ with U measured at 19,5 m above sea level. The exponent, n, was tenatively chosen to have values 2, 3, 4, 5. n = 4 seems to have given the best agreement with observations.

Kraus (1972) points out that attempts to find the exact dependence of the spectra on measurable quantities may have been unsuccessful for three basic reasons; (a) the wind speeds do not remain constant, (b) conditions are often contaminated by wave radiation from other regions, and (c) linear theories may be inadequate to describe the non-linear world.

Hasselmann et al (1973) found for the North Sea that Phillip's constant α in fact was not constant and decreased with fetch.

b) Practical Calculation of Power Spectra

The techniques of generating power spectra from digital records are now well known. Originating in the field of communications engineering, power spectrum analysis is now applied to economic as well as scientific problems. The following method for estimating the spectrum from the data is due to Blackman and Tukey (1958).

The first step is to form the autocovariance function from the original time series. Assuming zero mean, the autocovariance function $c(\tau)$ is defined in terms of ensemble averages by

$$c(\tau) = \langle x(t).\ x(t+\tau) \rangle \qquad \ldots\ldots\ldots\ldots \quad (2.25)$$

If the system is stationary and ergodic over the period of measurement, (2.25) can be replaced by the time averages for the record,

$$c(\tau) = \underset{T \to \infty}{\text{Limit}} \frac{1}{T} \int_{\frac{-T}{2}}^{\frac{+T}{2}} x(t).\ x(t+\tau)\, dt \qquad \ldots \quad (2.26)$$

The auto correlation function is the normalised form of (2.26) viz. $\frac{c(\tau)}{c(o)}$. The power spectrum is then defined by the cosine transform of the auto-covariance function:

$$\Phi(\sigma) = \int_{-\infty}^{\infty} c(\tau) \cos(\sigma\tau)\, d\tau \qquad \ldots\ldots\ldots\ldots \quad (2.27)$$

In practice, one has to deal always with a finite record. If the record has N points the number of lagged products, m, taken in (2.26) is less than N. (2.26) becomes

$$c(\tau) = \frac{1}{N-\tau} \sum_{r=1}^{N-\tau} x(r).\ x(r+\tau) \qquad \ldots\ldots\ldots\ldots \quad (2.28)$$
$$\tau = 1, 2, \ldots m < N$$

The spectral estimates V_p at frequency $\frac{p}{2m\,\Delta t}$ where Δt is the time spacing of the original data, are given by a numerical approximation of (2.27), which using the trapezoidal rule and values of $c(\tau)$ from (2.28), gives

$$V_p = 2m\,\Delta t \cdot \frac{1}{m} \left[c(o) + 2 \sum_{r=1}^{m-1} c(r) \cos \frac{\pi p r}{m} + c(m) \right] \ldots \quad (2.29)$$

These spectral estimates can be smoothed by a number of techniques, one of which is known as "Hanning":

$$\begin{aligned} U_o &= 0,5\ (V_o + V_1) \\ U_r &= 0,25\ V_{r-1} + 0,5\ V_r + 0,25\ V_{r+1} \qquad 1 \leq r \leq m-1 \\ U_m &= 0,5\ (V_{m-1} + V_m)\,. \end{aligned} \qquad \ldots\ldots\ldots\ldots \quad (2.30)$$

When designing the data capture to be analysed by power spectrum methods, there are several important features to note. The process must be sampled at such a rate that there is no appreciable energy content in cycles with frequencies less than twice the digitised interval. If this criterion is not observed, aliasing will take place and high frequency components will be falsely reported at the low frequency end of the spectrum. This cutoff frequency is known as the Nyquist frequency and is equal to $\frac{1}{2\Delta t}$. This is the highest frequency truly represented. The band width or resolution of the spectral estimates is governed by the choice of the total lag number m. The band width is $\frac{1}{2m\Delta t}$ (Hz). However, as we are dealing with a probabilistic process, a very good frequency resolution leads to poor energy resolution and vice versa. A compromise is required and Kinsman (1965) gives $m \approx 0,1N$ as a rule of thumb value. This implies about twenty degrees of freedom (see later) and gives adequate energy resolution.

The confidence limits of each spectral estimate may be calculated assuming that these quantities are distributed as a fixed multiple of Chi - square for each frequency, p, $1 \leq p \leq \ldots \leq m - 1$. The degrees of freedom of a fairly level spectrum are given by

$$df = 2\left(\frac{N}{m} - \frac{1}{4}\right) \approx \frac{2N}{m}\,. \qquad \ldots\ldots\ldots\ldots \quad (2.31)$$

For the energy of zero lag, the degrees of freedom are approximately half of (2.31) and for a narrow spectral peak, the degrees of freedom are about one. Tables to calculate the confidence limits for the spectral estimates as a function of the number of df are given in Blackman and Tukey (1958) (p. 22).

For example, a data record of 1800 pts, $\Delta t = 1$ sec, $m = 100$ has 36 degrees of freedom. The true value of the estimates will lie in the range 0.75 - 1.43

times the computed value with 80% confidence.

TABLE 2.1

Spectral computation parameters of various workers

VALUE \ WORKER	Munk et al (1963)	Snodgrass et al (1966)	Cartwright (1971)	Harris et al (1972)
Record length	210 min	180 min	160 min	30 min
Δt (sec)	4	2	1	1
N	3000	5400	9600	1800
m	100	250	160	100
Δf (mHz)	1,25	1,00	3,125	5,00
Degrees freedom	60	43	120	36
80% conf. limits	0,81-1,30	0,77-1,37	0,85-1,20	0,75-1,43

2.5 Statistical wave analysis

It is difficult to derive statistical functions of wave heights theoretically unless the exact probability structure of the distribution governing the wave heights is known. If the wave records have been spectrally analysed as described in the previous section, then two interesting aspects of the analysis are present. One is the statistical distribution of the wave heights and various expectation values, while the other is the frequency distribution of energy which is described later.

Using the assumption that only a narrow band of frequencies is present and that wave energy arrives from a large number of sources in random phase, Longuet-Higgins (1952) was able to calculate three basic statistical ratios. These are,

(a) the ratio of the average of 1/p of N wave amplitudes in a record (written $a^{(p)}$) to the root mean square amplitude, $\bar{a}$.

(b) the ratio of the expectation of the maximum expected amplitude, $E(a_{max})$, to the rms wave amplitude, $\bar{a}$, as a function of the number of waves, N.

(c) the ratio of the most probable maximum wave amplitude, $U(a_{max})$, to the rms wave amplitude, $\bar{a}$, as a function of N.

The narrow spectral distribution of amplitudes leads to the use of a Rayleigh probability distribution for the amplitudes which is as follows,

$$P(a) = \frac{2a}{\bar{a}^2} . \exp\left(-\frac{a^2}{\bar{a}^2}\right) \qquad \ldots\ldots\ldots\ldots (2.32)$$

where

$$\bar{a} = \sqrt{\frac{a_1^2 + a_2^2 + \ldots + a_N^2}{N}} \qquad \ldots\ldots\ldots\ldots (2.33)$$

Average of upper 1/p waves

The mean value of 1/p amplitudes $a_1, a_2, \ldots . a_p$ that exceed a value r is given by

$$a^{(p)} = \frac{1}{p}\int_r^\infty r.P(r).dr \qquad \ldots\ldots\ldots\ldots (2.34)$$

The proportion p of amplitudes exceeding r is

$$p = \int_r^\infty P(r).dr = e^{-r^2/\bar{a}^2} \qquad \ldots\ldots\ldots\ldots (2.35)$$

So

$$\frac{a^{(p)}}{\bar{a}} = \frac{r}{\bar{a}} + \frac{1}{p}\int_r^\infty \frac{e}{\bar{a}}^{-r^2/\bar{a}^2} dr$$

$$\frac{a^{(p)}}{\bar{a}} = \sqrt{\log_e\left(\frac{1}{p}\right)} + \frac{\sqrt{\pi}}{2p}\left[1 - H\left(\sqrt{\log_e\left(\frac{1}{p}\right)}\right)\right] \ldots . \quad (2.36)$$

where

$$H(x) = \frac{2}{\sqrt{\pi}}\int_0^x e^{-\theta^2} d\theta \qquad \ldots\ldots\ldots\ldots (2.37)$$

Equation (2.36) can be evaluated for particular values of p, the most common values being p = 1, 3, 10, which are listed below

$$\frac{a^{1}}{\bar{a}} = 0,886, \quad \frac{a^{(3)}}{\bar{a}} = 1,416, \quad \frac{a^{(10)}}{\bar{a}} = 1,800 \quad \ldots\ldots\ldots\ldots \quad (2.38)$$

Maximum expected wave:

The expectation value of a variable is defined in terms of its probability density, f(x), by

$$E(x) = \int_{o}^{\infty} x.f\,(x).dx \quad \ldots\ldots\ldots\ldots \quad (2.39)$$

According to Longuet-Higgins the probability distribution of a_{max} is given by

$$N(1-\phi)^{N-1} \,.\, P \text{ where } P = -\frac{d\phi}{dr} \quad \ldots\ldots\ldots\ldots \quad (2.40)$$

and $\phi(r) = p = e^{-r^2/\bar{a}^2}$

Therefore

$$E(a_{max}) = \int_{o}^{\infty} r\,.\,P\,(a_{max})\,dr$$

$$= \int_{o}^{\infty} r.N.(1-\phi)^{N-1}.P.dr$$

$$= \int_{o}^{\infty} r.d\left[1 - (1-\phi)^{N}\right] \quad \ldots\ldots\ldots\ldots \quad (2.41)$$

On evaluating the integral (which is non trivial),

$$\frac{E\,(a_{max})}{\bar{a}} = \left[\log_e N\right]^{\frac{1}{2}} + \tfrac{1}{2}\gamma\left[\log_e N\right]^{-\frac{1}{2}} + \text{order}\left(\log_e N\right)^{-3/2} \ldots \quad (2.42)$$

γ = Euler's constant = 0,57722 ....

Maximum probable wave:

The alternative method of determining the maximum wave likely to be measured is to find the maximum of the probability distribution. We want

the maximum of

$$N.(1 - \phi)^{N-1}.P \text{ as defined in (2.40).}$$

i.e. maximum of

$$N.\left(1 - e^{-r^2/\bar{a}^2}\right)^{N-1} .e^{-r^2/\bar{a}^2}. \frac{2r}{\bar{a}^2} \qquad \ldots\ldots\ldots\ldots \quad (2.43)$$

By putting $\frac{r}{\bar{a}} = \theta^{\frac{1}{2}}$, $\frac{d}{dr} = \frac{2\theta^{\frac{1}{2}}}{\bar{a}} . \frac{d}{d\theta}$

and

$$\frac{d}{d\theta}\left[(1 - e^{-\theta})^{N-1} e^{-\theta} \theta^{\frac{1}{2}}\right] = o \qquad \ldots\ldots\ldots\ldots \quad (2.44)$$

will give the maximum probable wave. After differentiating and removing constants it can be shown that

$$\theta = \log_e N + o\left(\frac{1}{\sqrt{\log_e N}}\right)$$

or

$$\theta^{\frac{1}{2}} = \frac{U(a_{max})}{\bar{a}} = \sqrt{\log_e N} + o\left(\frac{1}{\log_e N}\right)^{3/2} \quad \ldots\ldots \quad (2.45)$$

The difference between (2.45) and (2.42) is seen to be the factor $\frac{1}{2}\gamma(\log_e N)^{-\frac{1}{2}}$. The following table shows the difference in the two method's results.

TABLE 2.2
(after Longuet-Higgins, 1952)

N	$\frac{E(a_{max})}{\bar{a}}$	$\frac{U(a_{max})}{\bar{a}}$
50	2.124	2.010
100	2.280	2.172
200	2.426	2.323
500	2.609	2.509
1000	2.738	2.642
2000	2.862	2.769

Subsequent papers, e.g. Draper (1963), have adopted the maximum probable amplitude and converted it to wave height.

Cartwright and Longuet-Higgins (1956) using concepts developed by Rice (1944, 1945) have given a general probability distribution for the maxima of a random function, without the restriction to narrow spectra.

The random function is represented by

$$f(t) = \sum a_n \cos(\sigma_n t + \alpha_n) \qquad \ldots\ldots\ldots\ldots (2.46)$$

where the frequencies σ_n are distributed densely on the interval (o, ∞) and the phases α_n are random and distributed uniformly between 0 and 2π. In any small frequency band

$$\sum_{\sigma}^{\sigma+d\sigma} \tfrac{1}{2} a_n^2 = E(\sigma)d\sigma \qquad \ldots\ldots\ldots\ldots (2.47)$$

where $E(\sigma)$, a continuous function of frequency is the energy spectrum of $f(t)$. The moments of $E(\sigma)$ about the origin are

$$m_n = \int_o^\infty E(\sigma)\, \sigma^n \, d\sigma \qquad \ldots\ldots\ldots\ldots (2.48)$$

The energy per unit length of record is defined by the zeroth moment

$$m_o = \int_o^\infty E(\sigma)\, d\sigma \qquad \ldots\ldots\ldots\ldots (2.49)$$

so that $m_o^{\frac{1}{2}} = \bar{a}$ from previously. The probability distribution of crest maxima ξ_m is dependent only on ε and $m_o^{\frac{1}{2}}$ as follows:

($\eta = \xi_m / m_o^{\frac{1}{2}}$ - ratio of crest maxima to $m_o^{\frac{1}{2}}$),

$$P(\eta) = \frac{1}{\sqrt{2\pi}} \left[\varepsilon . \exp\left(-\tfrac{1}{2}\left(\frac{\eta}{\varepsilon}\right)^2\right) + (1-\varepsilon^2)^{\frac{1}{2}} . \eta . \exp\left(\tfrac{1}{2}\eta^2\right) . \int_{-\infty}^{\frac{\eta}{\varepsilon}(1-\varepsilon^2)^{\frac{1}{2}}} \exp\left(\tfrac{1}{2}x^2\right) dx \right] \qquad \ldots\ldots\ldots\ldots (2.50)$$

where

$$\varepsilon^2 = 1 - \frac{m_2^2}{m_o m_4} \qquad \ldots\ldots\ldots\ldots (2.51)$$

The ratio of the maximum probable wave height, $H_{max} = 2\xi_m$, to the rms amplitude $m_o^{\frac{1}{2}}$ for the general distribution is derived from (2.50) in a similar way as (2.45) was derived from the Rayleigh distribution. The result, $U(H_{max})/m_o^{\frac{1}{2}}$, is dependent on N and ε as

$$\frac{U(H_{max})}{m_o^{\frac{1}{2}}} = 2^{3/2}\left\{\left[\log_e(1-\varepsilon^2)^{\frac{1}{2}}N\right]^{\frac{1}{2}} + 0.5\gamma\left[\log_e(1-\varepsilon^2)^{\frac{1}{2}}N\right]^{-\frac{1}{2}}\right\} \quad \ldots\ldots\ldots\ldots \quad (2.52)$$

γ is Eulers constant and ε as in 2.51. The limiting form with $\varepsilon = o$ reduces to the same expression as for the Rayleigh distribution, while a form for $\varepsilon \longrightarrow 1$ is also known, corresponding to the Gaussian distribution.

Cartwright and Longuet-Higgins (1956) show that the ratio of $\frac{a^{(p)}}{m_o^{\frac{1}{2}}}$ decreases with increasing epsilon and that the ratio of $\frac{U(H_{max})}{m_o^{\frac{1}{2}}}$ increases with epsilon for large N.

In practice, epsilon, which is interpreted as giving a measure of the rms width of the spectrum, can be calculated either from (2.51) or from

$$\frac{N_o^2}{N_1^2} = 1 - \varepsilon^2 \quad \text{where} \quad \ldots\ldots\ldots\ldots \quad (2.53)$$

N_o - average density of zero up crossings. N_1 - total density of maxima. Equation (2.53) can be made even more managable by letting T_o be average zero crossing period and T_c average crest period, where a crest is a point of f(t) which is a maximum, i.e. the water level falls on both sides of the crest. Then

$$\varepsilon^2 = 1 - \left(\frac{T_c}{T_o}\right)^2 \quad \ldots\ldots\ldots\ldots \quad (2.54)$$

Cartwright (1962) points out that a sensitive recording of the sea surface, as for example obtained by a surface wave recorder, may show high frequency ripples which increase m_4 relative to the other moments. This tends to give epsilon a value only just less than one. In this case, the best description of m_o is provided by ξ_m^2 which has expectation $m_o(2 - \varepsilon^2)$.

2.6 Extrapolation of measured statistics

In calculating wave statistics, the assumptions of stationarity and ergodicity are usually made for the duration of the recording. Over a long period of time these assumptions may not hold. Considering then that the period of actual measurement is only a small fraction of the total time inbetween records, it may be desirable to extrapolate the measured statistics to these longer periods. The following technique of estimating the value of the highest wave that is likely to occur in a given time interval is due to Draper (1963). Suppose half hour recordings are made every twelve hours. The value of the maximum wave height measured in the half hour, H_{max} (measured) is used to estimate the value of the maximum wave height in the twelve hour interval, H_{max} (12 hrs.). First, an approximate average zero crossing period, T_o must be known for the record. Then the total number of waves in the twelve hour period will be

$$N_{12} = (12 \times 60 \times 60)/T_o \text{ where } T_o \text{ is in seconds.}$$

Entering Table 2.3 at N_{12} then gives the ratio of the most probable maximum wave height to the rms wave height (H_{max} (12 hrs.): H_{rms}).

For example, assuming $T_o = 9$ seconds,

$$N_{12} = \frac{12 \times 60 \times 60}{9} \approx 5000$$

Then

$$H_{max} \text{ (12 hrs.): } H_{rms} = 8,28$$

Since there are $\frac{30 \times 60}{9} = 200$ waves in the 30 minute record,

$$H_{max} \text{ (12 hrs.)} = 1,26\ H_{max} \text{ (measured)}$$

TABLE 2.3

Ratio of most probable maximum wave height $U(H_{max})$ to H_{rms}, varying with the number of waves, N. (after Draper, 1963)

N	$U(H_{max})/H_{rms}$
10	6,14
200	6,57
500	7,09
1000	7,47
2000	7,82
5000	8,28
10000	8,61

CHAPTER 3

3.1 Description of the field site

The wave recordings presented in this thesis were made from a sea tower situated at latitude 33° 40',7S and longitude 18° 25',1E of Greenwich. Figure (3.1) shows the site in relation to the Cape Peninsula. The tower is at a point 28 Km north of Cape Town and 1 Km offshore near the village of Melkbosstrand. The mean sea level at the tower is 13m above the sea bottom. Ocean gravity waves arriving from the Atlantic Ocean can be measured in the sector between 202° and 312°E of true North. The cutoff at 202° in the south is due to Robben Island, 15 Km distant. The cutoff of 312°E in the north is due to Dassen Island, 40 Km away. A very narrow open passage for waves exists between Dassen Island and the mainland. This is considered to be unimportant.

The symmetrical shape of the bay near Melkbosstrand indicates that the net wave energy approach is normal to the average coastline direction. Darbyshire and Pritchard (1966) shows the predominant wave direction in this area to be from the South West. A perpendicular line from the beach is at 248°E of true North and the sea bottom slopes downward uniformly at an average gradient of 1:150 (Van Ieperen, 1970). Apart from isolated reefs, the sea bottom in this area is sandy and bathymetric charts show the bottom contours to be regularly spaced. A study of wave refraction diagrams by Van Ieperen (1970) (and unpublished) shows that minimal refraction effects are present between 230°E and 315°. Refraction may be important from a southerly direction, just before the cut off direction of 202°E is reached.

3.2 Sea Tower

The sea tower on which the wave recorder is mounted, was designed and erected by Christiani and Nielsen, Pty. Ltd. The central tube is 0,98 m in diameter and 20 m in length. The bottom of the tube is supported on a 17 m square, pyramidal shaped base, the corners of which have piles jetted into the sea bottom. A 3,9 m square cabin is attached to a flange on the top end of the tube, and houses the wave recorder, batteries and other

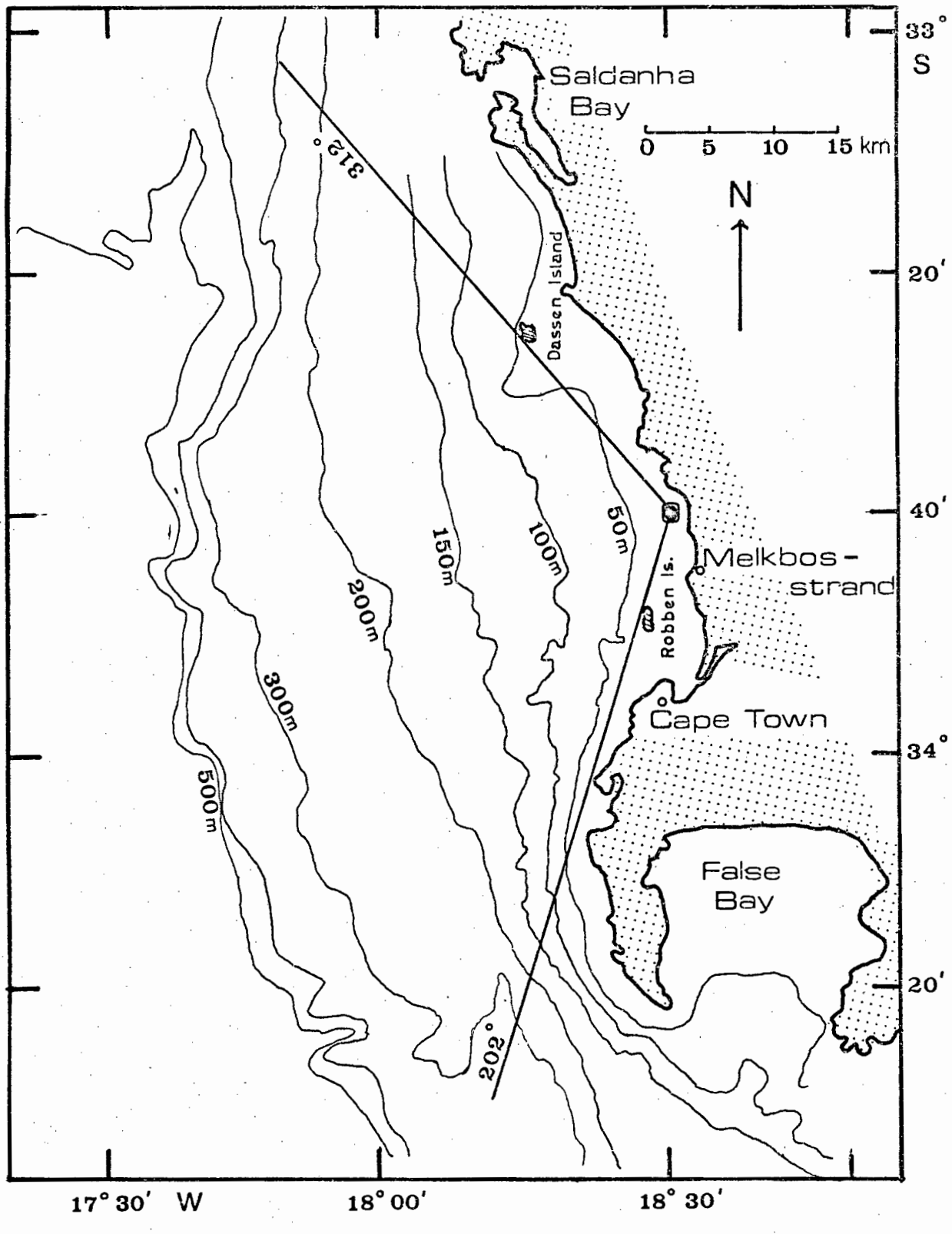

Fig. 3.1. Wave recorder site at Melkbosstrand.

tools necessary for maintenance.

In situ there is about 7 m clearance between mean sea level and the bottom of the cabin. A cat ladder welded to the central tube allows access to the cabin under most conditions. Because the ladder is on the western, seaward side of the tower, difficulty is sometimes experienced in boarding the tower in rough weather. An anemometer is attached to the top railing of the tower.

3.3 Wave Recorder

The wave recorder is a Wemelsfelder float operated wave height recorder, type W.R. 67 manufactured by Van Essen. It has a recording range of twelve metres. Although the main features of the recorder are described, full details are contained in Van Essen (1970).

The float, made of copper, weighing 1.5 Kg., has two nylon wearrings; one on either end, to protect the float from wear against the float tube. Float movement is transmitted to a drum by a nylon line which is kept taut by a counterweight. A reduction of ten to one is made from the float movement to the counterweight movement. Float movement is also reduced by 50:1 before the wave information is recorded.

The float tube, made of hot dipped galvanised steel, has an internal diameter of 130 mm. This tube is perforated with 30 mm diameter holes arranged in an ascending spiral so that the vertical distance from the centre of one hole and its nearest neighbour is 31 mm. The holes are spaced at 90^{o} intervals around the circumference of the tube.

The profile of the sea surface, as recorded by the float, is stored on a special waxed paper chart. Modifications to the wave recorder also allow digital wave heights to be telemetred ashore once per second for half hour records.

Breaks in the continuity of records are present due to equipment failure. During severe storms with maximum wave heights of the order of 5 m, the

float is unable to follow the wave profile exactly, because some waves break at and before the tower. Under these circumstances, the nylon line becomes entangled and the float breaks free.

3.4 Data storage - analogue and digital

An analogue record of the wave heights is stored on the waxed paper chart. The chart is driven by a small motor run by six 1.5 v dry cells. The trace on the chart is scratched by a ballpoint pen tip. Recordings can be initiated manually, or automatically as desired.

The present study uses records that are made with a chart speed of 1 mm per second with a duration of 30 minutes. Twice daily records are made automatically at twelve hour intervals. Because each record uses 1,8 m of paper, the waxed rolls have to be replaced every two weeks.

The 50:1 reduction from float movement to pen movement, implies that 1 mm of chart scale corresponds to 5 cm of wave height. One millimetre on the time axis corresponds to one second of time. Five centimetres of wave height is considered to be the resolution of the instrument.

An alternative data storage unit was designed and built by Diel, Pty., Ltd. A rotating, binary encoded disc allows wave heights to be stored in a solid state memory bank. These wave heights are then transmitted as a sequential pulsed signal every second to a shore station. At the shore station, a receiver decodes the signal and stores the information as a binary number on eight channel computer punch tape. The resolution of these wave heights, digitised at one second intervals, is 5 cm. These records, of half hour duration, are made at two hourly intervals.

Each computer punch tape record, 6 m long with 1800 characters is read into the U. C. T. Univac 1106 digital computer. The sequence of numbers is stored on disc and labelled according to the day and time the computer reads the tape. The values that are on disc can then be used for the various statistical calculations. A close check on the reliability of the digital information is

made by forming a five minute analogue signal from the radio information received at the shore. The digital signal is sometimes contaminated with spurious radio interference.

3.5 Computer handling of Data

Whenever the data stored on disc or magnetic tape is accessed, it is searched by a two pass scanning program that checks for spurious values. This check is achieved as follows. The mean and standard deviation of the record is calculated with all the original points. Each point is then checked against the value of four times the standard deviation. If the value of the point lies outside this range, it is replaced by the mean of its two neighbours. The record is then scanned a second time, the mean and standard deviation re-calculated, and points checked against a factor multiplying the standard deviation. In the second scan, the factor can be chosen, the usual value being 3,5.

The corrected record is then available as data for spectral calculations as outlined in Chapter 2, section 2.4. The output of the spectral computation program is in the form of a line printer graph. Numerical values of the smoothed energy densities can then be plotted on frequency time diagrams as will be discussed in Chapter 5, section 5.1.

A graph plotter subroutine is available to convert the digital values to an analogue record. This procedure is invaluable for studying the exact nature of telemetering errors that do occur in some of the records.

A statistical program is available for extracting maximum wave heights, upper one third heights, upper one tenth heights, as well as zero crossing periods and the ratios used in Chaper 2, section 2.6.

3.6 Analogue to Digital conversion

In order to glean the maximum information from wave records, it is necessary to have the wave heights in a digital format. That is to say, a time series of spot heights spaced at some interval Δt in time.

In this experiment, analogue to digital conversion is handled in two ways. Firstly, an electromechanical digitiser attached to the wave recorder converts the analogue recording to a digital series of wave heights at one second intervals. These wave heights are then transmitted to the shore station and recorded on eight channel computer punch tape. The second method employs a semi-automatic line follower which is used to make wave height measurements every millimetre on the analogue trace. The apparatus used in the Oceanography Department, U.C.T., was designed and built by Diel, Pty. Ltd.

The line follower is operated by following the wave in the y-direction with a movable cursor. Operating a small switch then automatically records the measurement on eight channel computer punch tape, and advances the record one millimetre (corresponding to $\Delta t = 1$ sec). An experienced user can digitise a half hour record (1800 readings) in forty-five minutes. Seventy-five analogue records were digitised on this machine for May and eight days in June 1973.

CHAPTER 4

The results of measurements made from thirty minute analogue recordings are presented in this chapter. The records, covering the period July 1972 - November 1973 have been used to obtain cumulative excedence curves of upper one tenth wave height and maximum wave height; histograms of zero crossing periods and spectral width parameter, epsilon; persistence information about duration of wave heights; design wave extrapolation; and statistical ratios for seventy five records in May and part of June 1973.

4.1 Time series of wave heights - 1972 - 1973

The twice daily analogue records for July 1972 to November 1973, excluding breaks due to equipment failure, were analysed for the maximum wave height H^1, which is defined as the vertical distance from the highest crest to the lowest trough in the half hour recording, and the average upper one tenth wave heights $H_{1/10}$. These two statistics are plotted as a time series in appendix 1 for all the available records.

4.2 Excedence curves of wave heights

From the time series of wave height measurements, percentage excedence curves of the number of times a given wave height was exceeded during the period July 1972 - June 1973 were calculated for both the average upper one tenth wave heights and the maximum wave height. These curves are shown in figure 4.1. The maximum heights can be multiplied by a factor depending on the period chosen (as discussed in Chapter 2, section 2.6) to determine the most probable maximum wave height in the twelve hour period when the wave recorder is not operating. In this case, assuming 9 second periods, H_{max} (twelve hours) = 1,26 H^1. The median of the curve gives $H_{1/10}$ = 1,5m, H^1 = 2,5m, H_{max} (12 hr.) = 3,2m

4.3 Histogram of zero crossing periods

To get the zero crossing periods from the half hour analogue records, the following procedure was used. A fifteen minute section was marked off, a

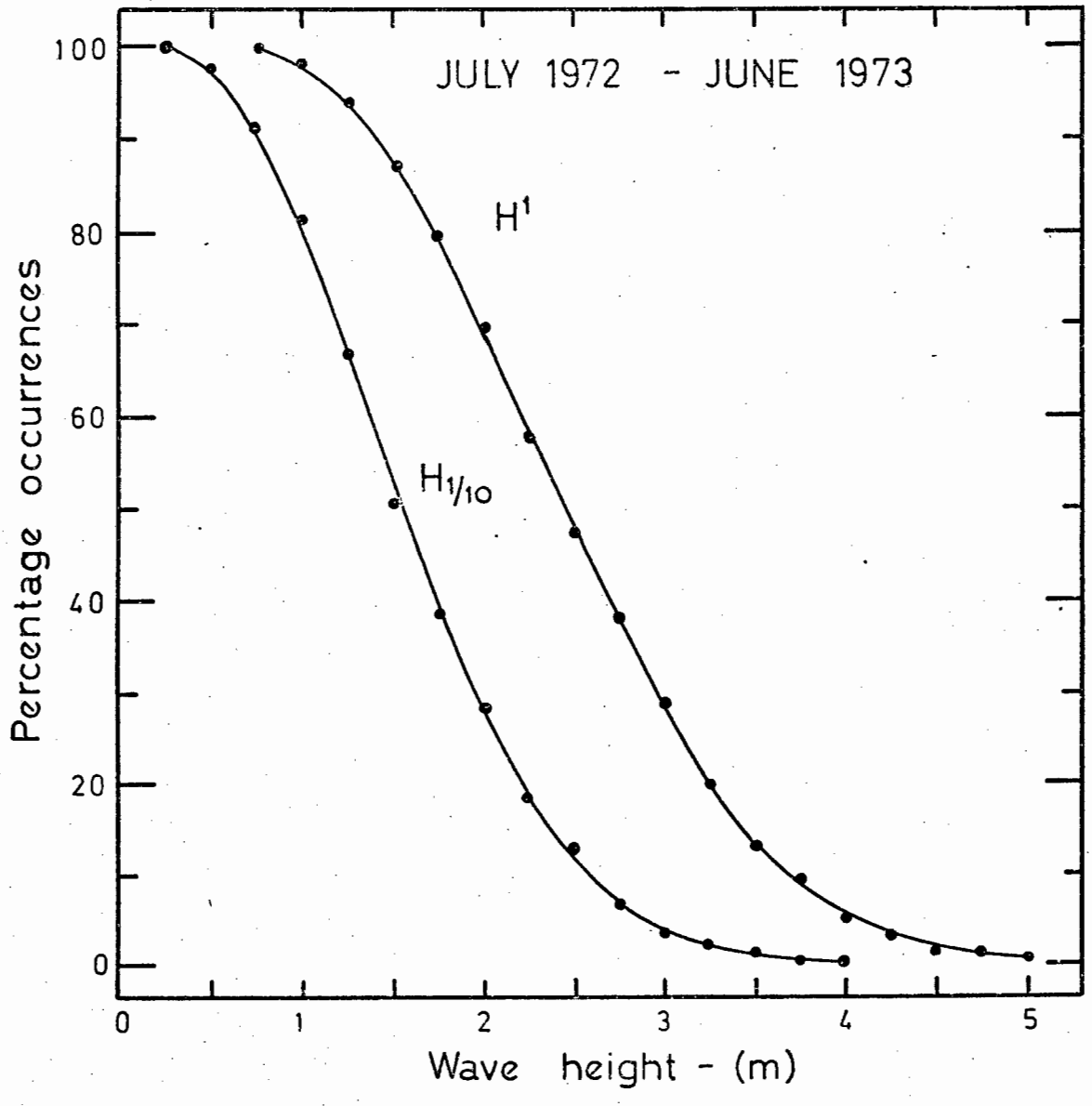

Fig. 4.1. Excedence curves of H^1 and $H_{1/10}$ for July 1972 - June 1973.

mean wave height line drawn in by eye, and the number of up crossings of this mean line noted for the fifteen minute period. These zero crossing periods were then grouped in one second intervals and graphed as in figure 4.2. Most common periods were from 6 - 11 seconds.

An attempt to distinguish between the distribution of zero crossing periods tabulated for different seasons was not considered to be meaningful.

4.4 Histogram of spectral width parameter, Epsilon

There are two equivalent ways of calculating the spectral width. One technique is to generate the zeroth, second and fourth moments from the spectrum, which are defined by (see equation 2.48);

$$m_n = \int_0^\infty E(\sigma)\, \sigma^n \, d\sigma$$

and then epsilon, the spectral width is given by (see equation 2.51):

$$\varepsilon^2 = \frac{m_o m_4 - m_2^2}{m_o m_4} .$$

An alternative method is to use a relation which involves measuring the crest period T_c and zero crossing period T_o. The crest period, T_c, is defined by the total number of crests (above and below the mean line) in the wave record, divided into the length of the record in seconds. Epsilon can then be calculated according to Cartwright (1962),

$$\varepsilon^2 = 1 - \left(\frac{T_c}{T_o}\right)^2 .$$

Figure 4.3 shows a histogram of occurrence of the values of epsilon for 1972-1973 calculated from T_c and T_o. A check on the values of epsilon was made by calculating it from the two different methods. The results were identical.

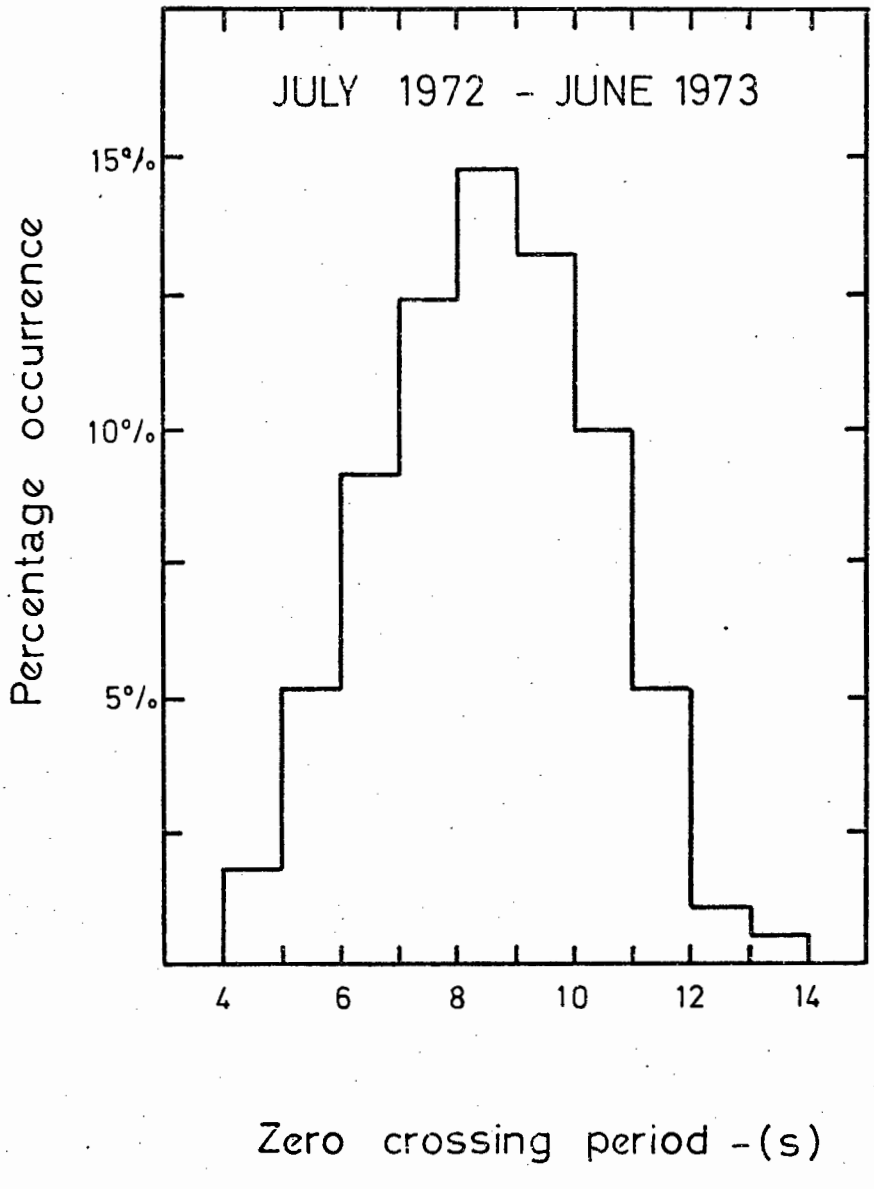

Fig. 4.2. Zero crossing periods for July 1972 - June 1973.

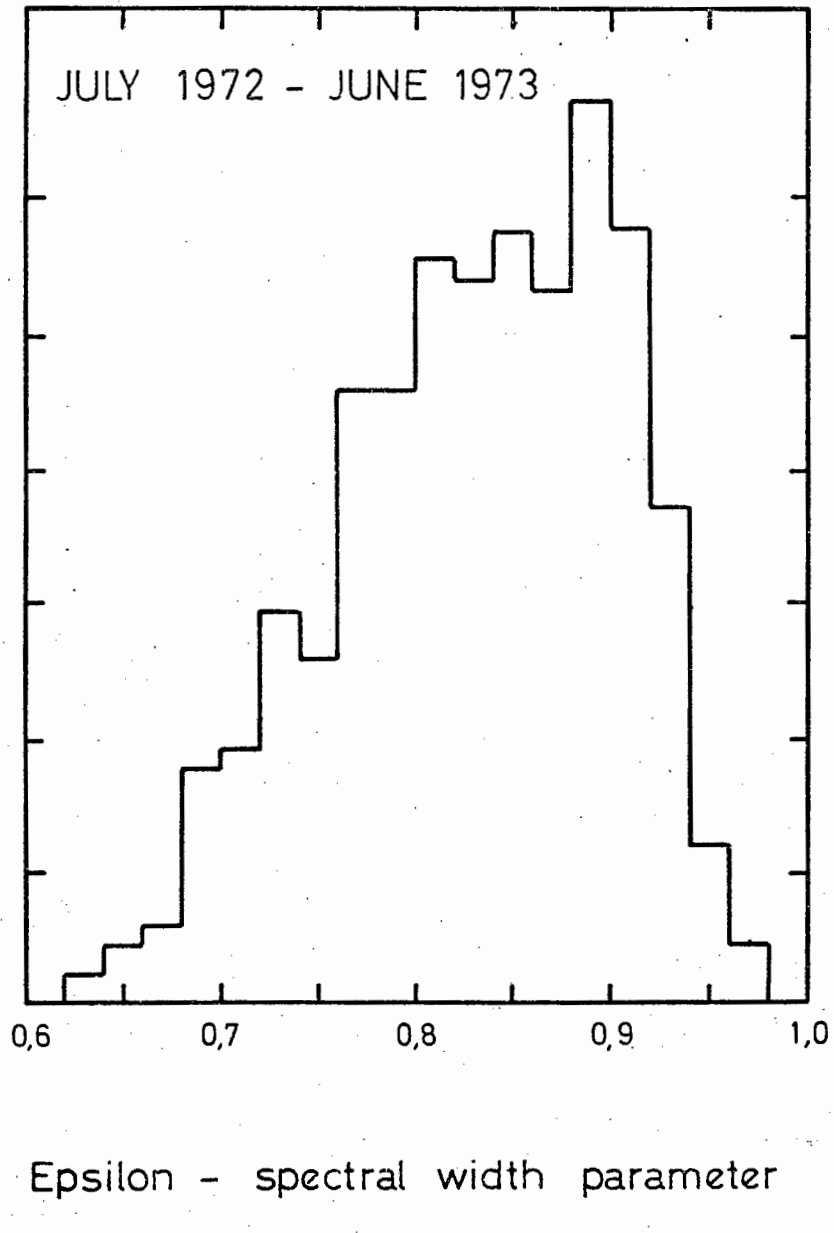

Fig. 4.3. Spectral width, epsilon for July 1972 - June 1973.

4.5 Wave height versus zero crossing period

A scatter diagram of upper one tenth wave heights versus zero crossing periods is given in figure 4.4. From this diagram it can be seen that the most common conditions were ones with average $H_{1/10}$ between 1 - 2m and T_o between 7 - 9 seconds.

Plotted on the same diagram are lines of wave slope, $\frac{H}{L}$, calculated from the classical equation

$$L = \frac{gT^2}{2\pi}\left[\tanh\ (\frac{2\pi d}{c\,T})\right].$$

The numerical figures were adapted from Shipley (1964) Table II.

4.6 Persistence information

From the time series of wave heights in appendix 1, duration periods for which upper one tenth wave heights were greater than or equal to 1,5m, 2,0m, 2,5m, and 3,0m were calculated. This data is plotted against a logarithmic time scale in figure 4.5. Entering the graph from the ordinate gives the number of occurrences during the year that the wave heights were greater than or equal to the value specified by the solid line curves. The duration is given for these heights on the abscissae.

4.7 Design wave information

If the maximum wave heights are known for a location for a period of time, an estimate of the highest wave most likely to occur in the future can be predicted. Darbyshire (1956b) has shown that by plotting the proportion of time for which a wave height is exceeded, against the wave height on logarithmic normal paper, a linear relationship is established. This can then be extrapolated to find the maximum height a wave might reach in say, ten years. In figure 4.6 the cumulative probability of waves exceeding a certain height is plotted on probability paper with a Weibull scale. An extrapolation is then made to estimate the maximum wave likely to occur in 10 years. This is 7,5m. The low value of this result is discussed later.

JULY 1972 - JUNE 1973

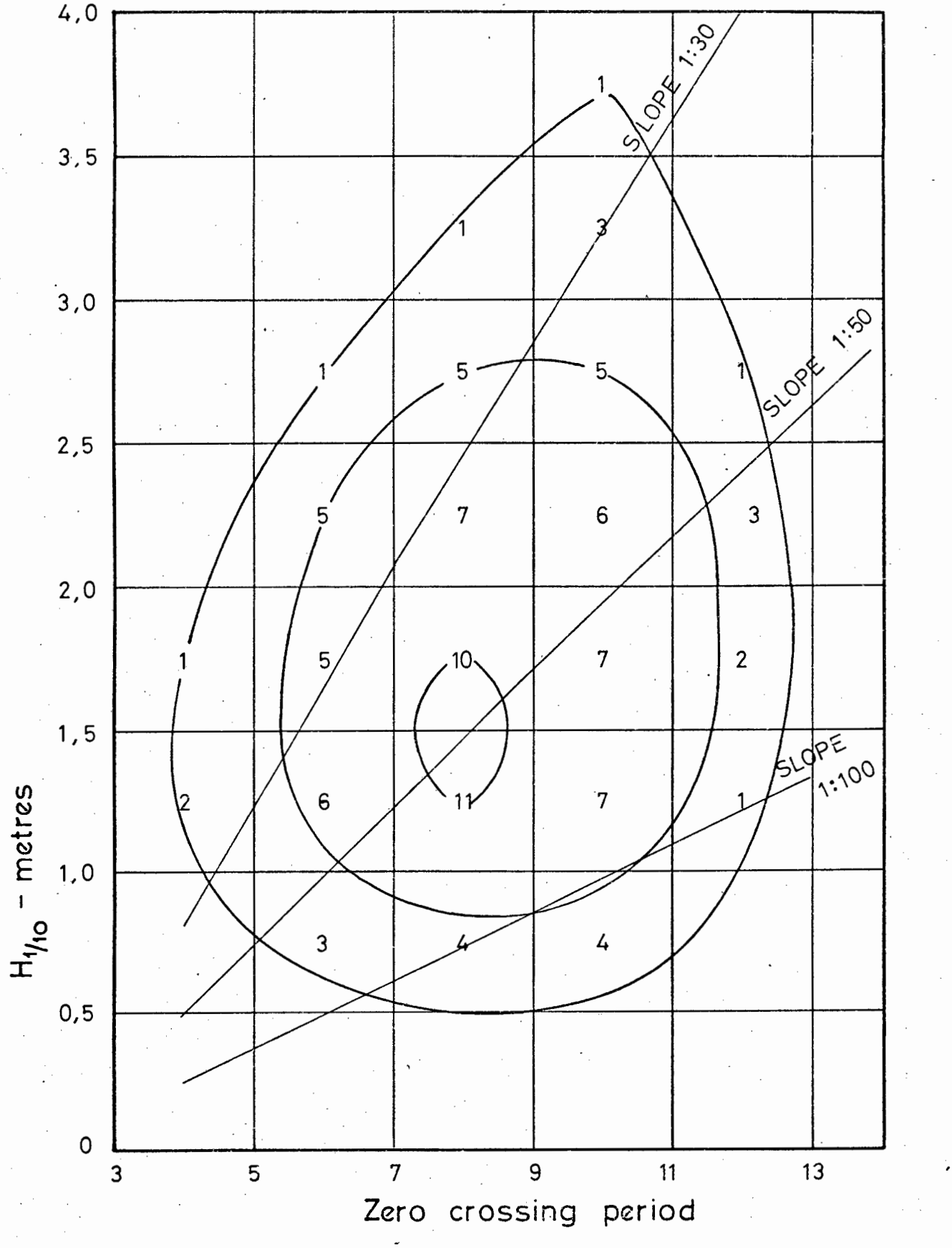

Fig. 4.4. Wave height, $H_{1/10}$, versus zero crossing periods, with lines of equal wave slope $\frac{H}{L}$.

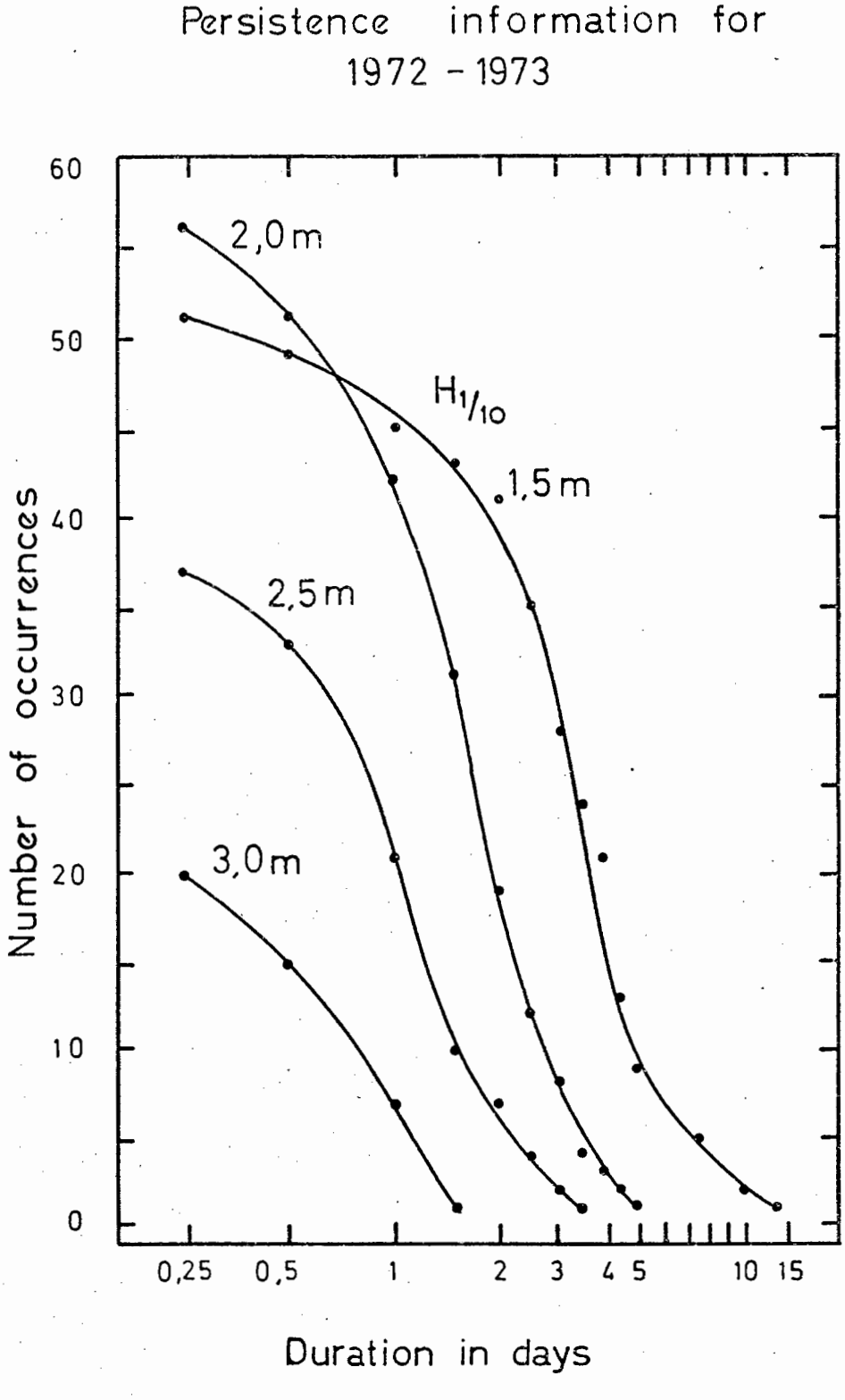

Fig. 4.5. Wave height persistence for July 1972 - June 1973.

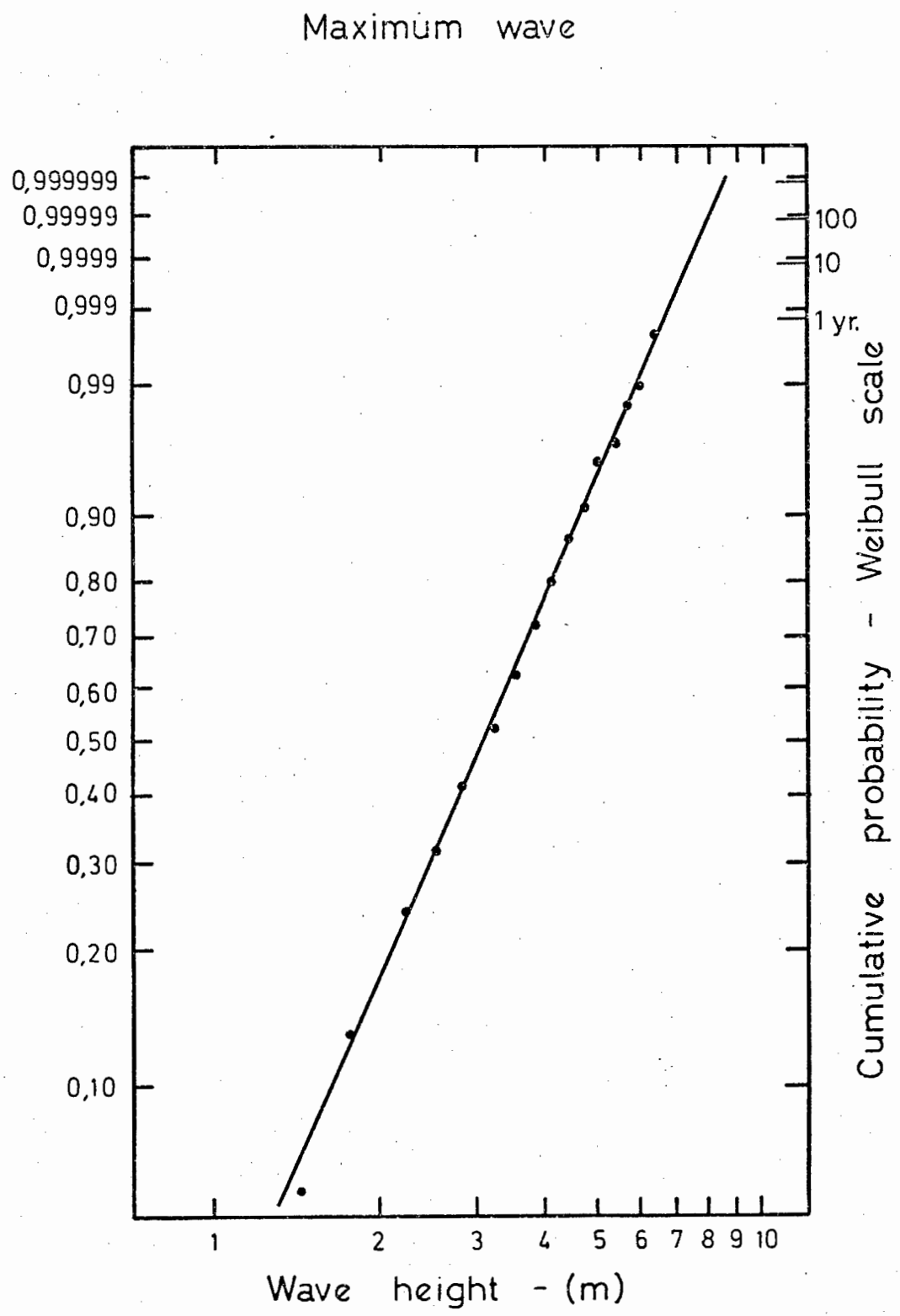

Fig. 4.6. Design wave extrapolation for July 1972 - June 1973.

4.8 Statistical Ratios for May 1973

As discussed in section 2.5, Longuet-Higgins (1952) proposed two methods for estimating the maximum wave amplitude divided by the rms amplitude. Wave amplitudes have in this section, been converted to wave heights and the tables modified accordingly, e.g. Draper (1963).

The conversion of $\frac{a_{max}}{\bar{a}}$ to $\frac{H_{max}}{H_{rms}}$ is as follows:

$$a_{max} = \tfrac{1}{2} H_{max}$$

$$\bar{a}^2 = \tfrac{1}{2} H_{rms}^2$$

so

$$\frac{H_{max}}{H_{rms}} = 2\sqrt{2^{-}} \cdot \frac{a_{max}}{\bar{a}}$$

Table 4.1 gives the variation of the ratios of expected maximum height to H_{rms} and most probable maximum height to H_{rms} for different numbers of waves.

TABLE 4.1

(adapted from Longuet-Higgins, 1952)

N	$\frac{E(H_{max})}{H_{rms}}$	$\frac{U(H_{max})}{H_{rms}}$
50	6,01	5,68
100	6,45	6,14
200	6,86	6,57
1000	7,38	7,09

Seventy-five half hour records for May and part of June 1973 were hand digitised once per second. From these records the maximum height, H^1, upper one tenth height $H_{1/3}$, and H_{rms} were measured. The values of the ratios:

$H^1 : H_{rms}$, $H^1 : H_{1/10}$, $H^1 : H_{1/3}$, $H_{1/10} : H_{1/3}$, $H_{1/10} : H_{rms}$, $H_{1/3} : H_{rms}$

were calculated. The hand digitised records have a scale resolution of $\pm$ 1 mm which corresponds to a height resolution of $\pm$ 5 cm. The response of the wave recorder also has this order of accuracy, so that scatter of the order of 10 cm of wave height has been assumed.

TABLE 4.2

Results compared with other workers

Worker	$\frac{H^1}{H_{rms}}$	$\frac{H^1}{H_{1/10}}$	$\frac{H^1}{H_{1/3}}$	Nº waves	$\frac{H_{1/10}}{H_{1/3}}$	$\frac{H_{1/10}}{H_{rms}}$	$\frac{H_{1/3}}{H_{rms}}$	$\frac{H_{1/10}}{\bar{H}}$	$\frac{H_{1/3}}{\bar{H}}$
Longuet-Higgins (1952) Theoretical	5,68	1,12	1,42	50					
	6,14	1,21	1,53	100					
	6,57	1,29	1,64	200	1,271	5,091	4,005	2,03	1,60
Watters (1953)	-	-	-	70-90	1,23	-	-	1,94	1,58
Bretschneider (1954)	-	1,32	1,62	-	1,23				
	-	1,24	1,58	-	1,27				
	-	1,39	1,7	-	1,22				
	-	1,38	1,76	-	1,28				
Darbyshire (1952)	5,66	-	-	120-180					
(1959a)	6,79	1,20	1,45	70-100	1,21	5,66	4,68		
(1959b)	6,51	1,24	1,60	70-100	1,29	5,25	4,07		
Shillington	6,15	1,37	1,65	160-300	1,20	4,47	3,71		

Notes:

(1) Longuet-Higgins' (1952) most probable maximum height has been used.

(2) Darbyshire (1952) used 20 – 30 minute wave records. Assuming T_o = 10 sec gives 120 - 180 waves.

(3) Darbyshire (1959a) is for 64 records free from swell, 7 - 10 minutes duration - if T_o = 6 seconds, 70 - 100 waves.

(4) Darbyshire (1959b) is similar to (3) except that it is for 84 coastal records.

No variation of the ratios with ε^2, the square of the spectral width parameter, was found. To gain a better understanding of the distribution of wave heights, a very narrow spectrum of twenty second period waves and two wider storm spectra of twelve second waves were fully analysed. The results are tabulated below, together with the theoretical values from Longuet-Higgins (1952), and the average values of the 75 records. The percentage error is calculated from (measured - theoretical)/theoretical.

TABLE 4.3a

Ratios independent of N

	$\bar{H}$: H_{rms}	$H_{1/2}$: H_{rms}	$H_{1/3}$: H_{rms}	$H_{1/10}$: H_{rms}	$H_{1/10}$: $H_{1/3}$
Swell	3,08	3,02	3,89	4,33	1,11
% error	+23%	-15%	-3%	-15%	-13%
Storm 1	2,95	3,36	3,73	4,17	1,12
% error	+18%	-5%	-7%	-18%	-12%
Storm 2	2,88	3,62	3,94	4,50	1,14
% error	+15%	+2%	-2%	-12%	-10%
Theor.	2,51	3,54	4,01	5,09	1,27
Ave.	-	-	3,71	4,47	1,20
% error	-	-	-8%	-12%	-6%

Table 4.3a shows that for wave heights between $H_{1/2}$ and $\bar{H}$, the Rayleigh distribution is generally exceeded. The remaining heights with exception of $H_{1/3}$ are smaller than the theoretical distribution. There is no systematic difference between the regular swell record and the two storm records. From Table 4.3b it is apparent that the value of H^1 is also reduced, compared with the Rayleigh distribution.

The net effect is a selective reduction in height of the upper 50% of waves, with the ratio H^1: $H_{1/10}$ being very close to the theoretical value. The ratios

that have been discussed above are graphed in figures 4.7 to 4.10, with least square regression lines drawn through zero.

TABLE 4.3b

Ratios dependent on N

	$H^1 : H_{rms}$	$H^1 : H$	$H^1 : H_{1/2}$	$H^1 : H_{1/3}$	$H^1 : H_{1/10}$
N. Waves	70	70	70	70	70
Theor.	5,87	2,34	1,66	1,46	1,15
Swell	4,98	1,62	1,65	1,28	1,15
% error	-15%	-31%	-1%	-12%	0%
N. Waves	150	150	150	150	150
Theor.	6,36	2,53	1,80	1,59	1,25
Storm 1	5,42	1,73	1,61	1,45	1,30
% error	-15%	-32%	-11%	-8%	+4%
Storm 2	5,67	1,97	1,56	1,34	1,26
% error	-11%	-22%	-13%	-16%	+1%
N. Waves	200	200	200	200	200
Theor.	6,57	–	–	1,64	1,29
Ave.	6,15	–	–	1,65	1,37
% error	-6%	–	–	+1%	+6%

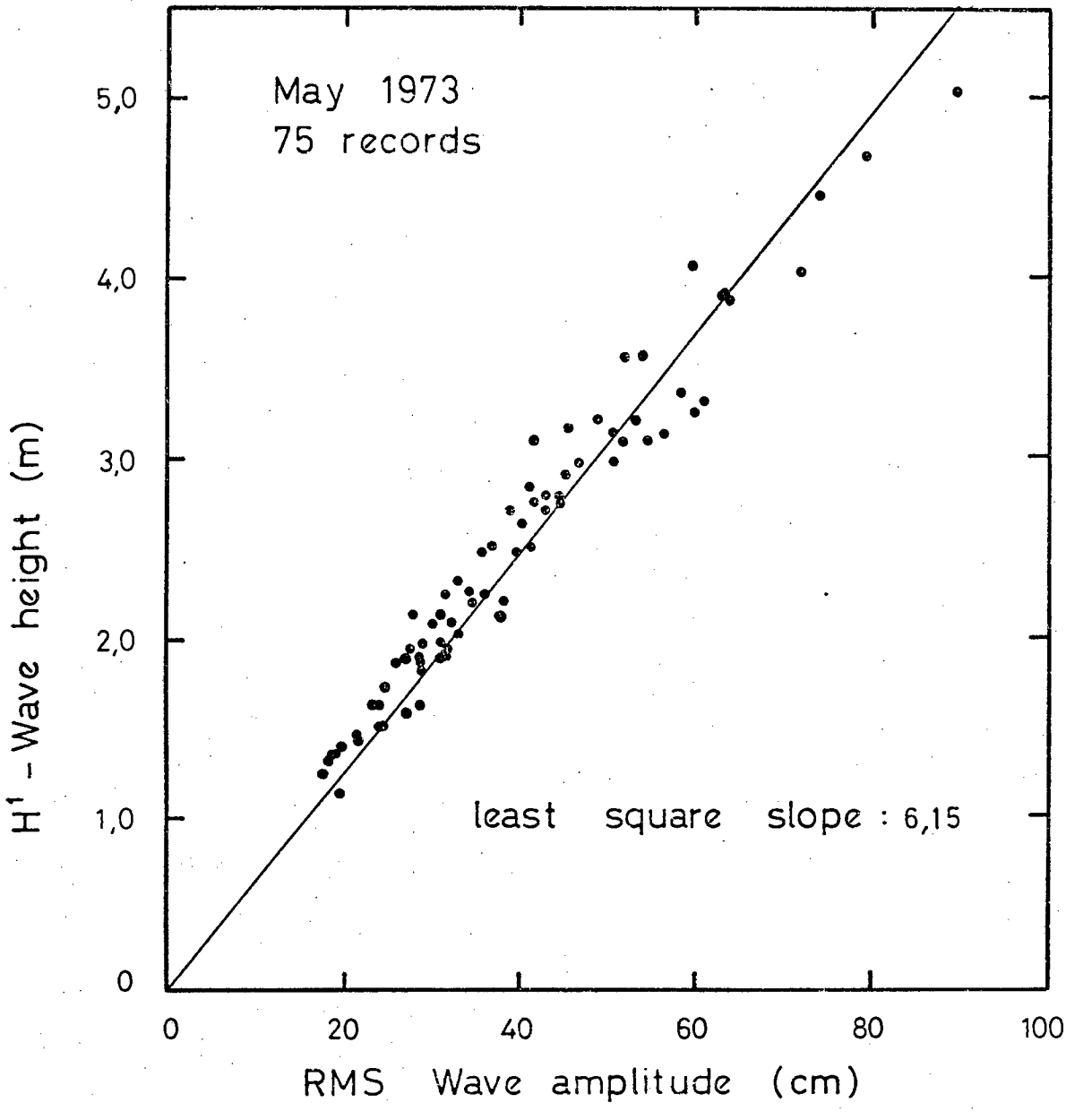

Fig. 4.7. Ratio of H^1 vs. H_{rms}.

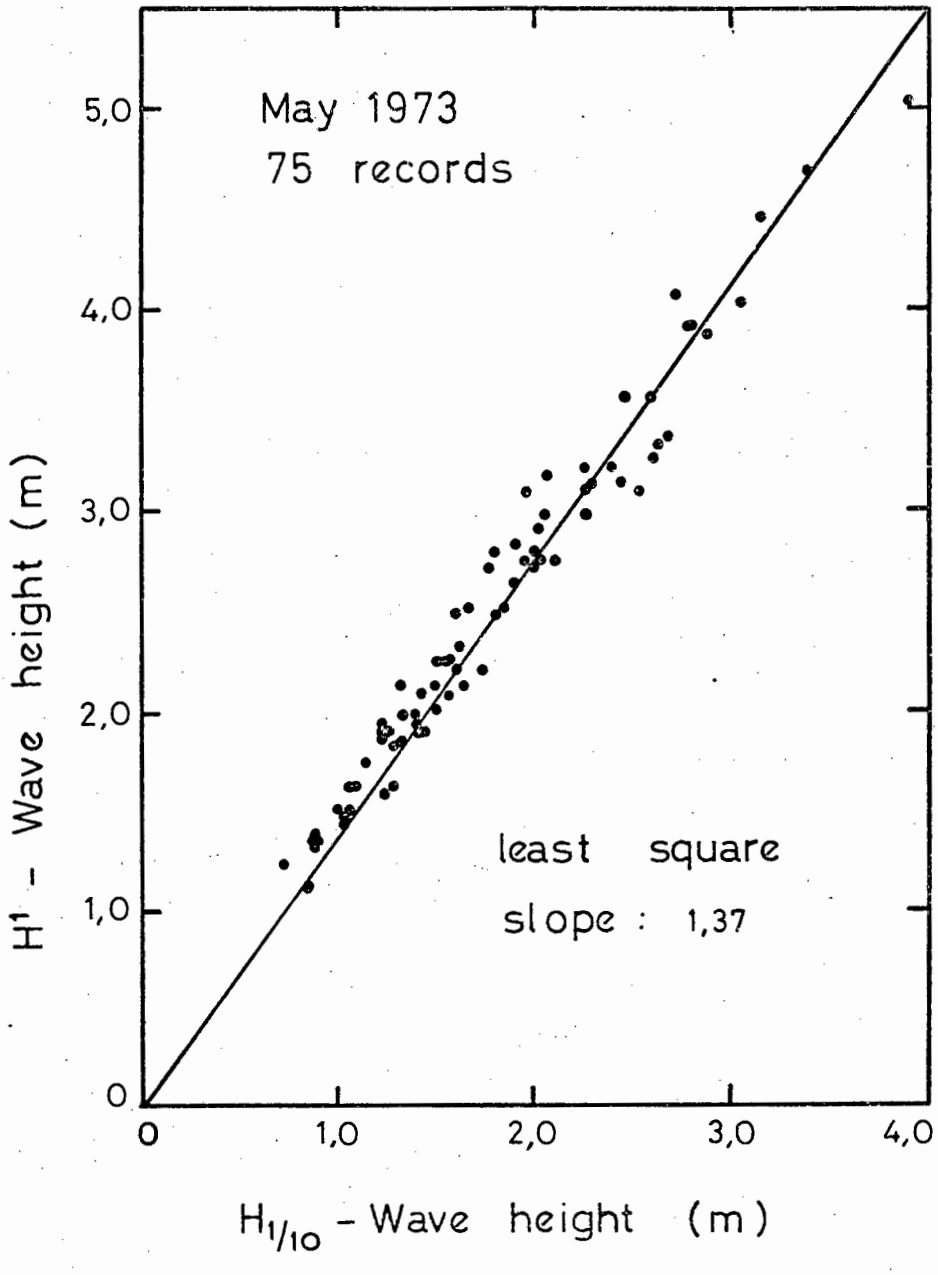

Fig. 4.8. Ratio of H^1 vs. $H_{1/10}$.

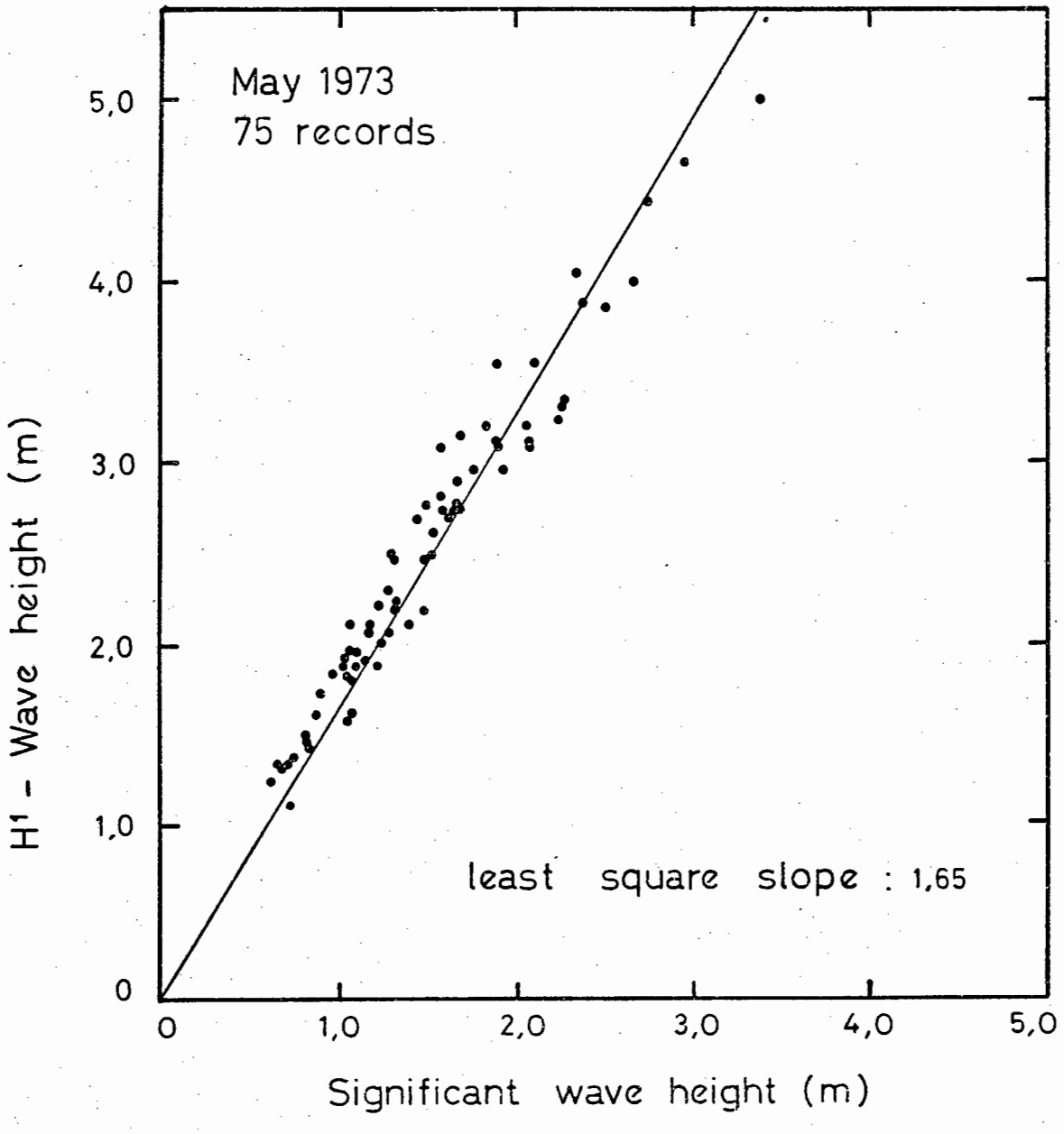

Fig. 4.9. Ratio of H^1 vs. $H_{1/3}$.

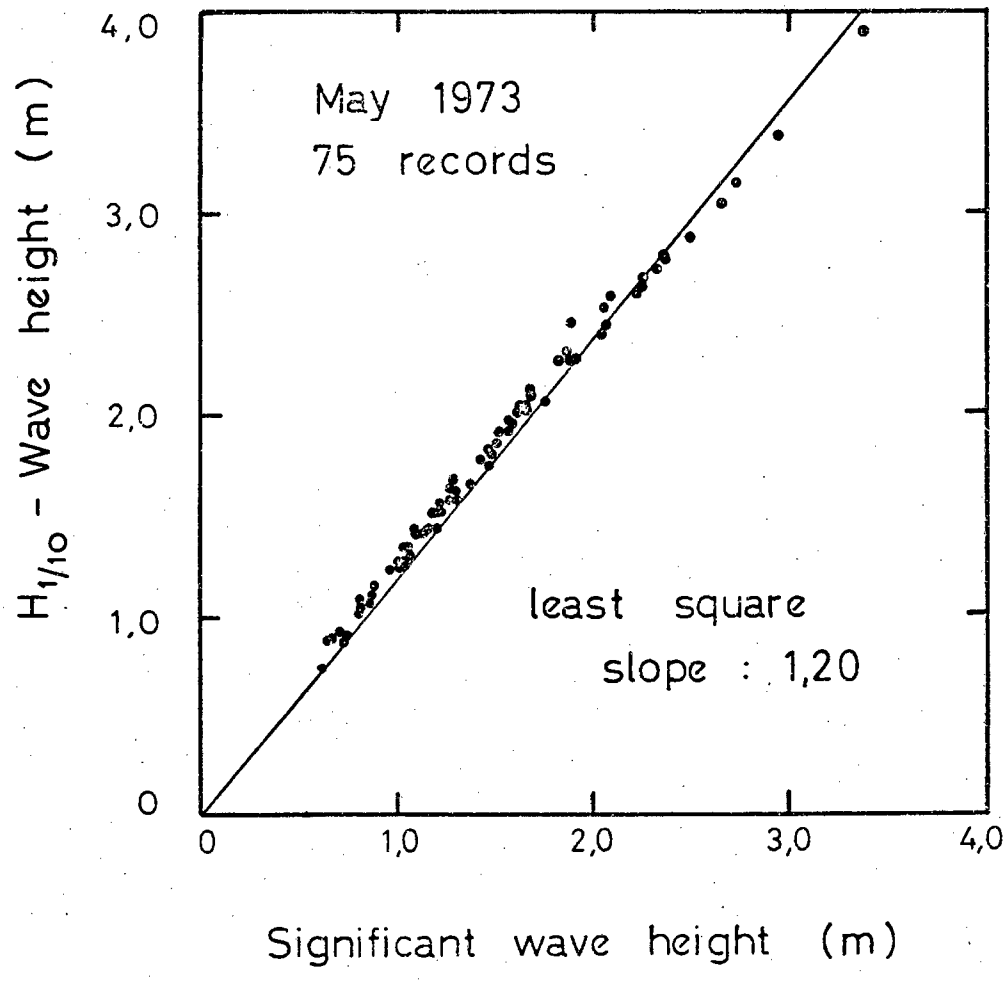

Fig. 4.10. Ratio of $H_{1/10}$ vs. $H_{1/3}$.

CHAPTER 5

5.1 Energy, frequency, time diagrams

If digital recordings of wave heights are available, the data can be satisfactorily represented by calculating the spectra and then by plotting each spectrum to form an energy, frequency, time diagram. A grid of twice daily wave height measurements spectrally analysed at one to five milleherz intervals, provides sufficient data for such a diagram to be graphed. The ordinate is used for frequency, the abscissa for time, and equal energy values are contoured. Munk, Miller, Snodgrass and Barber (1963) were the first workers to use this technique extensively.

The immediately obvious features from such a plot are sharp ridges and steep energy rises. If ridge lines are drawn in satisfying $\frac{\partial E}{\partial t} = 0$ or $\frac{\partial E}{\partial f} = 0$ and are projected back to the zero frequency axis, the time of origin of the wave source is known. The ridge lines can be accounted for by classical dispersion theory. If x is the distance of a wave generating source, t_o the time of origin of generation, t the time of recording, then the group velocity V(f) of component with frequency f is

$$V(f) = \frac{x}{t - t_o} \qquad \ldots\ldots\ldots\ldots \quad (5.1)$$

In deep water,

$$V(f) = \frac{g}{4\pi f} \qquad \ldots\ldots\ldots\ldots \quad (5.2)$$

$$f = \frac{g(t - t_o)}{4\pi x}$$

or

$$\frac{df}{dt} = \frac{g}{4\pi x} \qquad \ldots\ldots\ldots\ldots \quad (5.3)$$

Equation 5.3 is a straight line. An alternative form of 5.3 is

$$x = \frac{g}{4\pi} \cdot 1/\frac{df}{dt} \qquad \ldots\ldots\ldots\ldots \quad (5.4)$$

Numerically, if Δf is measured in Herz and Δt in hours,

$$x = 1,51 \frac{\Delta t}{\Delta f} . \qquad \ldots\ldots\ldots\ldots \quad (5.5)$$

The following variables can be measured from the prominent ridges appearing on E(f,t) diagrams,

a) time of origin t_o, of the storm, given by the intercept of the ridge line with the zero frequency axis.

b) The distance Δ, of the source determined by the slope of the ridge line according to equation 5.5.

c) storm duration, calculated from the sharpness of the ridge.

Munk et al (1963) mention that ridge lines stand out against the spectral background more than their associated storms stand out from run of the mill storms. This may indicate that high winds, concentrated in space and time, are missed in the loose meteorological observation grid.

Snodgrass et al (1966) found that spectra were peaked at 80 mHz in the generating area but when recorded at a distance, were peaked at 60 - 70 mHz. This red shift of frequencies implies a selective frequency attenuation in favour of high frequencies which appears to occur within the first thousand miles of the storm.

Munk and Snodgrass (1957) have investigated the situation leading to an enhancement of energy on the E(f,t) diagram at frequencies whose component's group velocity is the same as the velocity of the storm. Generally, the storm's approach velocity, W, is less than the group velocity V(f) of the lowest frequency wave generated. However, if the storm approaches on a great circle path at a velocity W comparable to the group velocity V(f), there will be an amplification of energy at the frequency given by,

$$f = \frac{g}{4\pi W} . \qquad \ldots\ldots\ldots\ldots \quad (5.6)$$

A similar type of energy enhancement could be created by winds within the storm whose wind velocities are twice that of the group velocity of the peak. Table 5.1 gives the amplification frequency as a function of the wind velocity U and approach velocity W.

TABLE 5.1

(After Munk and Snodgrass, 1957)

Storm velocity	Wind velocity	Ampl. freq.
W = 15 knots	U = 30 knots	f = 100 mHz
= 20 knots	= 40 knots	= 75
= 25 knots	= 50 knots	= 60
= 30 knots	= 60 knots	= 50

Thompson (1970) uses a novel, non-spectral method to calculate the time of origin t_o, the distance Δ, and by consulting the synoptic charts, the direction θ, of the swell. By plotting the storm's distance and velocity after the manner of Barber and Ursell (1948), he finds that the wave component with peak energy is propagated at a group velocity equal to that of the storm's approach velocity.

Cartwright (1971), measuring waves at St. Helena island in the Atlantic ocean was unable to positively correlate all of the events on his E(f,t) diagram with synoptic weather charts. He writes that winds appeared to be rather low to generate the dominant 60 - 80 mHz wave band appearing on his diagram. On some occasions he measured swell that originated west of the Drake passage and propagated through the narrow aperture offered by the Drake strait to St. Helena Island.

Snodgrass et al (1966), found that very little swell attenuation occurred at frequencies below 75 mHz. Recent studies by Hasselmann et al (1973) in the North Sea, have still not resolved exactly the mechanism responsible for wave attenuation. This study, which was mainly of the generation of waves showed that classical, dispersive swell systems appeared to be the

exception rather than the rule in the North Sea. Instead, the waves were "characterised by the signatures impressed by the particular space time structure of the generating wave field".

E(f,t) results

Energy, frequency time diagrams have been plotted for available data in figures 5.1 to 5.4. The results for July 1972 are from telemetred records, while those for the other months are from twice daily, hand digitised records. Over two hundred one dimensional spectra have been used in the compilation of these diagrams.

The wave energy is concentrated in the 50 - 100 mHz band in the diagrams. Pulsed maxima of short duration are present around 75 mHz for about half of the well defined events. On the other occasions, the maximum was usually around 80 mHz, with a few events having maxima below 75 mHz. Scanty evidence of high energy at and above 100 mHz indicates the general absence of local wind generated waves. The change of frequency with time $\frac{df}{dt}$, sometimes presents the classical type of ridges due to dispersion of waves from distant sources, but more often, is characterised by a steep, simultaneous rise in energy at a wide range of frequencies. The ridge patterns when present, are wide indicating long storm durations. Long fetches are evident from the synoptic weather charts and ridge time origins that are confirmed by suspected weather map sources are drawn in and labelled by the storms date of origin, and distance, Δ, in terrestrial degrees (1^{o} = 60 n.m. = 111 Km).

The change of energy with time, depicted in the E(f,t) diagrams by concentrated hills, and on the wave height time series by sharp rises, is strongly pulsed. The continually changing orientation of the fast moving fetches appears to be responsible for these bursts of wave energy being received at the Cape. An attempt has been made to group together similar patterns of this pulsed wave energy on the E(f,t) diagrams. (See figures 5.5, 5.6.) These patterns range in complexity from the simple swell system, to a mixed combination of swell and wind waves.

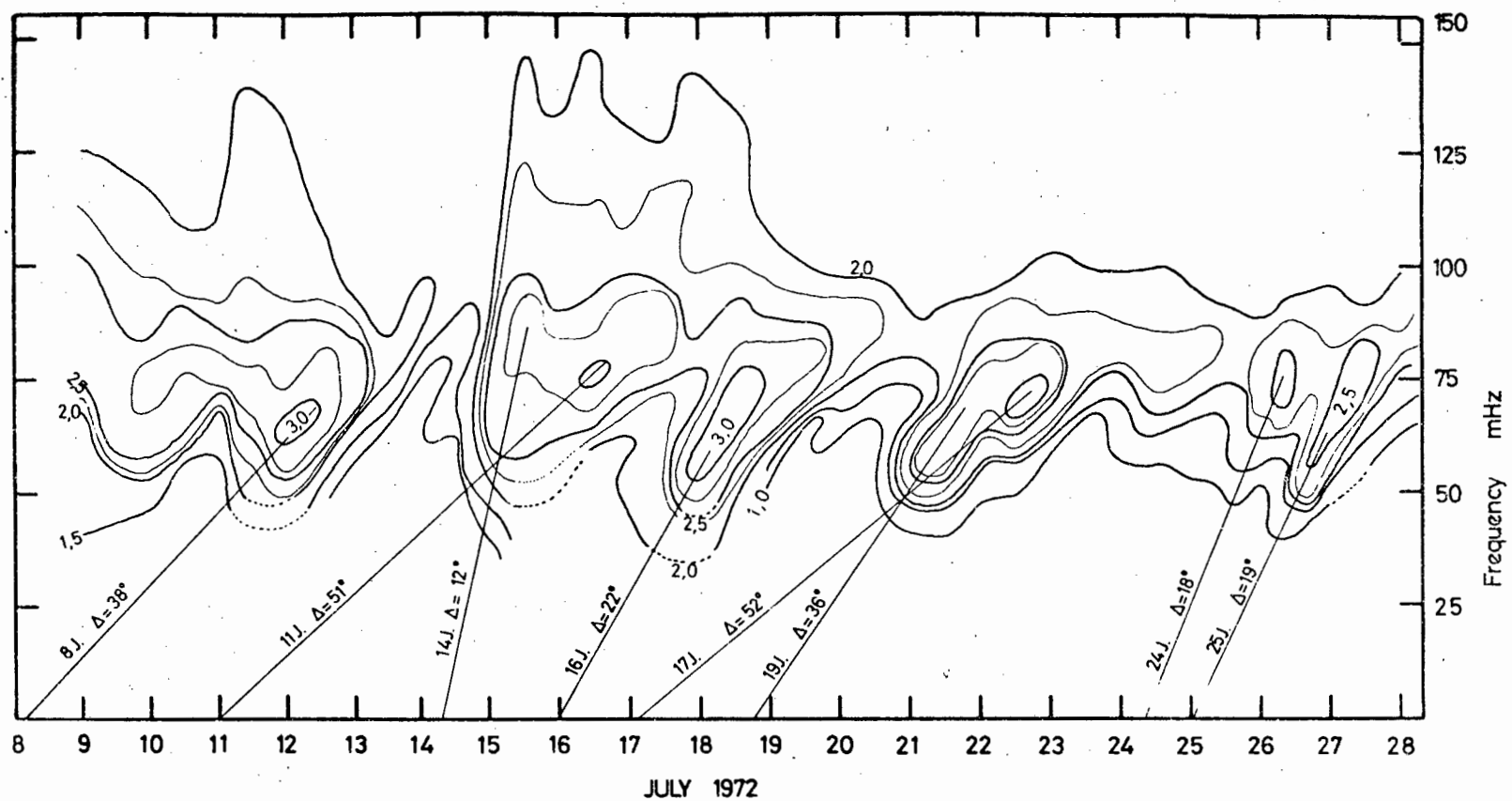

Figure 5.1. E(f, t) diagram contoured at $\log_{10} E/100$, where E is variance density per 5 mHz in cm^2 sec. Dates of origin of storms and distance, Δ, in terrestrial degrees marked in.

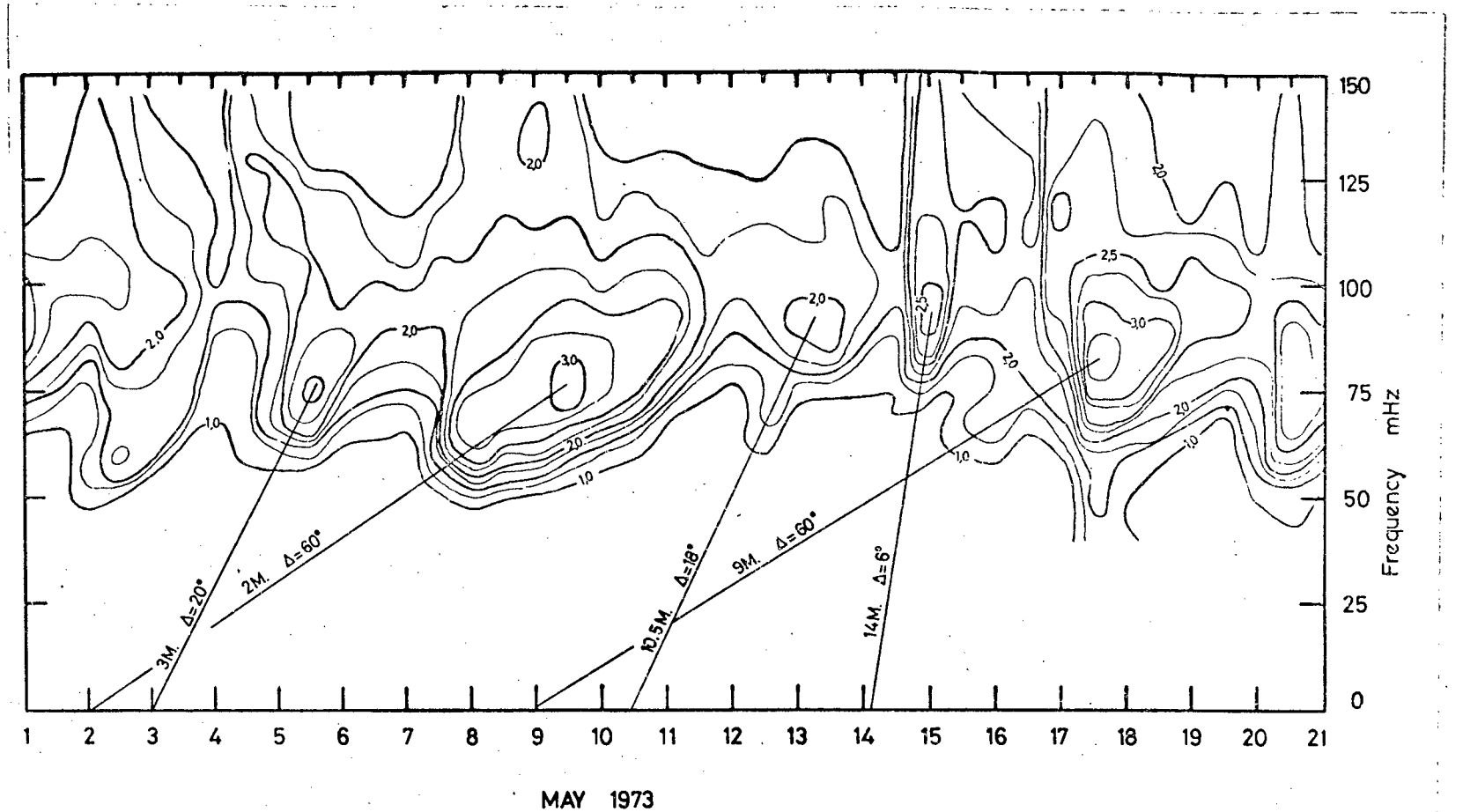

Figure 5.2. Legend as in 5.1.

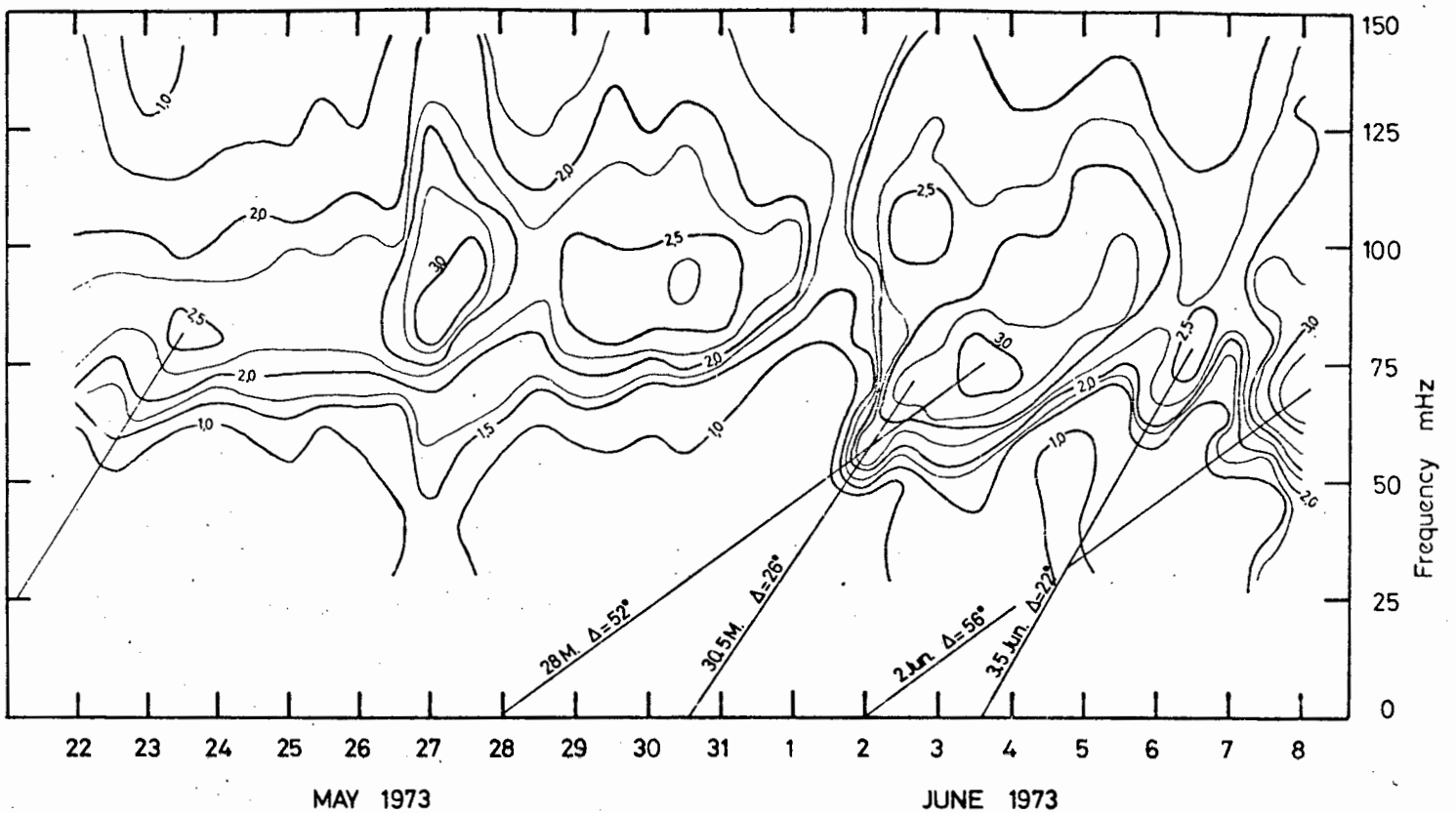

Figure 5.3. Legend as in 5.1.

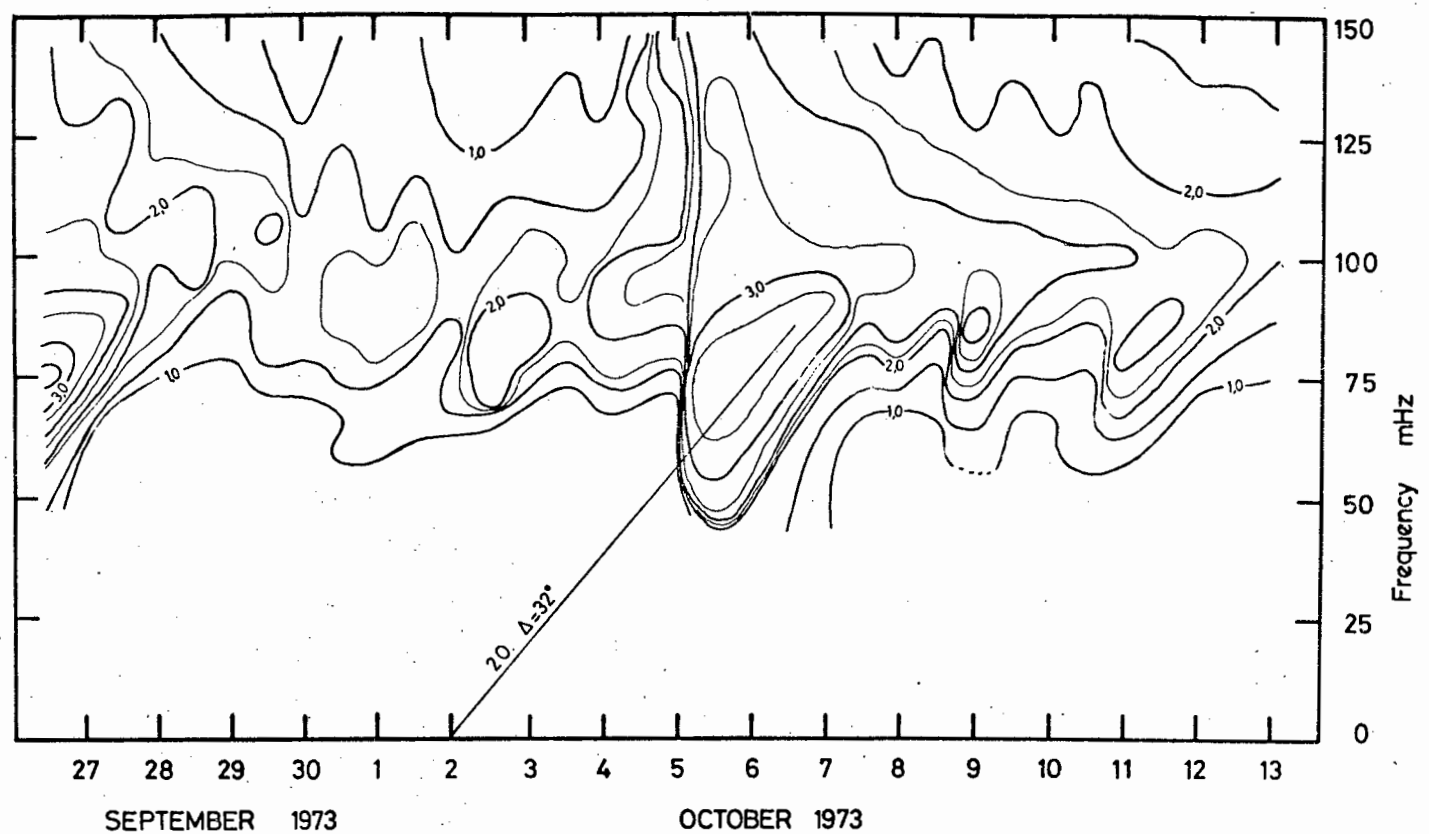

Figure 5.4. Legend as in 5.1.

One good example of local wind wave generation was recorded on and after the 30 July 1972. Because two hourly records were obtained, confidence could be placed in the growth pattern of energy at various frequencies. Frequencies travelling at the group velocity of the local winds were increased in energy at the fastest rate. (Unpublished work at the Institute of Oceanography, U.C.T.)

5.2 Individual storm events

Two distinct groups of patterns prevalent on the E(f,t) diagrams are shown in figures 5.5 number 1-4, and 5.6 number 5-8. The individual case histories are discussed in detail below.

A) Swell patterns (figure 5.5)

Case 1

A wide, sloping ridge, indicating pure swell which originated on 19.5 October 1973, at a distance of 38°. This is the clearest recorded instance of dispersive swell waves from a distant source. From the SAWB synoptic weather chart for 19 October 1973, 0600 SAST the wave generator appears to be an intense, occluded low pressure system centred on latitude 60°S, 25°W. Later charts show that the fetch, which was about 500 n.m. long, was advected towards Cape Town along a path which deviated southwards from a great circle passing at a tangent to 50°S and through Cape Town. Insufficient meteorological data was available to calculate the velocity of the cyclone and associated front.

Case 2

A wide sloping ridge indicating swell, that may have been enhanced by stronger winds or cyclone movement one day after origin. The earliest origin was on 17 July 1972, at a distance of 52°. A steepening of the ridge occurred on the 18th or 19th. The synoptic charts show a large fetch associated with a double low pressure field centred at 45°S, 15°W, on the 19th. On the 20th and 21st the passage of the low was blocked at 35°S, 0° by an anomalous

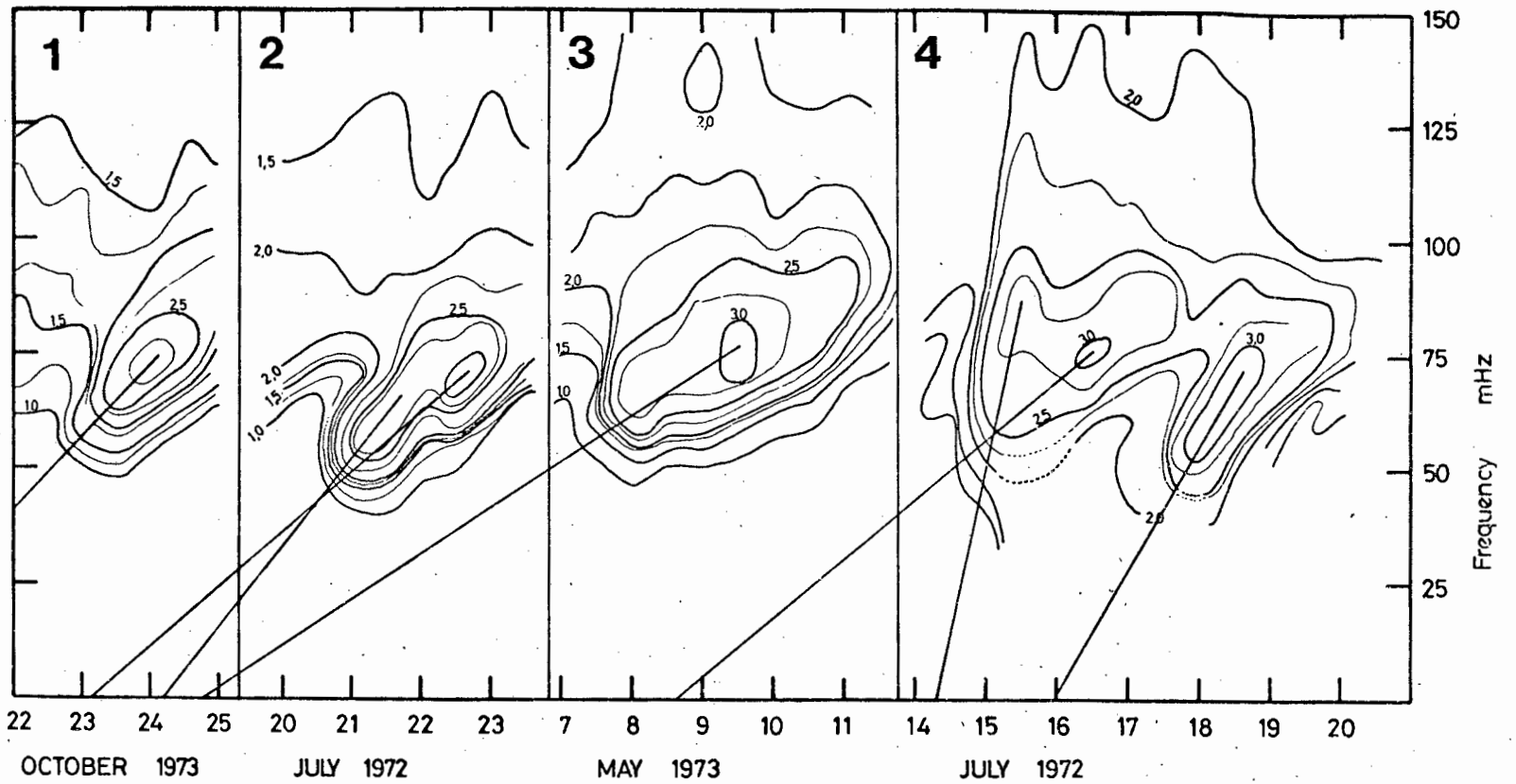

Figure 5.5. Swell case history studies.

positioning of the South Atlantic high pressure cell moving to the S.W. of the low. This effectively allowed the swell to emanate from a stationary source, with an unblocked passage over the last 1000 n.m. (about 2 days travel time). This accounts for the dispersive nature of the swell.

Case 3

A wide sloping ridge, indicating swell from a source on 2 May 1973, at a distance of 60^{o}. There is low local energy at 130 mHz. This is the most distant event recorded with the storm origin near South Georgia. From the synoptic charts, the swell generator appears to be an intense occluded low pressure cell centred on latitude 60^{o}S, 25^{o}W on the 3 May 1973. Similar to Case 1, later charts show that the fetch was advected along a great circle tangent to 50^{o}S passing through Cape Town. The low velocity of the cyclone ($\approx$15 knots) would have allowed an advanced arrival of the energy at 50 mHz early on the 7th. The peak energy at 75 mHz arrived two days later. Small scale hindcast synoptic charts show unfavourable winds for wave generation towards the Cape, over the time interval concerned.

Case 4

Two events were recorded, and the simpler second event is described first. A narrow, sloping ridge indicates swell originating on 16 July 1972, at a distance of 22^{o}. Synoptic weather charts show an occluded low with a large ESE component of velocity on the 16th and 17th. A southerly oriented fetch moved "out of view" eastwards on the 17th and allowed the swell waves to propagate without interference towards the Cape.

The first event shows a pattern that is not produced by a simple swell generator. The following explanation is proposed. A swell system originating on 11 July 1972, at a distance of 51^{o} was later complicated by a system originating on 14 July at a distance of 12^{o}. The synoptic charts in fact show a low which travelled fast ($\approx$27 knots) on the 13th, 14th. The sharp rise in energy at 60 - 80 mHz occurred on the 15th just after the passage of the front, which outstripped the low frequency swell. The swell generated earlier

by the system on the 11th, 12th, then arrived on the 16th.

B) Mixed swell and wind wave patterns (figure 5.6)

Case 5

This pattern represents local wind wave generation at high frequencies spreading to low frequencies. Winds were steady at 20 knots for 12 hours and came from the north to N.W. Synoptic weather charts indicate a fast moving front with ship measured wind velocities of 30 - 45 knots close behind the front. If the fast moving fetch had outstripped the swell waves generated by itself earlier, later arrival of these swell waves would explain the latter part of the pattern.

Since both fast and slow moving fronts do occur, see van Loon (1972), it seems that most of the E(f,t) patterns can be satisfactorily synthesised from a combination of swell patterns and wind wave growth patterns added with different time phases.

Case 6

Energy rising sharply in the 50 - 85 mHz band occurred from an intense occluded low at a distance of 32^{o} on 2 October 1973. This was the occasion when the highest waves recorded to date (H_{max} = 6,4 m) were measured. Frontal velocities were high ($\approx$30 knots) as were wind velocities measured by the weathership (60 knots on 4th and 5th at $14^{h}00$ SAST). It is shown later that the shape of the spectrum of these maximum waves is the closest to that of a fully developed sea, that has yet occurred at Melkbosstrand.

Case 7

This complicated pattern has the following possible explanation. The background is a dispersive swell system originating on 9 May 1973, at a distance of 60^{o}. This was enhanced by higher velocity winds on the 15th and because the front was moving fast ($\approx$25 knots) provided a sharp rise in energy between 75 - 85 mHz on the 17th. Although insufficient data is available to support the first part of the hypothesis, the developments from the

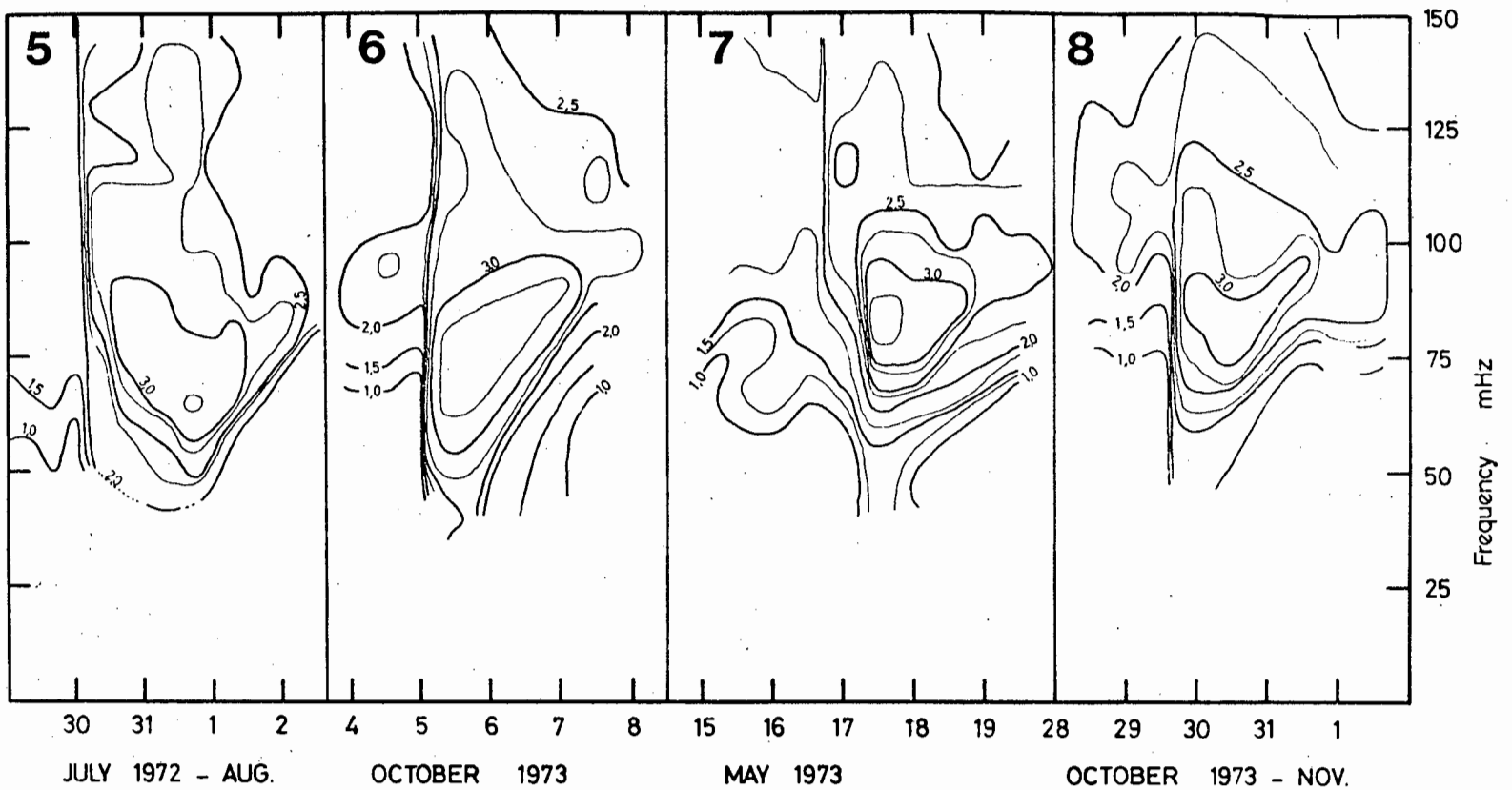

Figure 5.6. Mixed wind wave and swell studies.

15th onwards are satisfactorily supported by the synoptic weather maps. An occluded low moving eastwards had 40 knot measured winds 200 n.m. behind the front which passed over Cape Town on 17th at 14^h00 SAST. A patch of energy at 120 mHz indicated local wave generation which is explained by the winds close behind the front on the 17th.

Case 8

Synoptic weather charts indicate a single occluded low moving in an easterly direction. The frontal velocities were high ($\approx$35 knots) and the sudden rise in energy from 60 - 80 mHz followed shortly the passage of the front over the Cape on the 29th.

The most important feature common to the occluded low pressure cells generating cases 5, 6, 7, and 8, is that on each occasion, the centre of the cyclone lay between 40^o - 45^oS. This implies that a strong pressure gradient between the cyclone centre and Cape Town occurs (10 - 16 mbar) causing winds of 40 - 60 knots at 40^oS, 10^oE. In general the path of the cyclone was in an easterly direction between longitude 0^o to 30^oE. A sharp southerly component to the cyclone velocity then occurred.

A feature common to the conditions generating the swell cases 1, 2, 3, and 4 is that the cyclone centres all lay south of 45^oS.

Figure 5.7 shows selected SAWB hindcast maps depicting the similar conditions generating cases 5, 6, 7, 8. The fetches for the swell cases generally lie off these small scale maps.

Location of Storms

Events that appear on the E(f,t) diagrams and are confirmed by fetch locations on the SAWB synoptic charts, are shown in figure 5.8. The distance has been marked by both the most probable location from the synoptic charts and the distance as inferred from the slope of the ridge lines. The agreement in position of the suspected source from these two methods is satisfactory in

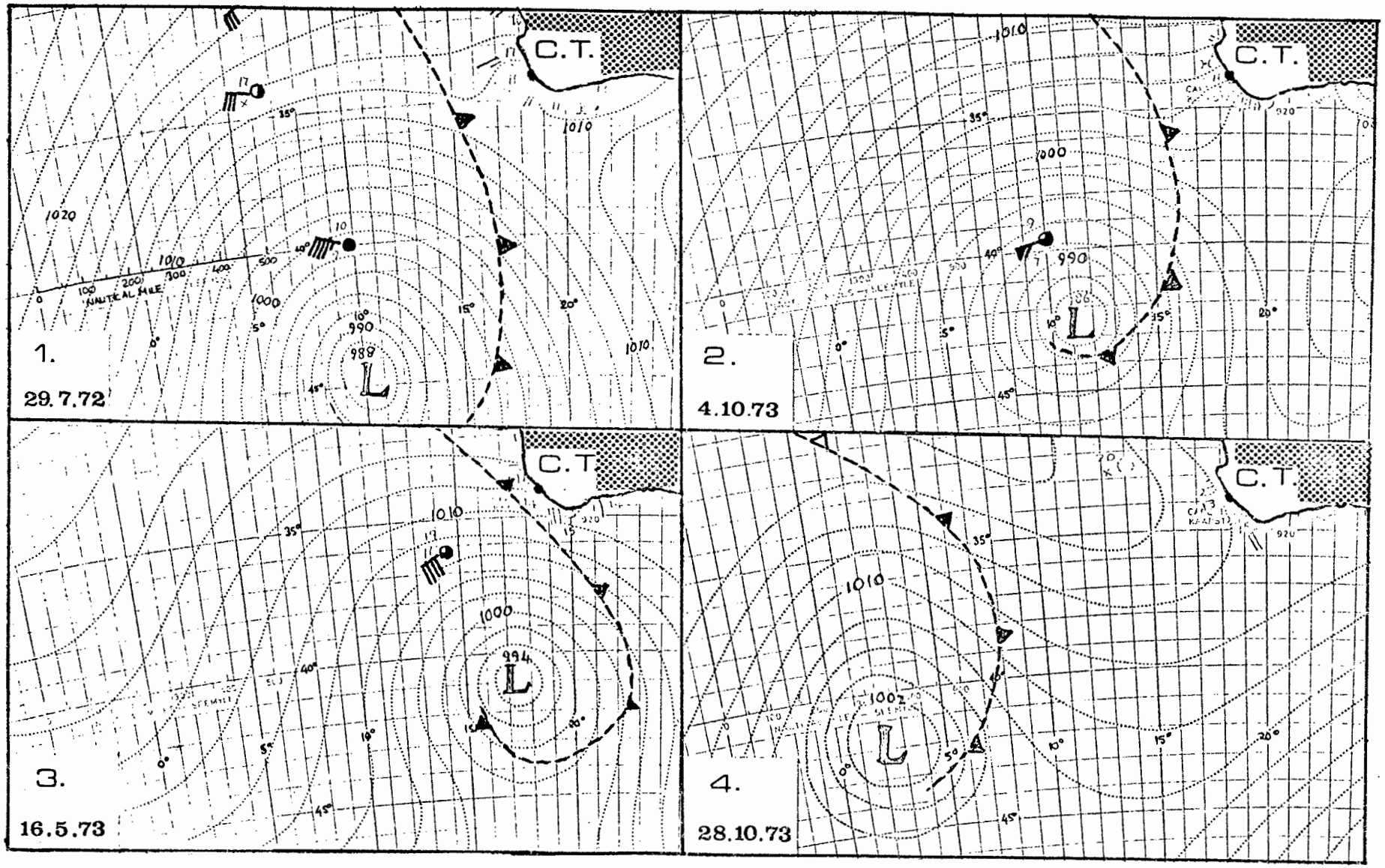

Fig. 5.7. Synoptic charts for $14^{h}00$ SAST compiled by SAWB, (for cases 5, 6, 7, and 8)

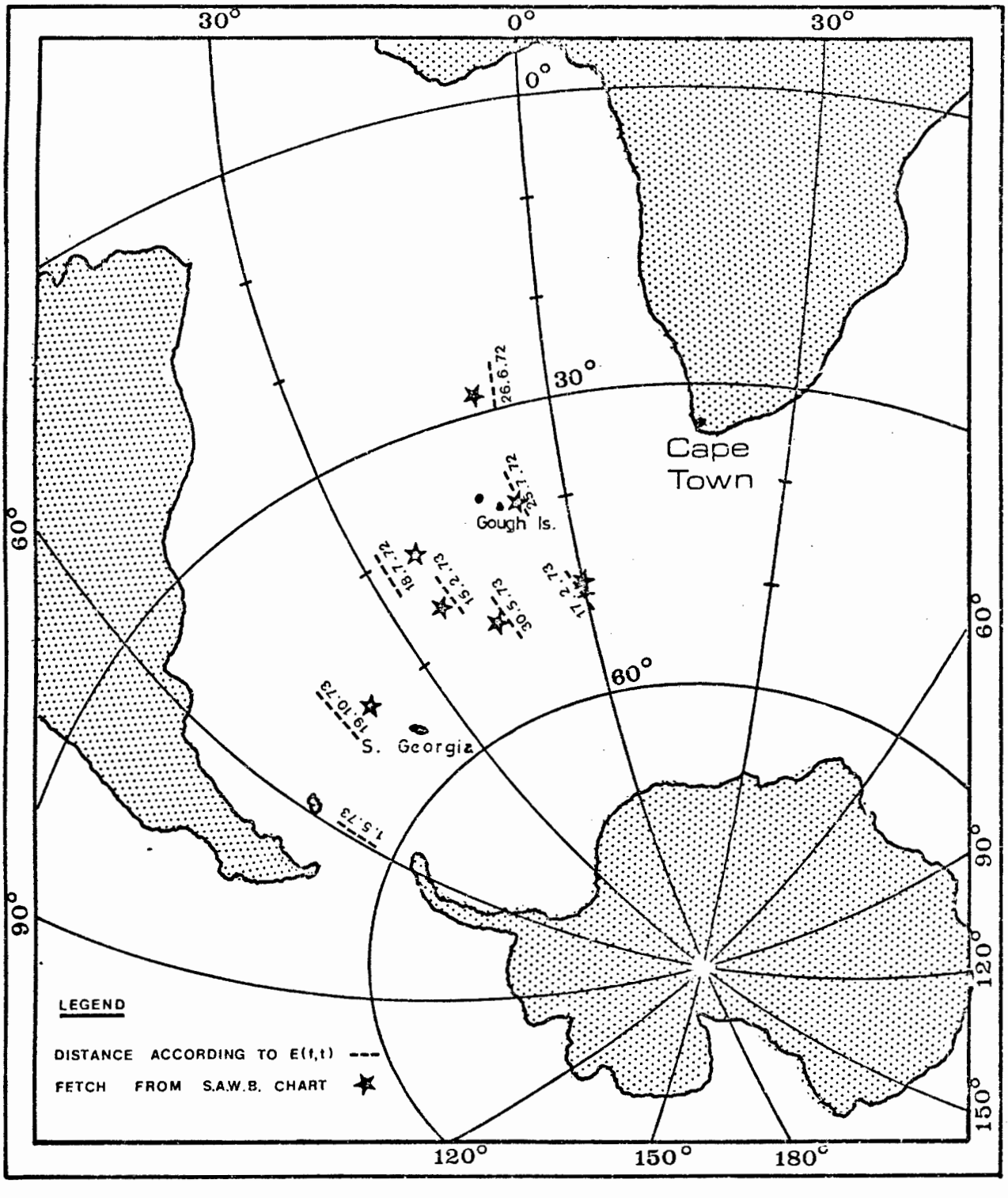

Fig. 5.8. Positions of fetches generating waves towards Cape Town.

most cases. A slight predominance of systems at distances of about 30^{o} - 40^{o} (1800 - 2400 n.m.) occurs.

5.3 Percentage occurrence of spectral frequencies associated with maximum spectral energy.

Figure 5.9 shows a histogram of the distribution of spectral frequencies associated with the spectral peak energy. The sample is 174 half hour records from May and part of June 1973 and part of September and October 1973. The range of frequencies is fairly wide, from about 75 - 100 mHz (10 - 13.3 second periods) with a peak at 95 mHz. The lack of spectral peak energy at the high frequencies seems typical of this region. Considering the usually short duration of the storms (see figures 5.1 - 5.4), a large percentage of low frequency (75 mHz) swell spectra are present. Occasionally fetches are advected close to the shore and wind waves of high frequency occur for short periods of time.

5.4 Spectral shape

Extreme spectra recorded at the Cape (maximum wave height $\geq$ 5 m) have been graphed together with a deep water spectrum from the T. B. Davie off Saldanha Bay (maximum wave height 10 m) in figure 5.10. On the same scale are spectra from Pierson and Moskowitz (1964), adapted from Silvester and Vongvisessomjai (1970), for fully arisen seas generated by 30, 35, and 40 knots. The different spectra are discussed in detail below.

Wind waves, 30 July 1972. This spectrum has a maximum peaked at a frequency corresponding to that of a 30 knot fully developed sea. The high frequency energy is low compared with the 30 knot case. It is possible that 45 knot winds near the weather ship (see figure 5.7,1) on the 29th generated the original sea which had a peak at 85 mHz and that local 20 knot winds filled up the high frequency end of the spectrum until it corresponded with the 25 knot Pierson/Moskowitz form.

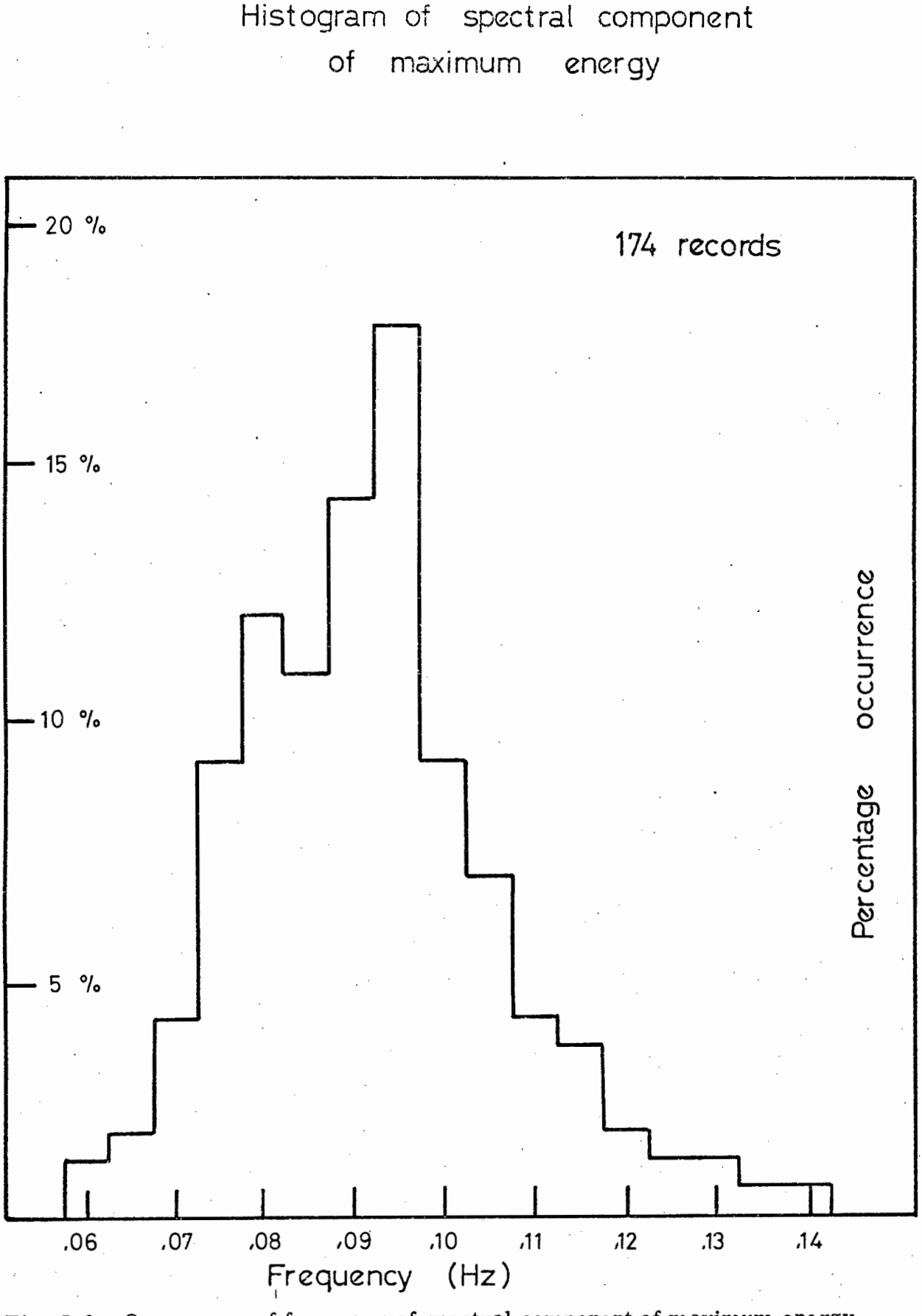

Fig. 5.9. Occurrence of frequency of spectral component of maximum energy.

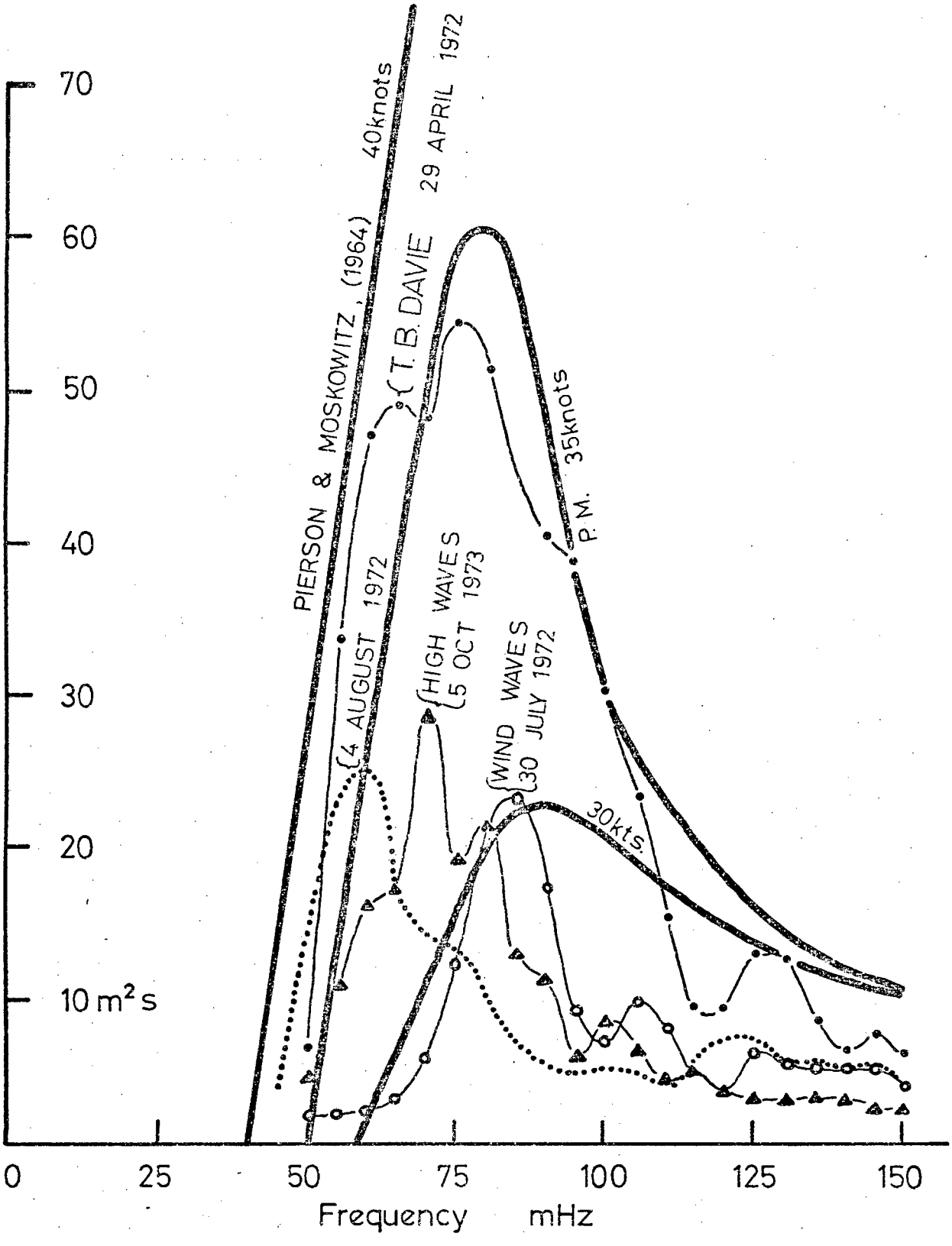

Fig. 5.10. Extreme spectra compared with Pierson and Moskowitz (1964) fully developed spectra.

High storm, 5 October 1973. Maximum wave height of 6.4 m was measured at 12^h00 SAST before equipment failure. Synoptic charts (see figure 5.7,2) show 60 knot winds at the weathership on the 4th and 5th. The spectrum shows a peak at 70 mHz; about the frequency of the 40 knot Pierson and Moskowitz case, but even allowing for a bottom friction factor of two, gives an energy spectrum somewhat comparable to the 35 knot case, but still lacking the high frequency waves.

High waves, 4 August 1972. This spectrum has a peak at 60 mHz, at a frequency similar to the 45 knot Pierson and Moskowitz form. Synoptic charts do not give a clear indication of the generation, but indicate very long south westerly fetches. No measured winds speeds are available.

Storm waves, 29 April 1972. The T. B. Davie measured maximum waves of 10 m on 29 April 1972, ($H_{1/3}$ = 7.2 m, T_z = 12 sec) while anchored six miles S.W. of Saldanha entrance in 100 m of water. The wind during the recording at 19^h00 SAST was 15 knots and had changed from 20 knots at 16^h00 to zero at 20^h00 SAST. The spectrum approaches the 35 knot fully developed form with an excess of energy at 65 mHz. This peak may have been generated by long distance swell. Synoptic charts indicate 40 knot winds at the weathership on 28th. This appears to be the best example of a nearly fully arisen wave spectrum off the Cape.

Not included in figure 5.10 is the very narrow, low energy swell spectrum of 26 June 1972 peaked at 50 mHz. This spectrum is only 15 -20 mHz wide at the half peak width. The frequency location of the peak was confirmed by a spectrum calculated from the NIO wave recorder aboard the weathership. The peak frequency is unexplained in terms of the geostrophic winds (20 - 30 knots).

CHAPTER 6

6.1 Discussion of Results

Zero crossing periods

In this work, only zero crossing wave periods and frequencies associated with the maximum energy of the spectrum, have been used to characterize the waves. Zero crossing periods are used extensively by engineers and naval architects. When the wave recordings are made in shallow water, solitary waves may occur on some occasions and it is sometimes difficult to estimate where the mean sea level should be drawn in. Draper (1966) suggests that a visual inspection of the record be made, and the mean level estimated by eye. If this procedure is adopted, two different workers may arrive at different mean levels, and so influence the value of the average zero crossing period, T_o. Another difficulty arising depends on the type of wave recorder used. A surface wave recorder may record waves that are included in the estimate of T_o, while a pressure or accelerometer instrument in the same place may fail to measure these waves as crossing the mean level. Thus two different values of T_o would be obtained for the same sea state.

D. L. Harris (1970) has made a critical comparison of wave periods estimated from wave records taken with different instruments. He finds the correlation between the differently defined periods poor and suggests that all frequencies that occur at a given site should be included in the design characteristics of sea structures.

Spectral width, epsilon

For wave records that have not been spectrally analysed, epsilon as defined by the zero crossing periods and crest periods, gives a measure of the rms spectral width. Values of epsilon calculated from both techniques described earlier were in excellent agreement with one another. However, as pointed out by Cartwright (1962), surface wave height recorders increase the fourth moment by virtue of small amplitude ripples present on the longer waves, and so make the value of epsilon difficult to interpret.

As an example, one record that contained only a narrow spectral range of frequencies, (see Harris, Marshall, and Shillington, 1972) gave an epsilon value of 0,93, indicating a broad spectrum. This value was higher than that obtained from storm wave records, which are the nearest to fully developed, wide spectra that have been obtained. The high value of epsilon measured is not considered to imply that Cape spectra are wide. Rather, because of the sensitivity of the recording instrument which registers small amplitude ripples, it is believed that the fourth moment is over emphasised. An attempt was made to cut off the high frequency end of the spectrum whilst calculating epsilon from the moment formula. However, it was found that the value of epsilon decreased almost linearly as the high frequency spectral density estimates were reduced. No satisfactory criterion could be chosen to limit the high frequency end of the spectrum used. Thus it is felt that an alternative method of describing the spectral width of records made by the Wemelsfelder surface wave recorder, is necessary.

Persistence Information

When studying the time series of wave heights given in Appendix 1, the sharp rise and fall of wave heights, and hence energy, over short intervals of time is most striking. It is even more apparent from the persistence curves that the high waves persist for short time intervals. As an example, average upper one tenth heights were greater than or equal to 3 m for a one day duration on only seven occasions from July 1972 - June 1973. The higher waves had even shorter durations.

Design wave

To calculate the maximum wave height likely to occur over a long interval of time, extreme value statistics are involved. An important aspect of this type of prediction is to know how long the sea state can be considered to be stationary. At the Melkbosstrand site, all indications are of a quickly changing wave height regime. A sampling interval of half an hour every twelve hours is thus likely to be too widely spaced in time to measure the highest waves in every storm. This factor, coupled with the restrictions of the measurements

being made in shallow water, and a number of maximum wave heights not being measured because of equipment failure, may account for the rather low maximum one in ten year wave (7,5 m) predicted for this site.

Statistical Ratios

From the ratios investigated, it appears that at this site, the wave heights are selectively reduced in amplitude. The maximum reduction in height is suffered by the highest wave, while the "lowest 50% of wave heights" are unaffected. This is deduced from the fact that the ratio of the maximum wave height to the upper one third and upper one tenth wave heights are comparable to the theoretical values. The ratio of maximum height to rms height is low as are the ratios of upper one third and upper one tenth wave heights to rms heights. Van Ieperen (1973) found that at this site there was no selective frequency attenuation, but that on some occasions the energy density of the spectral peak increased between the depths 20 m - 10 m. This would imply a selective height attenuation. From the results tabulated in Chapter 4, the statistics $H_{1/10}$ and $H_{1/3}$ predicted from H^1 using Longuet-Higgins (1952) figures are closest to the theoretical values. Energy calculations from the measured $H_{1/10}$ and $H_{1/3}$ will be too low by up to 15% if the theoretical ratios are used.

Van Ieperen (1973) found that refraction effects at this site were generally small. The most affected waves are those approaching between the southern cutoff (202^{o} east of north) and a south westerly direction. In this work, the direction of the source has been unknown unless the event could be linked with a storm on the synoptic charts, and no refraction corrections have been applied.

No variation of the ratios with different width spectra, as defined by epsilon were found. This is in agreement with the work of Koelé and de Bruyn (1964) working in shallow water off the Netherlands coast. Koelé and de Bruyn did find significant varations of ratios $\tilde{H}_{1/10}$: $\tilde{H}_{mean}$ where all wave heights $\tilde{H}$ were used, and not only those separated by a zero crossing. This type of measurement is very dependent on the type of wave recorder used and the

criterion adopted, as to which small waves to neglect (wave heights of 5 - 10 cm and periods < 1 second in their case). The implication of the above result is that the assumptions used by Longuet-Higgins (1952) of a narrow spectrum are satisfied in Cape waters. This is confirmed by the lack of variation in the relatively narrow spectral shape of the sharply peaked Cape spectra. It would have been useful to have been able to test more wind wave type spectra, had these been available.

Frequency distribution of energy

In agreement with other workers, Munk et al (1963), Snodgrass et al (1966), Cartwright (1971), it was found that the major frequency spread of energy was between 50-100 mHz. Also apparent in the $E(f,t)$ diagrams was a sharp pulsing of energy. The high energy events are satisfactorily explained by three classes,

a) pure swell from distant or slow moving sources;

b) pure local wind wave generation;

c) varying mixtures of the above systems depending to a large degree on the velocity of the front associated with the cyclone causing the wave generation.

It may be possible to synthesize all of the recorded patterns on the $E(f,t)$ diagrams by combining swell and wind wave patterns with different time phases.

Location of storms

Of the events confirmed by the synoptic weather charts, the generation centres seem to fall in two categories.

a) Occasional very distant generation by fetches that are advected towards Cape Town, on or near great circle paths. The velocity of the cyclone and associated front is usually slow and a classical dispersive pattern of energy occurs on the $E(f,t)$ diagram. In cases where the velocity has not been low (>20 knots), the cyclone centre has been to the south of 45^{o}S.

b) the more usual generation of waves from fetches that are from 1000 - 2000 n.m. distant. These fetches tend to be associated with the north western aspect of an occluded low, situated behind the front. The cyclone and its associated front are fast moving (25-30 knots), with the cyclone centre passing between 40^{o} - 45^{o}S as the cyclone nears Cape longitudes (0^{o} - 20^{o}E). Measured wind velocities have been from 40 - 60 knots in a westerly to south westerly direction near the weather ship (see figure 5.7). These types of fetches lead to a sudden increase of wave energy in a wide frequency band, (50 - 90 mHz), shortly after the passage of the front over the Cape.

Spectral shape

An interesting result of this work is that fully developed sea conditions do not seem to prevail off the Cape. It is not known whether the spectra obtained are representative of the deep water conditions. If they are, then it will be difficult to establish a wave prediction scheme until the exact shape of the spectrum in the generating area is known.

6.2 Conclusions

A continuous time series of wave height measurements made twice daily for a period of more than one year has revealed the sharply pulsed nature of the wave regime off the Cape. Maximum wave heights measured did not exceed 6.4 m and were generated on relatively few occasions. The values of statistical ratios that are important to engineers were measured and some of these (H^{1}: $H_{1/3}$; H^{1}: $H_{1/10}$; $H_{1/10}$: $H_{1/3}$) were found to be in close agreement with those predicted by Longuet-Higgins (1952) for a narrow wave spectrum. Other statistics (H^{1}: H_{rms}; $H_{1/3}$: H_{rms}; $H_{1/10}$: H_{rms}) were between 6 - 12% lower than the theoretical values. A selective height attenuation of the upper 50% of wave heights accounts for these low values.

In agreement with the work of Koelé and de Bruyn (1964), no variation of the ratios with spectral width epsilon, was found. When examining the shape of

the spectra, it is felt that the high value of epsilon does not reflect a wide spectrum. Rather, because the wave recordings were made with a sensitive surface recorder, the interpretation of epsilon is difficult. Small amplitude ripples are present on most of the wave records but are of low energy. An attempt to calculate the value of epsilon from the moments of the spectrum, using only the major peak, showed a systematic decrease in epsilon as the higher frequencies were neglected. Thus no suitable criterion could be adopted as to which ripples to include and which to neglect.

The second aspect of this project was to obtain spectra from the wave records and link up the events with the relevant meteorological systems. The extensive use of E(f,t) diagrams has revealed the nature in which the sharply pulsed wave energy arrives at the Cape. Comparing the results from these diagrams with the cyclones responsible for wave generation it has been established that there is a close correlation between the shape of the E(f,t) pattern and the velocity and latitude with which the cyclone passes the Cape. Slow moving fetches or fetches with the cyclone centre south of 45^{o}S result in a classical dispersive ridge pattern, while fast moving cyclones with their centres between 40 - 45^{o}S while in Cape longitudes, present a simultaneous arrival of energy at a wide band of frequencies.

Because the measurements were taken at a shore station which was generally out of the generating area, the spectra tended to have a narrow shape compared to the various Pierson and Moskowitz (1964) fully developed spectra. Pure wind wave spectra do occur, but the more usual system is one that presents a narrow swell type spectrum that is sharply peaked with the frequency of maximum energy in the spectrum between 75 - 100 mHz. Wind speeds of up to sixty knots are sometimes recorded, but the reported geostrophic winds appear to be lower than those required by Moskowitz (1964) to generate the lower frequency peaks.

6.3 Suggestion for future work

The most natural extension of the preliminary work reported in this thesis, would be the establishment of a wave prediction scheme. Shallow water

spectra have been available for some time, and with the extensive use of energy, frequency, time diagrams, some understanding of the nature in which the wave energy arrives at the shore has been made. What is severely lacking at present is a knowledge of wave spectra in the generating area. All indications near the Cape are of narrow spectra, often at low frequencies. Does this imply that waves are not fully developed even in the storm fetches? Analysis of a few weather ship spectra has not solved the problem, as low frequency peaks (0,05 Hz) are sometimes present in weathership wave records with considerable energy.

With the introduction of intensive atmospheric-oceanic studies in the near future, better meteorological coverage of the south Atlantic will be available. This input is an essential feature of wave prediction. Because of the quickly changing orientation of the meandering westerlies, wave energy input may be from a variety of directions. At present, there has been no attempt to obtain a directional wave spectrum. Experiments have been made to determine the wave direction from simple orbital motion measurements, as well as from radar studies. Both these experiments are recent.

Prediction of waves at the coastline assumes a thorough knowledge of the attenuation features of the coast. Preliminary studies by van Ieperen (1973) at Melkbosstrand indicate that the friction factors are larger than measured on other similar topographies. This, together with the fact that his work shows that a linear friction law may be better than a quadratic one, indicates that the bottom friction problem has not been completely solved.

The construction of a nuclear power station on the shore, requiring sea water for cooling, has posed a number of unanswered surf zone problems. For these particular problems, knowledge of the wave regime, and particularly the surf zone width are important. Expansion in this field is apparent and the understanding of some of the unexplained wave features may be promoted.

With the intensive surf studies, more effort has been placed into positioning several wave recorders in close proximity with one another. Unfortunately,

not all the wave recorders are of the same type, and an intercalibration program between recorders is essential. Some work of this nature between the Wemelsfelder float recorder and an NIO shipborne wave recorder on the T. B. Davie has been carried out, but the results were disappointing. Although frequency comparisons were good, there was a difference in spectral energies reported by the different instruments. The nature of this problem must be understood, as the only way to obtain deep sea records is with accelerometer instruments.

ACKNOWLEDGEMENTS

I am indebted to the following people and organisations for their help.

Dr. T.F.W. Harris and Dr. T.R. Hennessy, my supervisors, whose kind, unfailing help and personal attention have made this thesis possible.

Professor J.K. Mallory and members of staff of the Oceanography Department at U.C.T., for their continual interest and fruitful discussion. Mr. J.N. Marshall together with Messrs. D. Rattey, C. Maxwell and M. Price of the Marine Effluent Research Unit, who carried out the essential maintenance of equipment on the sea tower. Theirs is a difficult task, having to plan according to the whim of the natural elements.

The Computer Department provided an essential service and in particular programming help was obtained from Mr. T. Radford.

I am indebted to ESCOM for their permission to use the data here published and to ESCOM, VISKOR and U.C.T. for financial help.

My final thanks are to Mrs. P. Dobbie, whose special typing skills produced the immaculate final typed manuscript.

REFERENCES

BACKUS, G.E. (1962): The effect of the earth's rotation on the propagation of of ocean waves over long distances. Deep Sea Res., 9, pp. 185 - 197.

BARBER, N.F. and F. URSELL (1948): Generation and propagation of ocean waves and swell. Phil. Trans. Roy. Soc. Lond. A, 240, pp. 527 - 560.

BLACKMAN, R. B. and J.B. TUKEY (1958): The measurement of power spectra from the point of view of communications engineering. New York: Dover Publ. Inc. pp. 190.

BRETSCHNEIDER, C.L. (1954): Field investigation of wave energy loss in shallow water ocean waves. Tech. Memo. No. 46, Beach Erosion Board, Corps of Engineers.

CORNISH, V. (1934): Ocean waves and kindred geophysical phenomena. C.U.P. pp. 164.

CARTWRIGHT, D.E. (1962): Analysis and Statistics, Chapter 15, pp. 567 - 589, in The Sea, ed. M. N. Hill. New York: John Wiley and Sons.

CARTWRIGHT, D.E. (1971): Tides and waves in the vicinity of St. Helena. Phil. Trans. Roy. Soc. Lond. A, 270, pp. 603 - 649.

CARTWRIGHT, D.E. and M.S. LONGUET-HIGGINS (1956): The statistical distribution of the maxima of a random function. Proc. Roy. Soc. A, 237, pp. 212 -232.

DARBYSHIRE, J. (1952): The generation of waves by wind. Proc. Roy. Soc. A, 215, pp. 299-328.

DARBYSHIRE, J. (1955): An investigation of storm waves in the North Atlantic Ocean. Proc. Roy. Soc. A, 230, pp. 560 - 569.

DARBYSHIRE, J. (1956a): An investigation into the generation of waves when the fetch of the wind is less than 100 miles. Quart. J. Roy. Met. Soc. Lond. 82, pp. 461 - 468.

DARBYSHIRE, J. (1956b): The distribution of wave heights: a statistical method based on observations. Dock Harbour Author. 37, pp. 31 - 32.

DARBYSHIRE, J. (1959a): A further investigation of wind generated waves. Deut. Hydr. Zeit. 12, pp. 1 - 13.

DARBYSHIRE, J. (1959b): The spectra of coastal waves. Deut. Hydr. Zeit. 12, pp. 153 - 167.

DARBYSHIRE, J. (1963): The one dimensional wave spectrum in the Atlantic ocean and in coastal waters, in Ocean Wave Spectra, pp. 27 - 38. Engelwood Cliffs, N.J.: Prentice Hall Inc.

DARBYSHIRE, J. and M. DARBYSHIRE (1964): Wave observations in South African waters. S. Afr. J. Sci. 60, pp. 183 - 189.

DARBYSHIRE, M. (1962): A preliminary account of wave observation and prediction in South African waters. S. Afr. J. Sci. 58, pp. 353 - 361.

DARBYSHIRE, M. and E. PRITCHARD (1966): Sea waves near the coasts of South Africa. Deut. Hydr. Zeit. 19, pp. 218 - 225.

DRAPER, L. (1963): Derivation of a 'design wave' from instrumental records of sea waves. Proc. Inst. of Civil Eng. 26, pp. 291 - 304.

DRAPER, L. (1966): The analysis and presentation of wave data: a plea for uniformity. Proc. of 10th Conf. on Coast. Eng. Tokyo. New York: Amer. Soc. of Civil Eng. pp. 1 - 11.

HARRIS, D.L. (1970): The analysis of wave records. Proc. 12th Conf. Coast. Eng. Washington. New York: Amer. Soc. Civil Eng. pp. 85 - 100.

HARRIS, T.F.W., J. MARSHALL and F.A. SHILLINGTON (1972): Wind waves in Cape waters: features of their frequency spectra and associated generating conditions. ECOR Symposium on the ocean's challenge to South Africa's engineers, Stellenbosch, S.A.

HARRIS, T.F.W., J. MARSHALL and F.A. SHILLINGTON (1973): Quasi monochromatic 0,05 Hz waves in Cape waters. Nature, 244, pp. 154.

HASSELMANN, K., T.P. BARNETT, E. BOUWS, H. CARLSON, D.E. CARTWRIGH K. ENKE, J.A. EWING, H. GIENAPP, D.E. HASSELMANN, P. KRUSEMAN, A. MEERBURG, P. MÜLLER, D.J. OLBERS, K. RITCHER, W. SELL, H. WALDEN (1973): Measurements of wind wave growth and swell decay during JONSWAP, Deut. Hydr. Inst. Hamburg, pp. 95.

INTERIM REPORTS (1969, 1971): Oceanographic investigations being conducted for proposed ESCOM Nuclear power station project at Duynefontein. Oceanog. Dept. U.C.T. (Internal reports).

KINSMAN, B. (1965): Wind waves, their generation and propagation on the ocean surface. Prentice Hall Inc. Engelwood Cliffs, N.J. pp. 676.

KOELÉ, L.A. and P.A. DE BRUYN (1964): Statistical distribution of wave heights in correlation with energy spectrum and water depth. Proc. of 9th Conf. Coast. Eng. Lisbon, New York: Amer. Soc. Civil Eng. pp. 123 - 139.

KRAUS, E.B. (1972): Atmosphere-ocean interactions. Oxford, Clarendon Press. pp. 275.

LAMB, H. (1932): Hydrodynamics (6th ed.) Land. C.U.P. pp. 738.

LONGUET-HIGGINS, M.S. (1952): On the statistical distribution of the heights of sea waves. J. Mar. 11, pp. 245 - 266.

LONGUET-HIGGINS, M.S. (1957): The statistical analysis of a random moving surface. Phil. Trans. Roy. Soc. Lond. A 249, pp. 321 - 387.

MOSKOWITZ, L. (1964): Estimates of the power spectra of fully developed seas for wind speeds of 20 - 40 knots. J. Geophys. Res. 69, pp. 5161 - 5179.

MUNK, W.H., G.R. MILLER, F.E. SNODGRASS and N.F. BARBER (1963): Directional recording of swell from distant storms. Phil. Trans. Roy. Soc. Lond. A255, pp. 505 - 584.

MUNK, W.H. and F.E. SNODGRASS (1957): Measurements of southern swell at Guadalupe Island. Deep Sea Res. 4, pp. 272 - 286.

NEAL, A.B. (1972): MSL cyclones and anticyclones in November 1969 and June 1970. Aust. Met. Mag. 20. pp. 217 - 230.

NEUMANN, G. and W.J. PIERSON (1957): A detailed comparison of theoretical wave spectra and wave forecasting methods. Deut. Hydr. Zeit. 10, pp. 73 - 92, pp. 134 - 146.

OCEAN WAVE RESEARCH REPORT 1 (1968): Wave and Wind conditions for Natal and the western Cape coastal areas. CSIR report, MEG 665, Pretoria. (restricted).

OCEAN WAVE RESEARCH REPORT 2 (1969): Handleiding vir golf voorspellings aan die Suid Afrikaanse Kus. WNNR verslag, MEG 736, Pretoria.

PHILLIPS, O.M. (1958): The equilibrium range in the spectrum of wind generated waves. Journ. Fluid Mech. 4, pp. 426 - 434.

PHILLPOT, H.R., P.G. RICE, A.B. NEAL and F.A. LAJOIE (1971): GARP basic data set analysis project. The first experiment. November 1969, Aust. Met. Mag. 19, pp. 48 - 81.

PIERSON, W.J. (1955): Wind generated gravity waves. Advances in geophysics, II, New York: Academic Press Inc. pp. 93 - 178.

PIERSON, W.J. and L. MOSKOWITZ (1964): A proposed spectral form for fully developed wind seas based on the similarity theory of S.A. Kitaigorodskii. J. Geophys. Res. 69, pp. 5181 - 5190.

RICE, S.O. (1944, 1945): Mathematical analysis of random noise. Part I - IV, Bell system Tech. J. 23 pp. 282 - 332, 24, pp. 46 - 156.

ROLL, H. U. and G. FISCHER (1956): Eine Kritische bemerking zum Neumann-Spektrum des Seeganges. Deut. Hydr. Zeit. 9, pp. 9 - 14.

SHIPLEY, A.M. (1964): Some aspects of wave refraction in False Bay. S. Afr. J. Sci. 60, pp. 115 - 120.

SILVESTER, R. and S. VONGVISESSOMJAI (1970): Energy distribution curves of developing and fully arisen seas. J. of Hydraulic Res. 8, pp. 493 - 521.

SVERDRUP, H.V., M.W. JOHNSON, and R.H. FLEMMING (1942): The Oceans, their physics, chemistry and general biology. Prentice Hall Inc. Engelwood Cliffs, pp. 1087.

SVERDRUP, H. V. and W.H. MUNK (1947): Wind sea and swell: theory of relations for forecasting. U.S. Navy Hydrographic office Publ. No. 601, pp. 41.

SNODGRASS, F.E., G.W. GROVES, K.F. HASSELMANN, G.R. MILLER, W. H. MUNK and W.H. POWERS (1966): Propagation of ocean swell across the Pacific. Phil. Trans. Roy. Soc. Lond. A 259, pp. 431 - 497.

THOMPSON, W.C. (1970): Swell and storm characteristics from coastal wave records. Proc. of 12th Conf. on Coast. Eng. Washington. New York American Soc. of Civil Eng. pp. 33 - 52.

TALJAARD, J.J. (1967): Development, distribution and movement of cyclones and anticyclones in the southern hemisphere during IGY. J. Appl. Met. 6, pp. 973 - 987.

TALJAARD, J.J. (1972): Synoptic Meteorology in the Southern Hemisphere. Chapter 8, pp. 139 - 214 in Met. of the Southern Hemisphere, ed. C.W. Newton. Meteor. Monographs, 13, Amer. Met. Soc.

TALJAARD, J.J., W. SCHMITT, and H. VAN LOON (1961): Frontal analysis with application in the southern hemisphere. Notos, 10, pp. 25 - 58, Pretoria.

TALJAARD, J.J. and H. VAN LOON (1962): Cyclogenesis, cyclones and anticyclones in the southern hemisphere during the winter and spring of 1957. Notos, 11, pp. 3 - 20, Pretoria.

TALJAARD, J.J. and H. VAN LOON (1963): Cyclogenesis, cyclones and anticyclones in the southern hemisphere during summer 1957-8. Notos, 12, pp. 37 - 50, Pretoria.

VAN ESSEN (1970): Specification sheet for W.R. 67 wave recorder, Delft, Holland.

VAN IEPEREN, M.P. (1970); One dimensional wave spectrum analysis of wind waves off Cape Town. M.Sc. Thesis, University of Cape Town, South Africa.

VAN IEPEREN, M.P. (1973): Transformation of waves from deep to shallow water. Ph.D. thesis. University of Wales.

VAN LOON, H. (1972): Wind in the southern hemisphere. Chapter 5, pp. 87 - 99, in Met. of the southern hemisphere, ed. C.W. Newton, Meteor. Monographs, 13, Amer. Met. Soc.

VOWINCKEL, E. (1954); Synoptische Klimatologie vom gebiet Marion Island. Notos, 3, pp. 13 - 21, Pretoria.

WALDEN, H. (1963): Comparison of one dimensional wave spectra recorded in the Germany Bight with various theoretical spectra, in Ocean Wave Spectra, Prentice Hall Inc. Engelwood Cliffs.

WATTERS, J.K.A. (1953): Distribution of height in ocean waves. N.Z.J. Sci. Tech. 34, pp. 408 - 422.

ZWAMBORN, J.A., C. VAN SCHAIK, and A. HARPER (1970): Ocean wave research in Southern Africa. Proc. of 12th Conf. on Coastal Eng. Washington. New York: Amer. Soc. of Civil Eng.

APPENDIX 1

Monthly time series of wave heights H^1 and $H_{1/10}$ for July 1972 - November 1973. Breaks in continuity are due to equipment failure.

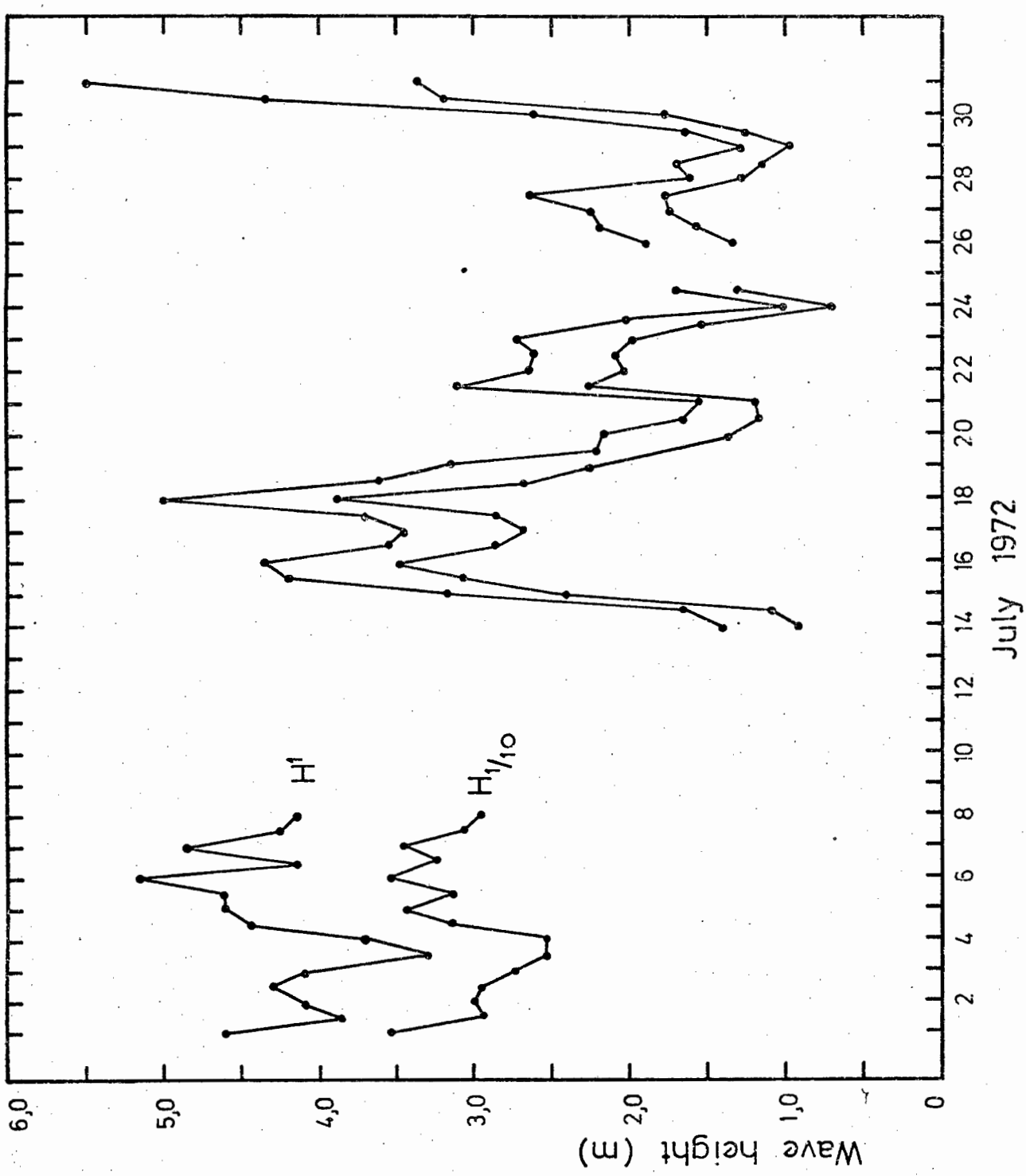
Wave height (m)
0
1,0
2,0
3,0
4,0
5,0
6,0
H'
H1/10
2
4
6
8
10
12
14
16
18
20
22
24
26
28
30
July 1972

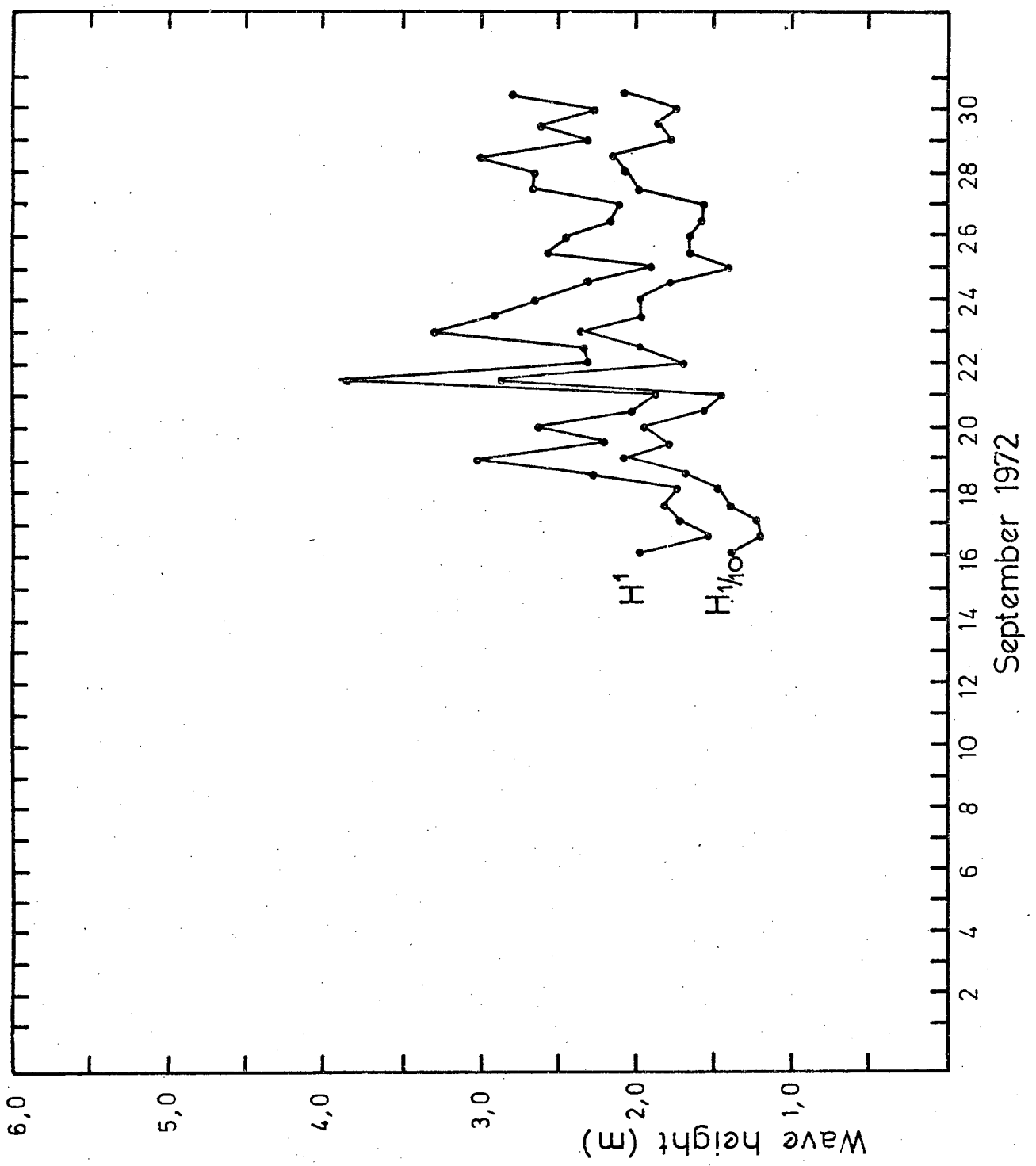
Wave height (m)
6,0
5,0
4,0
3,0
2,0
1,0
2
4
6
8
10
12
14
16
18
20
22
24
26
28
30
September 1972
H'
H1/10

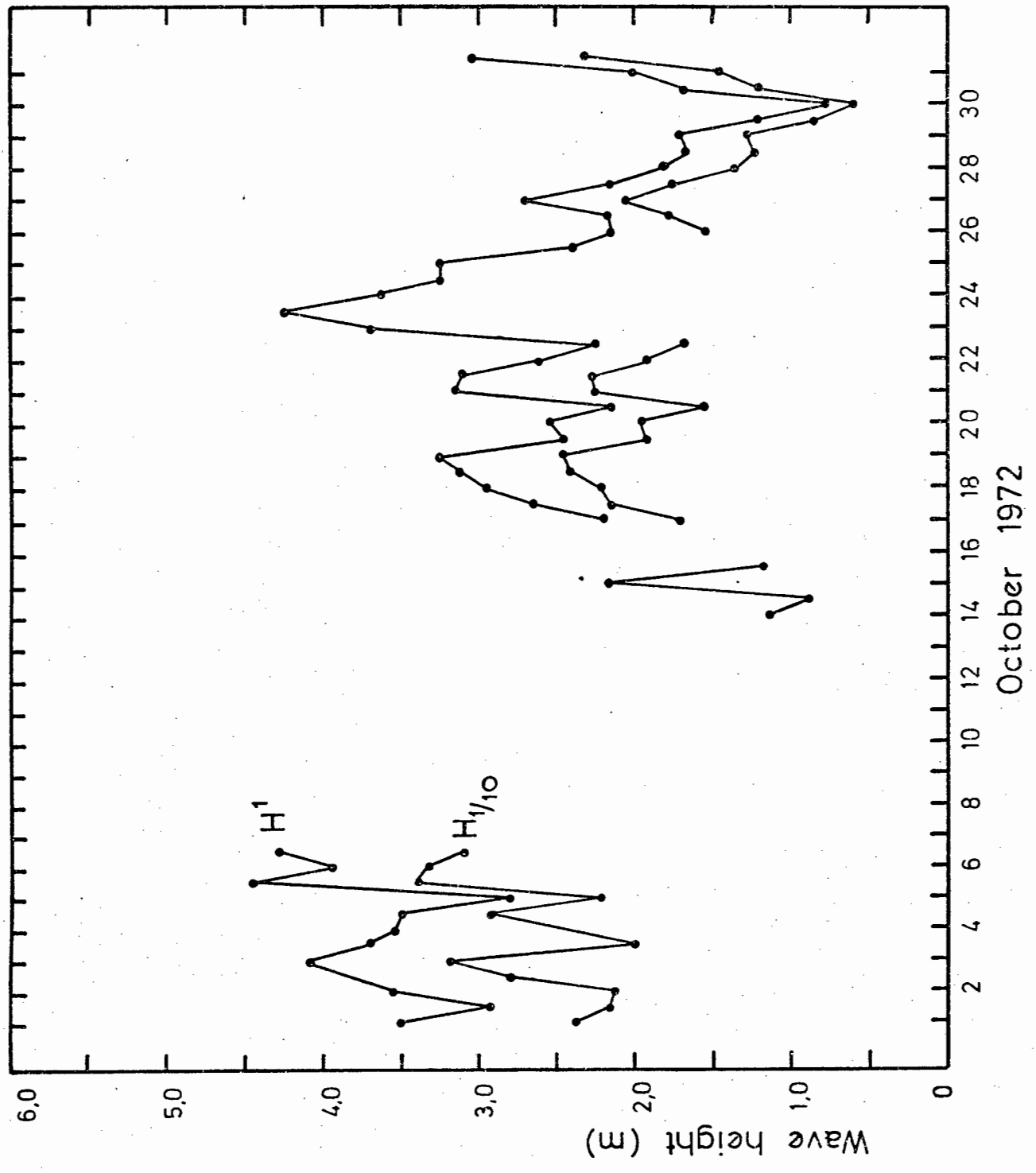
Wave height (m)
0
1,0
2,0
3,0
4,0
5,0
6,0
H'
H1/10
2
4
6
8
10
12
14
16
18
20
22
24
26
28
30
October 1972

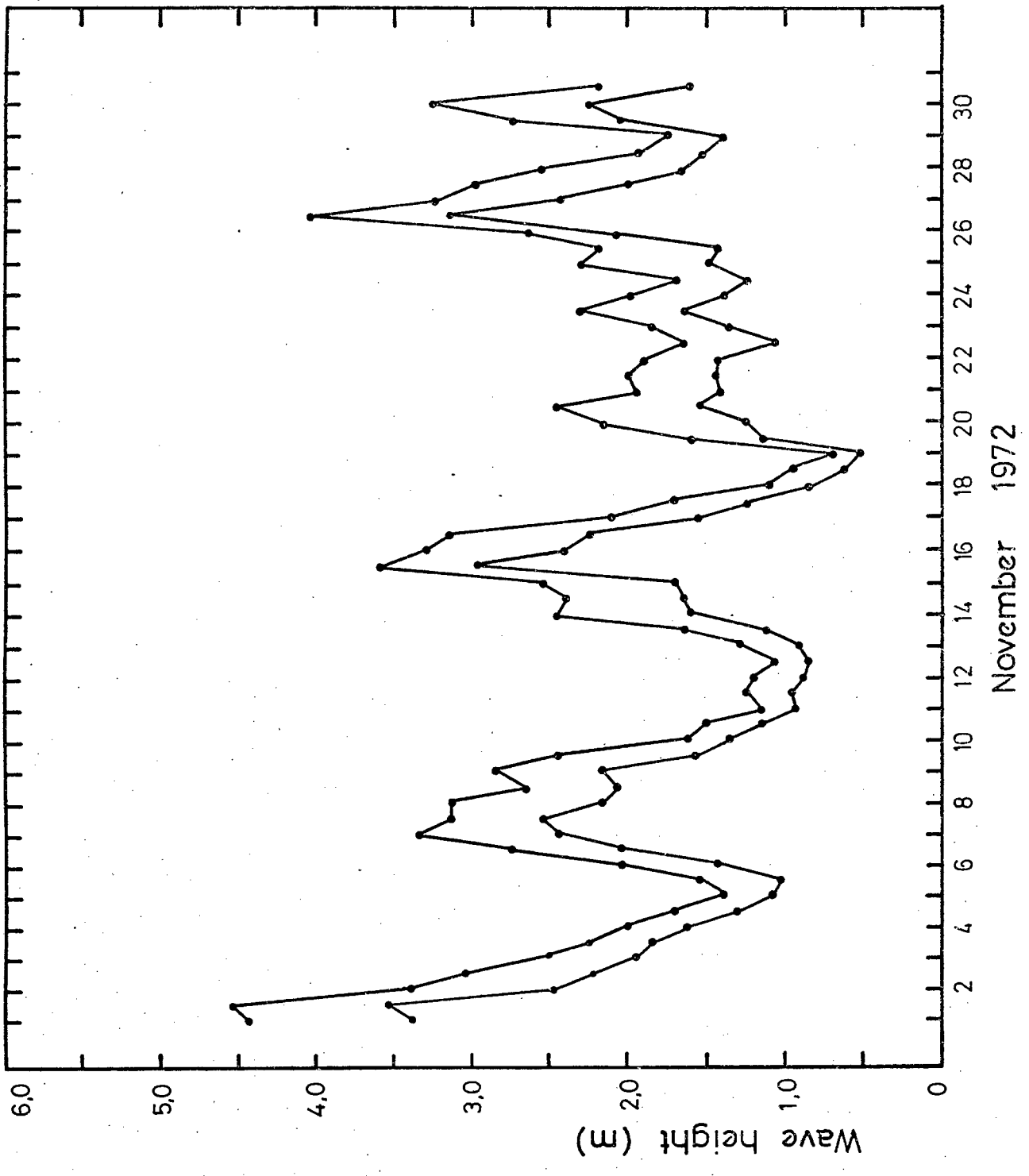
Wave height (m)
0
1,0
2,0
3,0
4,0
5,0
6,0
2
4
6
8
10
12
14
16
18
20
22
24
26
28
30
November 1972

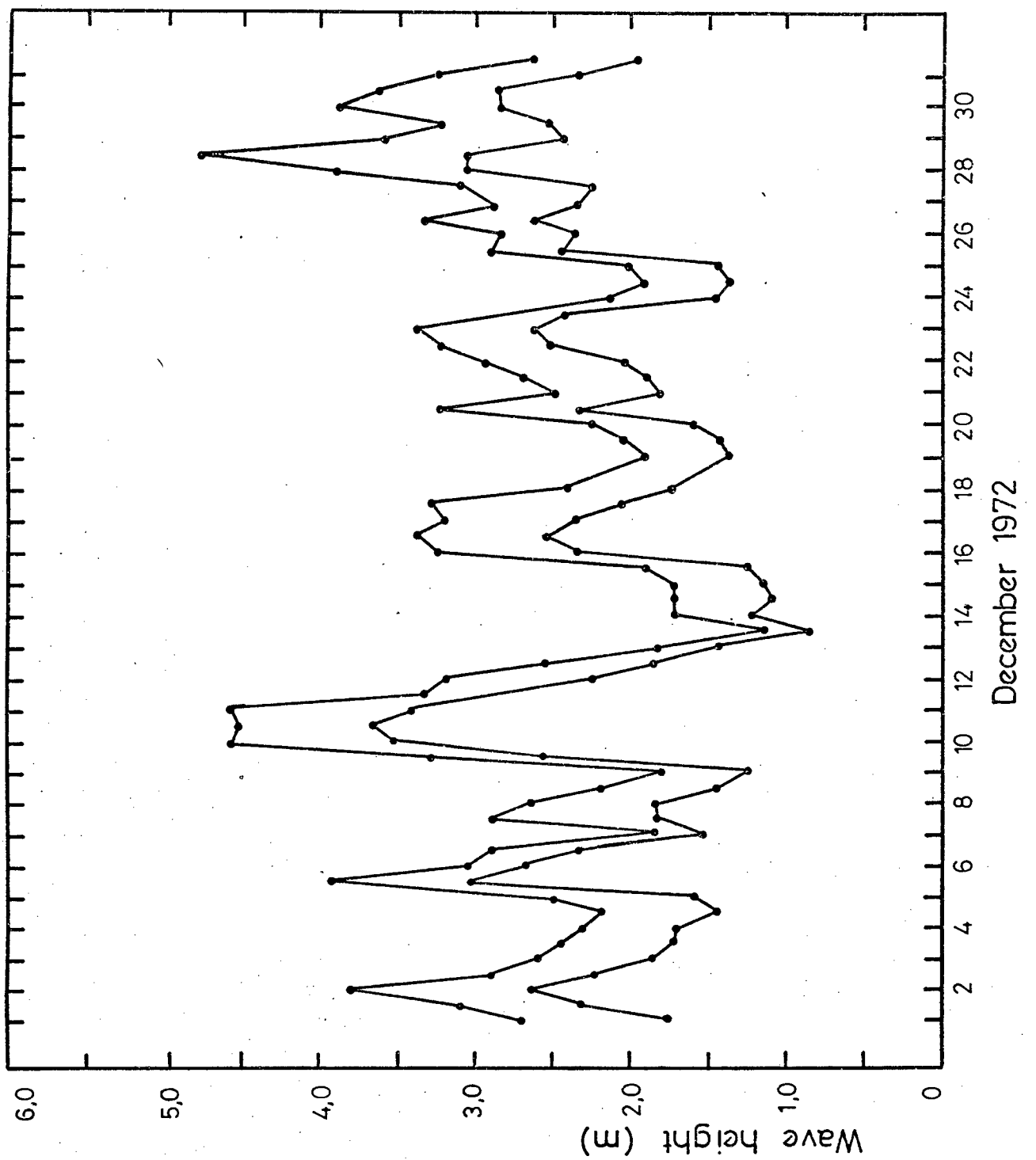
Wave height (m)
6,0
5,0
4,0
3,0
2,0
1,0
0
2
4
6
8
10
12
14
16
18
20
22
24
26
28
30
December 1972

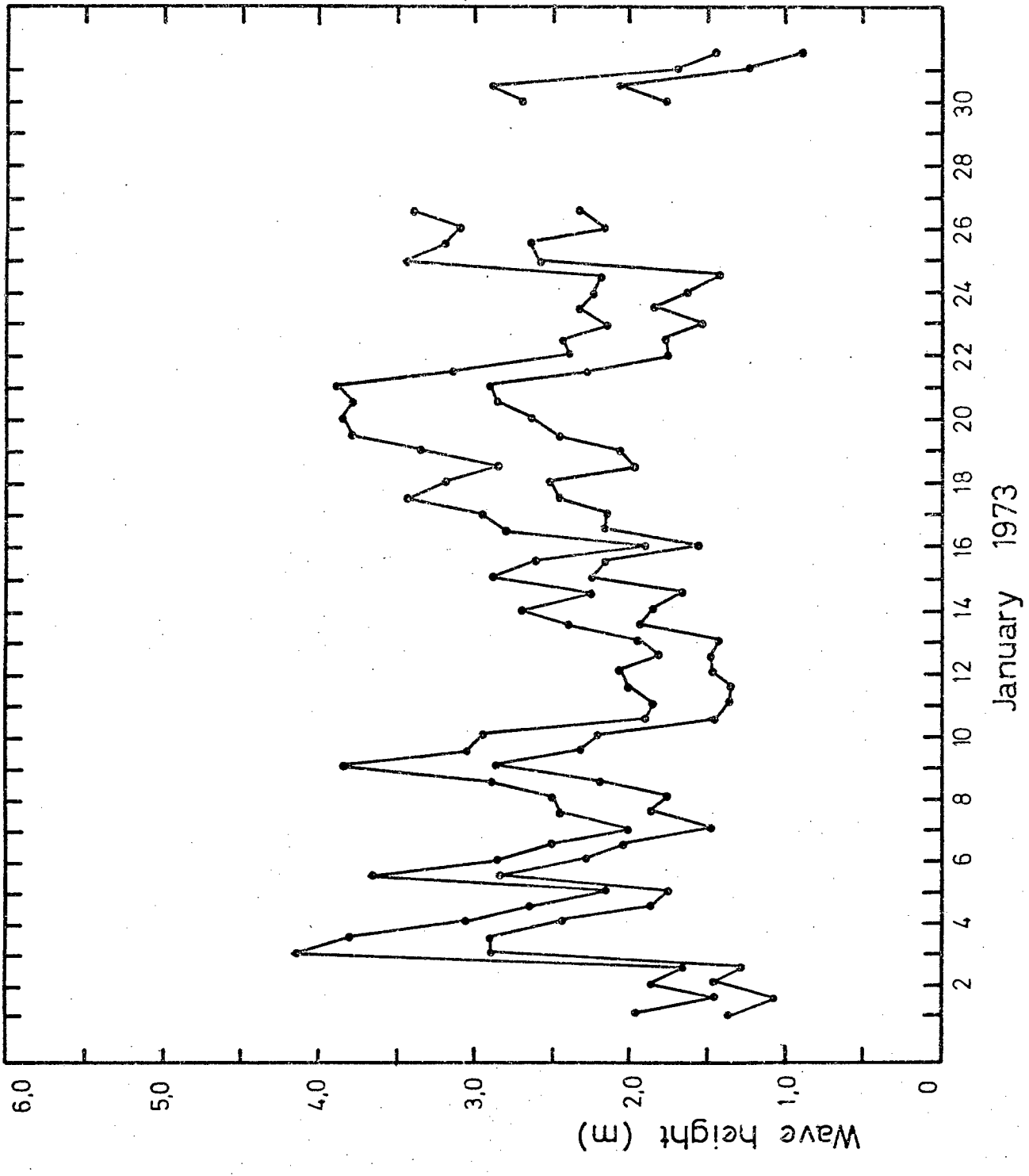
Wave height (m)
0
1,0
2,0
3,0
4,0
5,0
6,0
2
4
6
8
10
12
14
16
18
20
22
24
26
28
30
January 1973

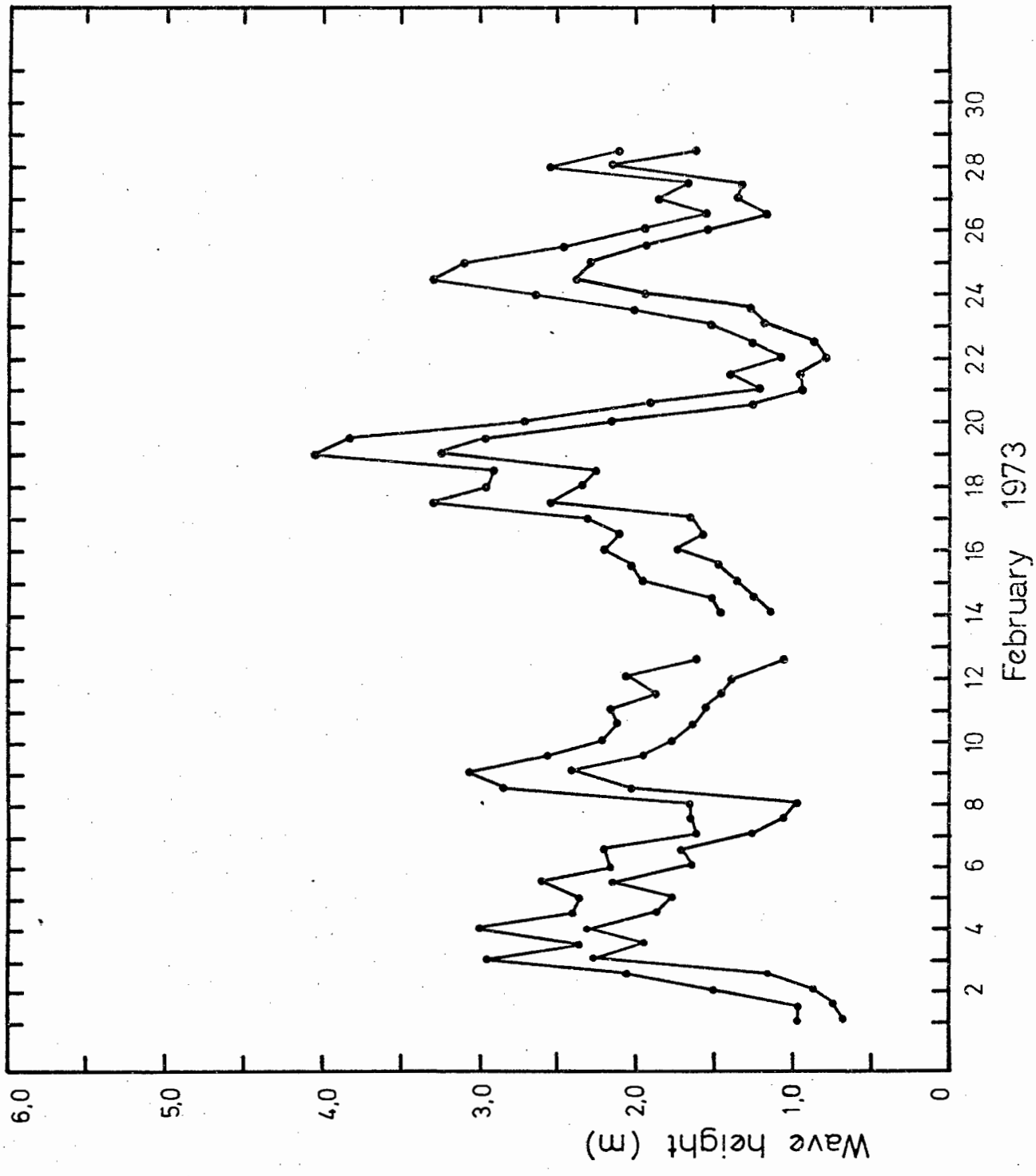
Wave height (m)
6,0
5,0
4,0
3,0
2,0
1,0
0
2
4
6
8
10
12
14
16
18
20
22
24
26
28
30
February 1973

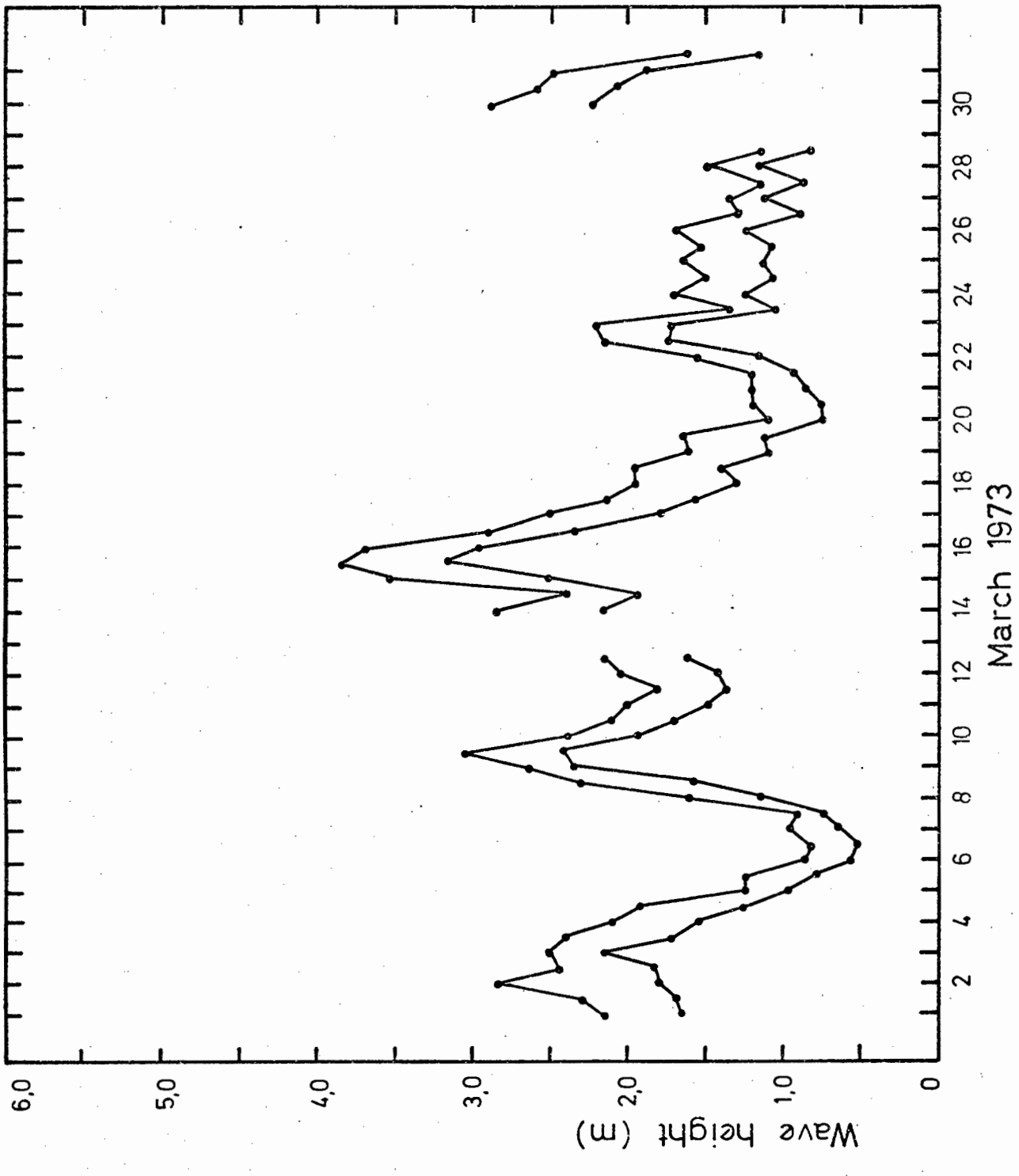
Wave height (m)
0
1,0
2,0
3,0
4,0
5,0
6,0
2
4
6
8
10
12
14
16
18
20
22
24
26
28
30
March 1973

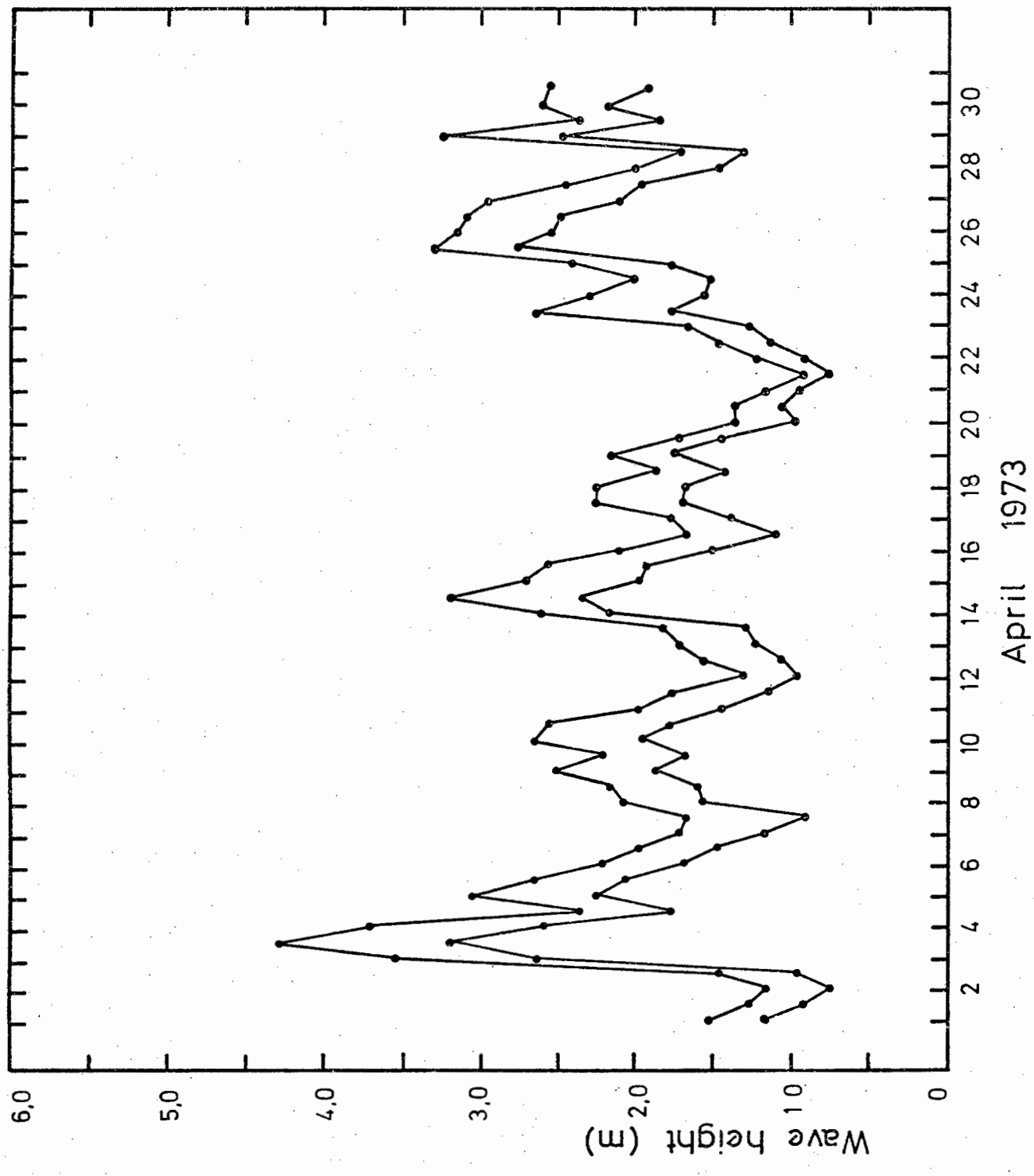
Wave height (m)
0
1,0
2,0
3,0
4,0
5,0
6,0
2
4
6
8
10
12
14
16
18
20
22
24
26
28
30
April 1973

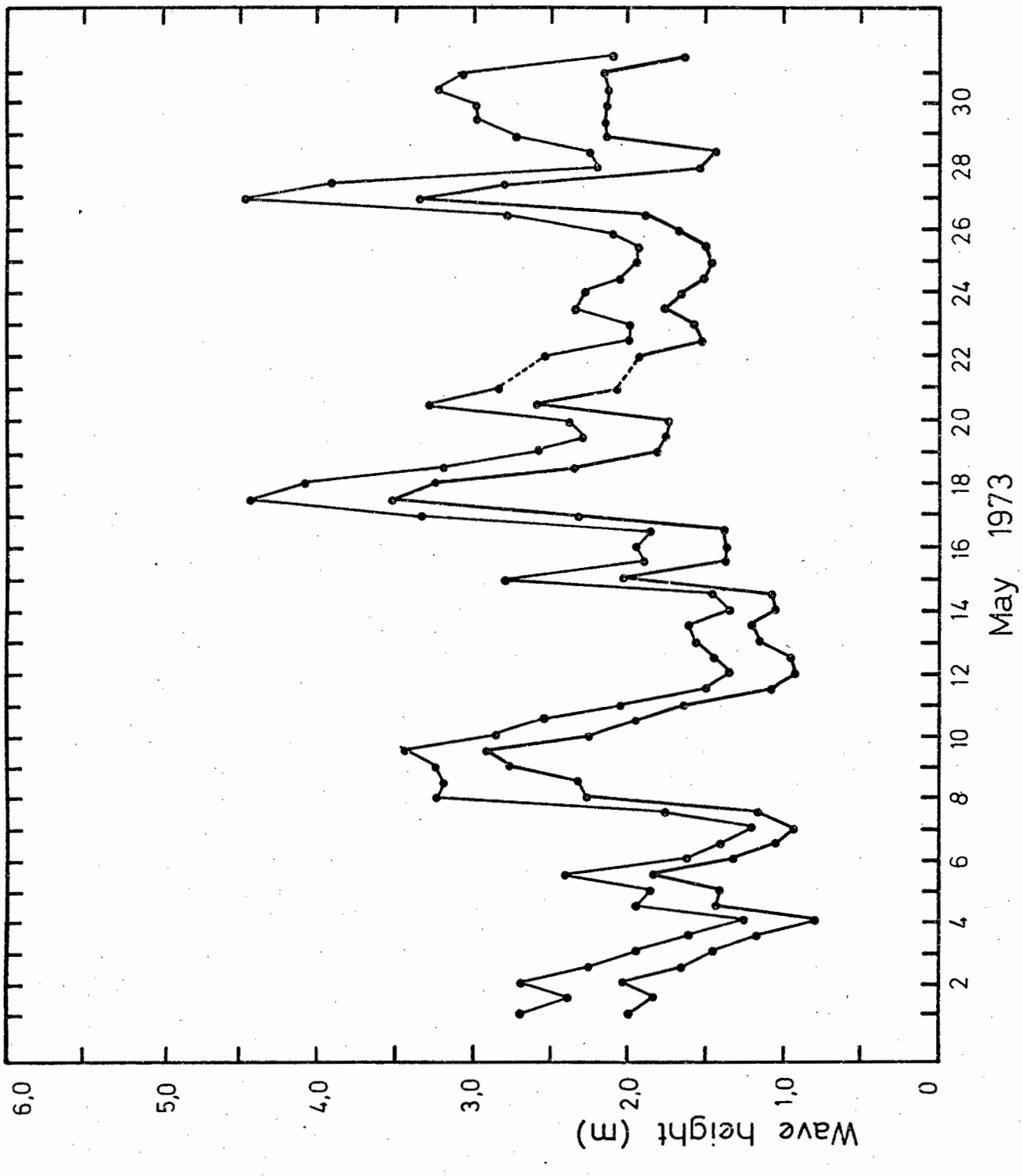
Wave height (m)
6,0
5,0
4,0
3,0
2,0
1,0
0
2
4
6
8
10
12
14
16
18
20
22
24
26
28
30
May 1973

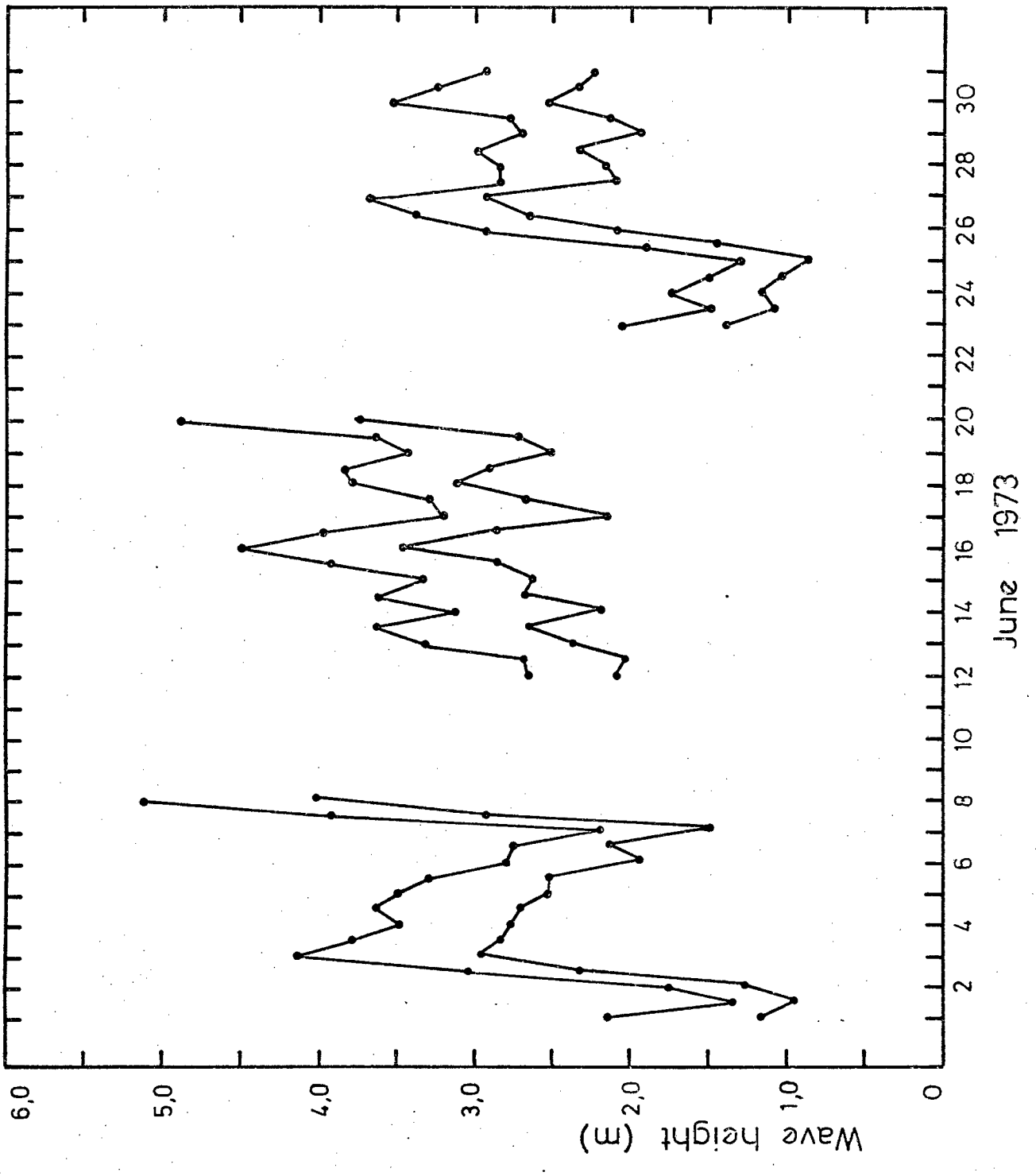
Wave height (m)
0
1,0
2,0
3,0
4,0
5,0
6,0
2
4
6
8
10
12
14
16
18
20
22
24
26
28
30
June 1973

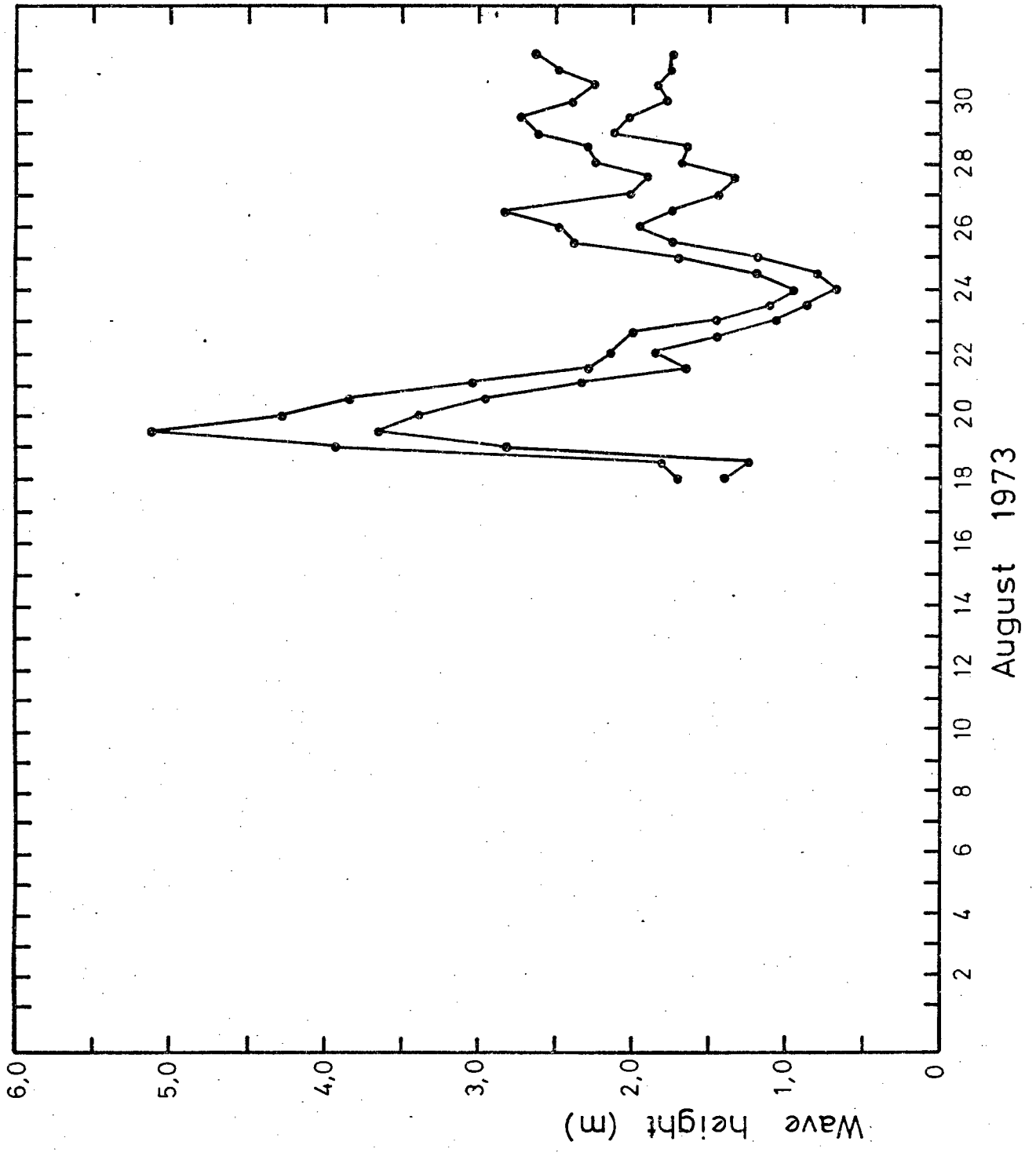
Wave height (m)
0
1,0
2,0
3,0
4,0
5,0
6,0
2
4
6
8
10
12
14
16
18
20
22
24
26
28
30
August 1973

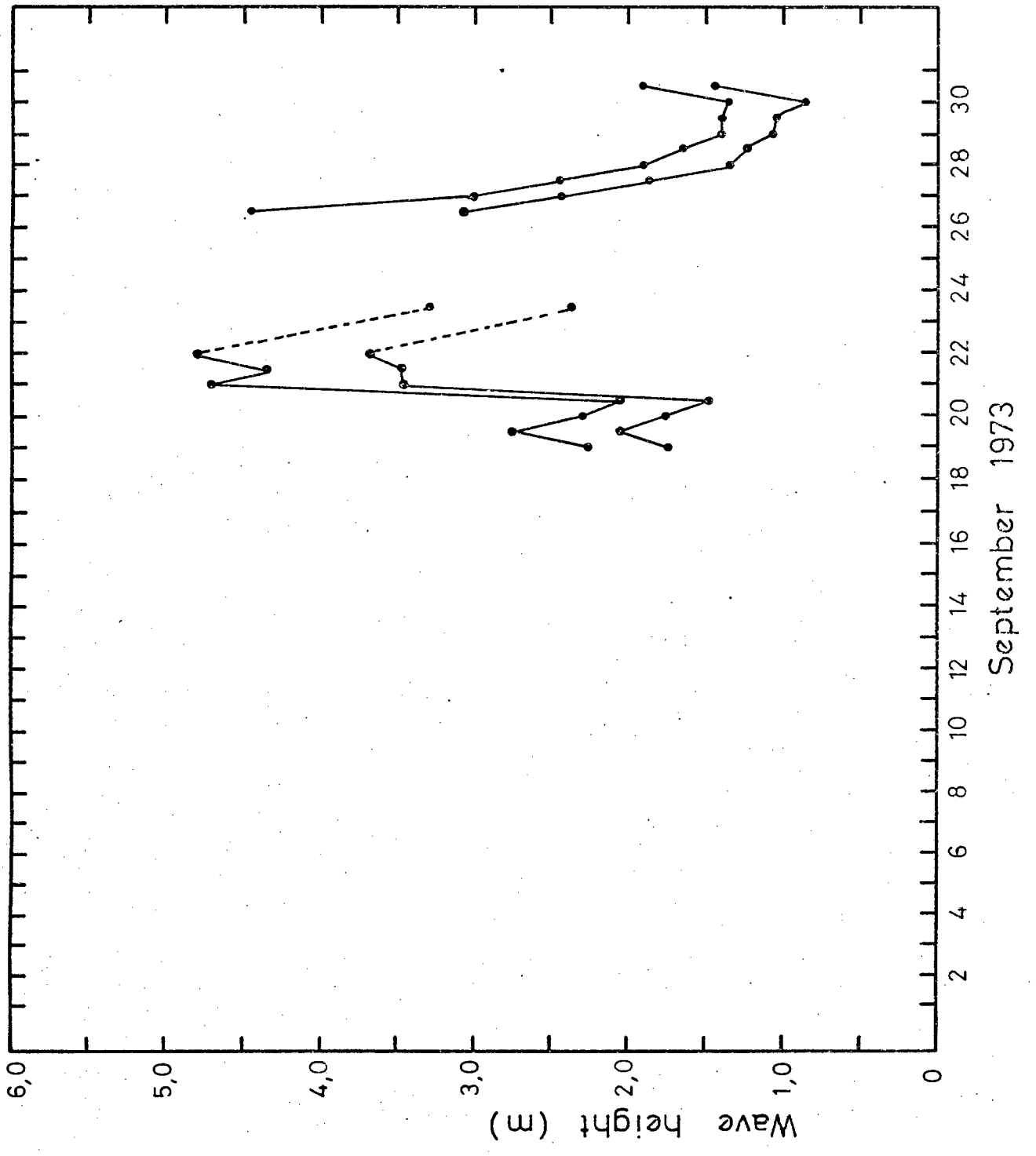
Wave height (m)
6,0
5,0
4,0
3,0
2,0
1,0
0
2
4
6
8
10
12
14
16
18
20
22
24
26
28
30
September 1973

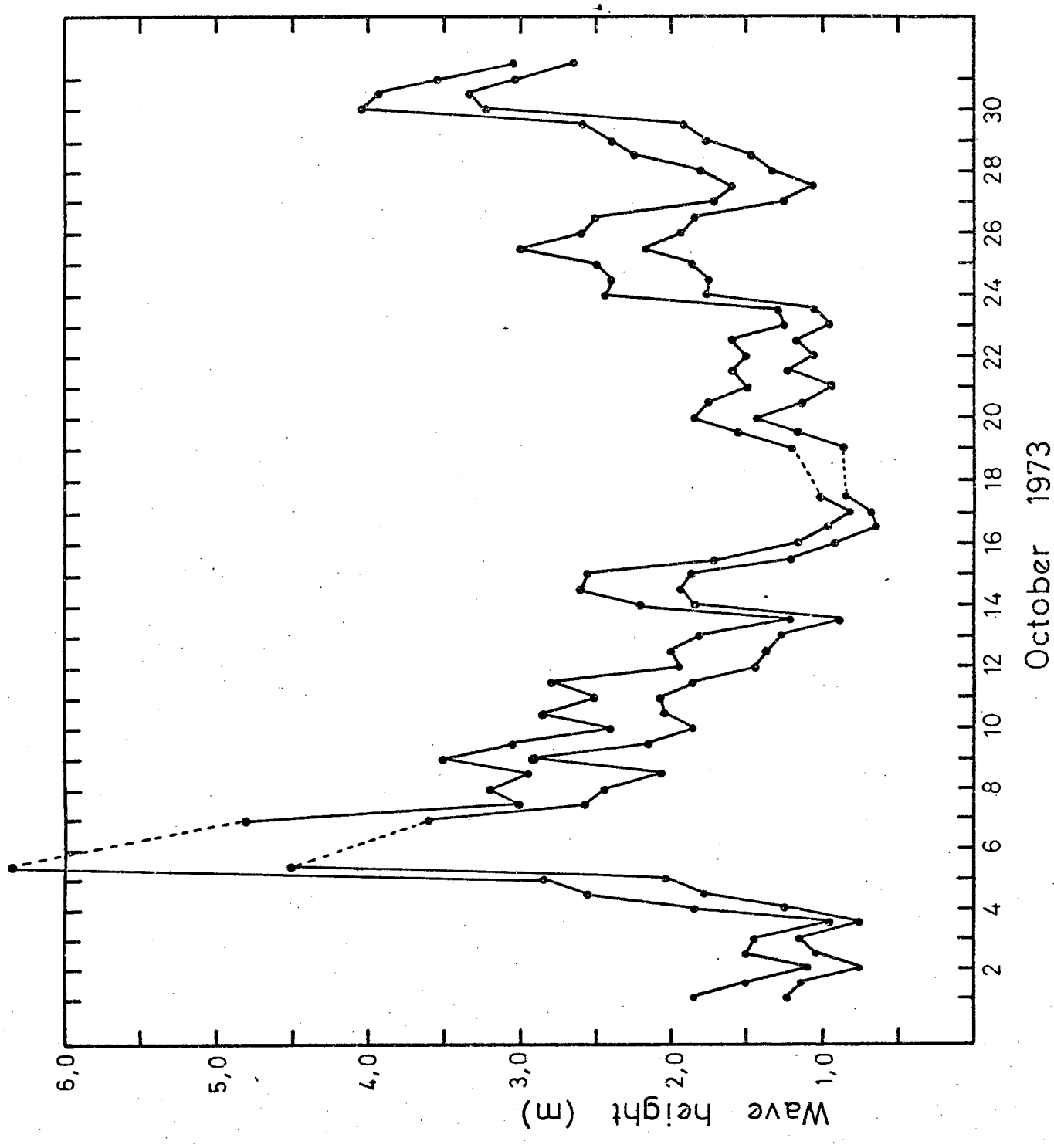
Wave height (m)
6,0
5,0
4,0
3,0
2,0
1,0
2
4
6
8
10
12
14
16
18
20
22
24
26
28
30
October 1973

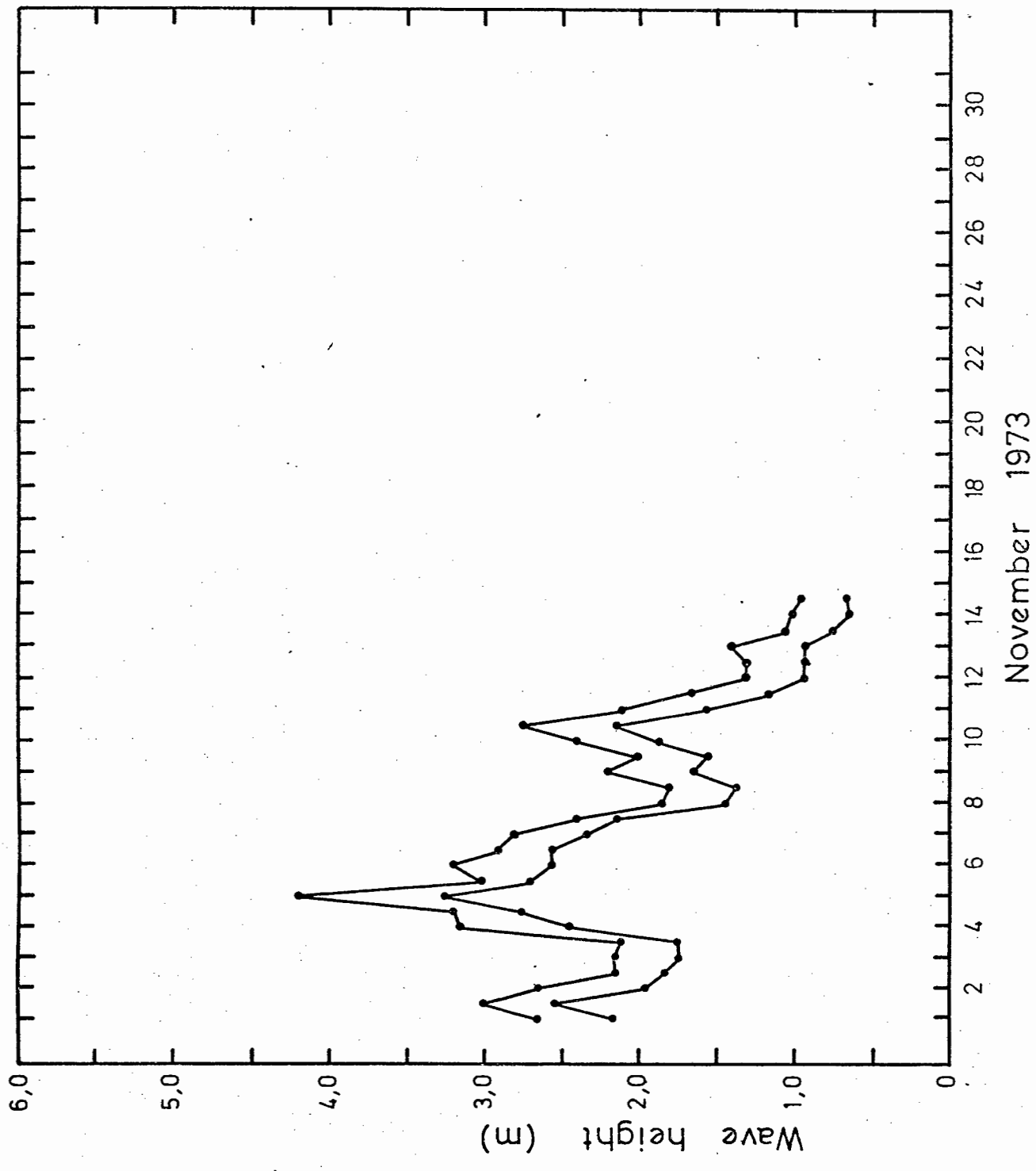
Wave height (m)
6,0
5,0
4,0
3,0
2,0
1,0
0
2
4
6
8
10
12
14
16
18
20
22
24
26
28
30
November 1973